Optimization of a gas flow proportional counter for alpha decay measurements

Elena Ceballos Romero

Master Thesis

Institut für Kernphysik
Mathematisch-Naturwissenschaftliche Fakultät
Westfälische Wilhelms-Universität Münster

Prof. Dr. Alfons Khoukaz

October 2012

I am among those who think that science has great beauty. A scientist in his laboratory is not only a technician: he is also a child placed before natural phenomena which impress him like a fairy tale. We should not allow it to be believed that all scientific progress can be reduced to mechanisms, machines, gearings, even though such machinery has its own beauty.

-Marie Curie

A magdalena, por ponerme en este camino.
A mis padres, por siempre acompañarme en él.

I certify that I have independently written this thesis and no other sources than the mentioned ones have been used.

Referent: Prof. Dr. Alfons Khoukaz

Correferent: Dr. María Villa Alfageme

Contents

1. Introduction

> *The basic motive which drives scientists to new discoveries and understanding of nature is curiosity. Progress is achieved by carefully directed questions to nature, by experiments. For many of these questions, precise measurement devices or detectors had to be developed. The development of particle detectors practically started with the discovery of radioactivity by Henri Becquerel in 1896.* Claus Grupen.

The effects produced when a charged particle passes through a gas is the base of several of the oldest and most widely used types of radiation detectors. The primary modes of interaction involve ionization and excitation of gas molecules along the particle track.

The first electrical devices designed for radiation detection were ionization detectors. Gas-filled detectors are the most used. They are based on sensing the direct ionization created by the passage of the radiation through the gas. These particular devices are in widespread use particle physics experiments. They are cheap, simple to operate and easy to maintain.

The present thesis is an attempt to present the different aspects of α detection with one of these gas-filled detectors: a windowless gas flow proportional counter, in a detailed manner. Its basic operation way is one of the simplest and originates an electronic output signal with the ion pairs formed within the gas filling it.

Proportional counters have several advantages. They are versatile in that they can be used for a variety of different applications. They can detect a variety of radiations (including α, β, γ, x-ray, and neutrons) and also distinguish among radiation types based on the shape of the pulses they create, so spectroscopy is possible. They have a low background for α particles and exhibit little or almost no dead time which allows the counting of higher activity sources. They are also available in a variety of shapes and sizes. In addition, for the particular case of the *windowless* counter, the presence of no window gives the great advantage of a high sensitivity. Because of the fact that α particles, whose decay detection is the main subject matter of this thesis, are stopped by a thin foil, the presence of no window avoid attenuation effects. The simplicity of these detectors and the possibility to make dosimetry, as well as spectroscopy with them, motivated the realization of a deeper study of them to optimize its operation focusing on α detection.

Starting from a commercial proportional counter, the currently available detector was rebuilt in the installations of the own university with the idea of implemented it for the practical exercises of the lesson of Nuclear Physics as radiation detector. The possibility of using of the detector regularly to make both counting and spectroscopy of radioactive unknown samples in the future by the students was the principal objective of this work. The idea of setting up a completely new device according to the objectives of its use,

motivated the initial studies with the gas flow detector. However, a large number of varied problems were found on its tuning. A short previous work developed with the gas flow detector with a lot of unanswered questions was the starting point for this present work. Complications in both α and β detection with, on principle, such simple device, promoted a Master Thesis focused on the device with the main aim of getting its good operation and gaining a good understanding of it. By measuring some certificated radioactive sources, the calibration of both the detector and its whole set up associated was carried out.

In the present thesis, the improvements and optimization of the device carried out will be described. That includes all the diverse complications that were observed in the use of the device and the systematic measurements implemented to identify the problems and get the mentioned improvements. The optimal nuclear electronics that must surround the detector and all the checking put through to decide it will be presented as well.

The structure of this thesis will follow this outline:

- In **Chapter 2** a brief introduction to natural radiations (α, β and γ) is presented. Their general characteristics and the different methods to detect them are explained. The concept of decay and activity will be introduced for a better understanding of these radiations.

- **Chapter 3** will be about gas-filled detectors in general. It will describe their common features and behaviour, giving some details about geometry aspects or operation regions depending on the different possible applications, focusing with particular emphasis on proportional counters.

- In **Chapter 4** the experimental set-up used for the measurements, including the detector and all the associated nuclear electronic, is presented in detail. The special type windowless gas flow proportional counters will be presented. Besides that, a description of the devices used in the chain and all their parameters selected as optimal for α decay detection are carefully explained.

- In **Chapter 5** the previous work with the detector will be summarized. That will include the old set-up used and the most important results from which this thesis continued. In addition, all the unanswered questions which motivated a Master Thesis about the device will be presented.

- **Chapter 6** is the main chapter of the thesis. In it will be shown all the systematic studies and measurements carried out to get the improvements of the whole set-up. An important point in this chapter is that it will provide the way to proceed with an unknown set-up to tune it up across all the difficulties that were found in this particular work during the various calibration measurements. It will include a description of the problems which came up in the detection, as well as the different ideas to check their possible causes and all the betterments obtained. That includes a study with a source of americium-241 used to make the detector calibration. Finally, a silicon detector included as a new tool for the detection techniques can also be found in this chapter. An explanation of its complete set-up and the results provided with this detector are given.

- In **Chapter 7** the different measurements with solid α sources will be exposed. That includes a stone containing natural uranium as well as several unknown elements, and a flat metal piece containing natural thorium. The shown results will include both the dosimetry and the spectroscopy analysis in a qualitative way.
- **Chapter 8** will describe the main features of β detection by using proportional counters. That will include the coming across difficulties found in the the qualitative analysis of two sources with a different range of energies, a strontium-90 source and a potassium chloride source present as salt.
- **Chapter 9** is a conclusion and an outlook of future work which has to be done to optimize the set-up completely with focus on β detection.

Besides this, a manual with more details of the whole set-up named *Manual for the windowless gas flow proportional counter* is available in the working group. This manual includes the details of the construction of the windowless gas flow proportional counter used, the electronic specifications of the devices of the nuclear chain for the proportional counter and the set-up associated to the Silicon detector in detail.

2. Introduction to natural radiations

An introduction to the concept of radioactivity and the decay laws that describe it is presented in this chapter. This brings to the main properties of natural radiations and the basic concepts for their measurement through the definition of activity. The principal differences between such radiations which characterize their interactions with matter like energy ranges or lifetimes are described.

2.1. Radioactivity

Nuclei can undergo a variety of processes resulting in the emission of radiation of some form.

Radioactivity is a natural and spontaneous process in our universe and our earth by which the unstable atoms of an element emit or radiate excess energy in the form of particles or waves. These emissions are collectively called *ionizing radiations*. Ionization is a particular characteristic of the radiation produced when radioactive elements decay. These radiations are of such high energy that when they interact with materials, they can remove electrons from the atoms in the material. This effect is the reason why ionizing radiation is hazardous to health, and provides the means by which radiation can be detected.

Depending on how the nucleus loses this excess energy either a lower energy atom of the same form will result, or a completely different nucleus and atom can be formed. In today's radioactivity is among other things for energy, nuclear medicine, and used in materials research.

Radioactive radiation is classified into α, β and γ radiation. These various types of radiation ionize to different extents. Seeing that the three of them were found along the studies with the detector, they must be explained with a little more depth. But before that, the introduction of some concepts is necessary.

2.1.1. Decay laws

In nuclear physics it cannot be predicted exactly when a nucleus will decay, it may only be given a probability with which the core will disintegrate. Just is possible to have statistical information about the decay process. Based on these, it is also possible to predict when a radioactive sample will be expected to disintegrate completely.

A nuclear decay process is governed by a transition probability per unit time, λ, characteristic of the nuclear species and known as *decay constant*. For a sample with N as the total number of existing nuclei, the mean number of nuclei decaying in a time dt according to:

$$dN = -\lambda N dt \tag{2.1}$$

The minus sign takes into account here that the number of existing nuclei decreases.

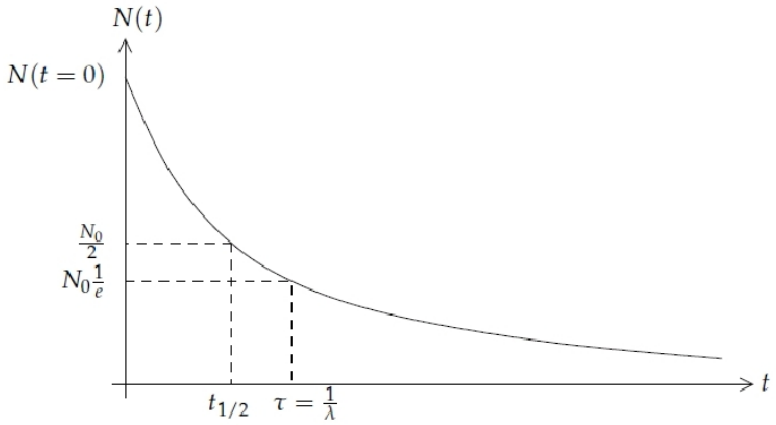

Figure 2.1. Representation of the decay law [Wei12].

In the previous equation it has been assumed that N is large so that it may be considered as continuous. Thus, equation (2.1) may be considered as the differential form of the radioactive decay law. By integration of the equation, yields the exponential decay law of radioactive cores:

$$N(t) = N(0)\exp(-\lambda t) \tag{2.2}$$

where $N(0)$ is the number of the nuclei at $t = 0$. Hence, the exponential decrease in activity of a sample is governed by the decay constant λ. The decay law is illustrated in Fig. 2.7

The reciprocal value of λ is called *mean life* τ, and is defined just like the average time during which a system, such as an atom, nucleus, or elementary particle, exists in a specified form, surviving before it decays.

Another concept is the *half-life time* $T_{1/2}$, which is defined as the time it takes for the sample to decay to one-half of its original quantity:

$$N(t = T_{1/2}) = \frac{N(0)}{2} = N_0 \exp(-T_{1/2}\lambda) \quad \Longrightarrow \quad T_{1/2} = \frac{\ln 2}{\lambda} \tag{2.3}$$

Consequently, the decay constant of the radioactive element is

$$\lambda = \frac{1}{\tau} = \frac{\ln 2}{T_{1/2}} \tag{2.4}$$

2.1.2. Activity

When a certain amount of radioactive material is given, it is customary to refer its quantity based on its *activity*.

The activity of a radioisotope source is simply the number of disintegrations or transformations the quantity of material undergoes in a given period of time. It is defined as its rate of decay by the fundamental law of radioactive decay

$$A = \frac{dN}{dt} = -\lambda N \tag{2.5}$$

In the *International System*, the activity is measured in becquerels (Bq). One Bq is defined as a decay per second.

This unit supersedes the old unit Curie (Ci). Historically, one Ci was the activity of one gram of radium

$$1\text{Ci} = 37 \times 10^{10}\text{Bq} \tag{2.6}$$

It should be emphasized that the activity measures the source disintegration rate, which is not synonymous with the emission rate of radiation produced in its decay. Frequently, a given radiation will be emitted in only a fraction of all the decays, so a knowledge of the decay scheme of the particular isotope is necessary to infer a radiation emission rate from its activity. Also, the decay of a given radioisotope may lead to a daughter product whose activity also contributes to the radiation yield from the source.

2.2. Decays

2.2.1. Alpha decay

Alpha decay (Fig. 2.2) is a radioactive process in which an α particle with two neutrons and two protons is ejected from the nucleus of a radioactive atom. The particle is a helium ^{4}He nuclei which are generally emitted by very heavy nuclei containing too many nucleons to remain stable (known as *neutron rich-atoms*).

For an atom with A its *mass number*, which gives the total number of protons and neutrons (together known as nucleons) and Z the *atomic number*, the number of protons found in the nucleus of an atom and therefore identical to the charge number of the nucleus, the parent nucleus ${}^A_Z X$ in the reaction is thus transformed via

$${}^4_2 X \longrightarrow {}^{A-4}_{Z-2} Y + {}^4_2 \alpha \tag{2.7}$$

where X and Y are the initial and final nuclear species.

The α particles appear in one or more energy groups that are monoenergetic. For each distinct transition between initial and final nucleus, a fixed energy difference or *Q-value* characterizes the decay. This energy is shared between the α particle and the recoil nucleus in a unique way, so that each α particle appears with the same energy given by $T_{kin} = Q(A-4)/A$.

α particles are very heavy and very energetic compared to other common types of radiation. These characteristics allow these particles to interact readily with materials

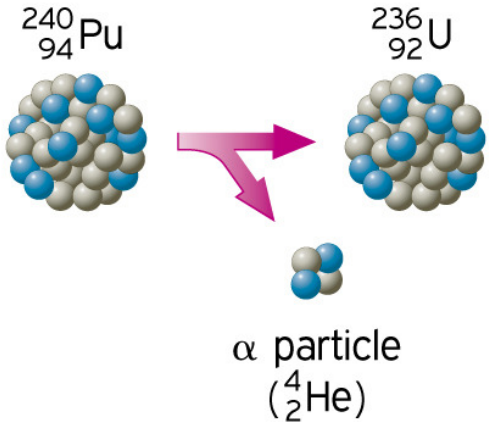

Figure 2.2. Example of a α decay [Isu12]: a plutonium-240 nucleus decays into an uranium-236 one by emitting an α particle. The mass number is reduced by four and the atomic number by two .

they encounter, including air, causing many ionizations in a very short distance seeing that they have a very high rates of energy loss in matter. Typical α particles will travel no more than a few centimeters in air and they can be shielded by a sheet of paper or the surface layer of our skin. For this reason it is necessary to make α sources as thin as possible in order to minimize energy loss and particle absorption in the source itself. Most α-sources are made, in fact, by depositing the isotope on the surface of a suitable backing material and protecting it with an extremely thin layer of metal foil.

Most α particles energies are limited between 4 and 6 MeV. There is a very strong correlation between the α particle energy and the half-life of the parent isotope. Those with the highest energies are those with the shortest half-life. Beyond about 6.5 MeV, the half-life can be expected to be less than a few days, and therefore the source is of very limited utility. For this reason, most α decays are directly to the ground state of the daughter nucleus since this involves the highest energy change. On the other hand, if the energy drops below 4 MeV, the half-life of the isotope becomes very large. In that case it is exceedingly long, the specific activity (defined as the activity per unit mass of the radioisotope sample) attainable in a practical sample of the material becomes very small and the source is of no interest because its intensity is too low [Kno96].

That is why for our experiments americium-241 was the α radioisotope selected, with an energy of $E_\alpha = 5.638$ MeV and a half-life of $T_{1/2} = 432.2$ years [Kae12]. Is must be noted that this source also emits gamma rays of approximately 60 keV, as shows its decay scheme depicted in Fig. 2.5

This source has three possible α decays summarized in Table. 2.1. However, in practice, for spectroscopic effects, due to the closure of these three energies, the decay is detected as a single peak corresponding to the decay energy, this is 5.673 MeV. So, the intensity of the decay is consider 100%.

Figure 2.3. α sample of americium-241 in the left-hand side and its decay scheme in the right-hand one [Web12a]. The source emits both, α and gamma radiation.

Isotope	Product	Decay Energy (MeV)	Particle Energy (MeV)	Intensity (percent)
^{241}Am	^{237}Np	5.673	5.4857	85.2
			5.4431	12.8
			5.3884	1.4
			others	<1

Table 2.1. Decay modes of americium-241 [Bau02].

2.2.2. Beta decay

Beta particles are fast electrons or positrons resulting from the weak-interaction decay of a neutron or a proton in nuclei which contain an excess of the respective nucleon. Atoms which undergo β decay are located below the line of stable elements on the chart of the nuclides, and are typically produced in nuclear reactors.

When a nucleus ejects a β particle, one of the neutrons in the nucleus is transformed into a proton or vice versa. Since the number of protons in the nucleus has changed, a new daughter atom is formed which has one less neutron but one more proton than the parent. Due to energy conservation required in nuclei the existence of the neutrino was proposed.

$$\begin{aligned} n &\rightarrow p + e^- + \overline{\nu_e} \quad (\beta^- \text{ process}) \\ p &\rightarrow n + e^+ + \nu_e \quad (\beta^+ \text{ process}) \end{aligned} \tag{2.8}$$

The most common source of fast electrons in radiation measurements is a radioisotope that decays by *beta-minus emission* (Fig. 2.4). The process is written schematically

$$^{A}_{Z}X \longrightarrow ^{A}_{Z+1}Y + \beta^- + \overline{\nu} \tag{2.9}$$

where X and Y are the initial and final nuclear species, and $\overline{\nu}$ in the antineutrino.

In this β decay an electron is emitted from the nucleus of a radioactive atom, along with a particle called an antineutrino. The neutrino is an almost massless particle that carries away some of the energy from the decay process. Because neutrinos and antineutrinos have an extremely small interaction probability with matter, they are not easy to detect. The recoil nucleus Y appears with a very small recoil energy, which is ordinarily below the

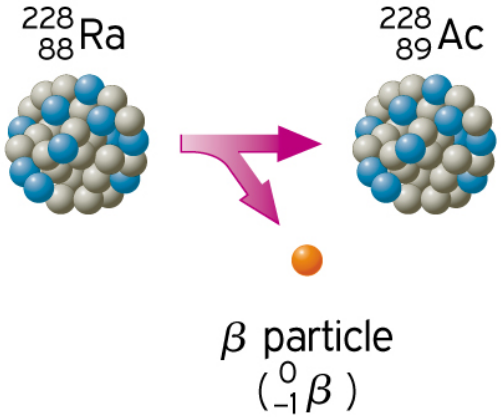

Figure 2.4. Example of a β^- decay [Isu12]: a Radius-228 atom decays into Actinium-228 by β^- emission. The parent is rich in neutrons which become into protons while emitting an electron (β^-) and an electronic antineutrino.

ionization threshold, and therefore it cannot be detected by conventional means. Thus, the only significant ionizing radiation produced by β decay is the fast electron or β particle itself.

β particles are single negative charged particles. As a result, they interact less readily with material than α particles. Depending on the β particles energy (which depends on the radioactive atom), β particles will travel up to several meters in air, and are stopped by thin layers of metal or plastic.

Each specific β decay transition is characterized by a field decay energy or Q-value. Because the energy of the recoil nucleus is close to zero, this energy is shared between the β particle and the *invisible* neutrino. The β particle thus appears with an energy that varies from decay to decay and can range from zero to the *beta endpoint energy*, which is numerically equal to the Q-value. For most β sources, this maximum value ranges from a few tens of keV to a few MeV.

Because most radionuclides produced by neutron bombardment of stable materials are beta-active, a large assortment of β emitters are readily available through production. Species with many different half-lives can be obtained, ranging from thousands of years down to as short half-life as is practical in the application.

In our case, the chosen β source was strontium-90, with a decay energy of $E_\beta = 0.546$ MeV. This isotope decays into yttrium-90 with a half-life of $T_{1/2} = 28.79$ years, which is much more energetic, $E_\beta = 2.280$ MeV and $T_{1/2} = 64.00$ hours [Kae12].

In very many β sources, the daughter nucleus is left in an excited state which decays immediately with the emission of one or more γ photons. These sources, therefore, are also emitters of γ radiation. Most β sources are of this type. *Pure* β sources exits but the list is astonishingly short. Since electrons lose their energy relatively easily in matter, it is important to β sources being thin in order to allow the beta's to escape with a minimum of energy loss and absorption.

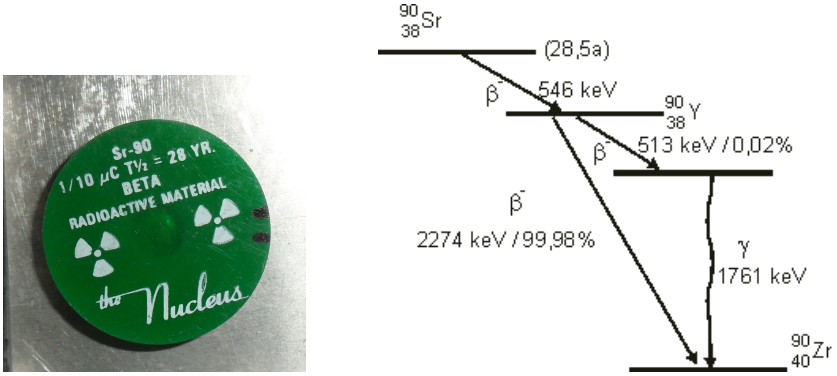

Figure 2.5. Beta sample of strontium-90 in the left-hand side and its decay scheme in the right-hand one [Web12b]. ^{90}Sr has a low decay energy of $E_\beta = 0.546$ MeV but its daughter ^{90}Y which decays with an energy of $E_\beta = 2.274$ MeV.

2.2.3. Gamma decay

After a decay reaction, the nucleus is often in an *excited* state. This means that the decay has resulted in producing a nucleus which still has excess energy to get rid of. Rather than emitting another β or α particle, this energy is lost by emitting a pulse of electromagnetic radiation called a γ ray (Fig. 2.6). This is identical in nature to light or microwaves, but of very high energy.

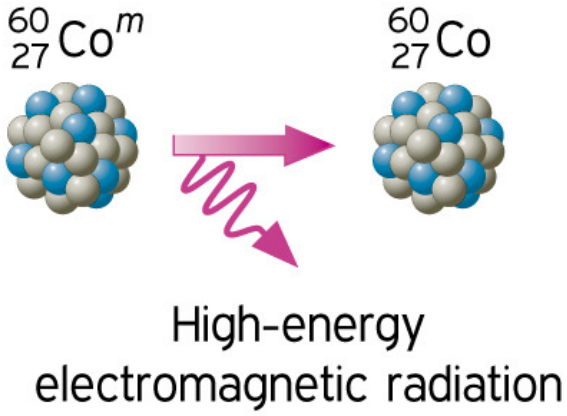

Figure 2.6. Example of a γ decay [Isu12]: metastable cobalt-60 is a nuclear isomer of cobalt-60 and decays in the 99.76% of the cases by internal transition to cobalt-60 emitting 58.6 keV γ rays, or with a low probability (0.24%) by β decay into nickel-60 [Kae12].

Like the electron shell structure of the atom, the nucleus is also characterized by discrete energy levels. Transitions between these levels can be made by emission (or absorption) of electromagnetic radiation of the correct energy, this is, with an energy equal to the energy difference between the levels participating in the transition.

The energies of these photons, from a few hundred keV to a few MeV, characterize the high binding energy of the nuclei.

Like all forms of electromagnetic radiation, the γ rays have no mass and no charge. They interact with material by colliding with the electrons in the shells of atoms. They lose their energy slowly in material, being able to travel significant distances before stopping. Depending on their initial energy, γ rays can travel from some to hundreds of meters in air and can easily go right through people. They are best shielded by thick layers of lead or other dense material. A comparison of the different penetration ranges of the three natural radiations described is shown in Fig. 2.7.

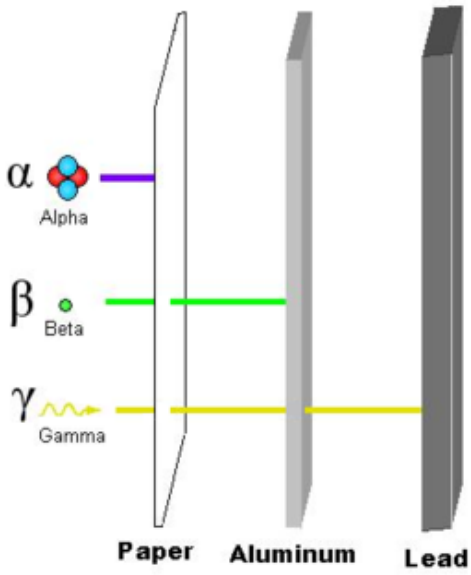

Figure 2.7. Penetrating distances of the different radiations [Isu12]. α particles have a very high rate of energy loss in matter, so they travel no more than a few centimeters in air and are stopped by a sheet of paper. On the other hand, β particles interact less readily with material than α particles do and are stopped by thin layers of metal or plastic. However, γ rays are only stopped by thick layers of lead or other dense material.

Most γ sources are *placed* in their excited states as the result of β-disintegration, although excited nuclear states are often created in nuclear reactions also. Since electrons and positrons are more easily absorbed in matter, they can be *filtered* out by enveloping them with sufficient absorbing material, leaving only the more penetrating gamma ray. There is no such thing as a*pure* gamma emitter.

3. Theoretical background: Gas-filled detectors

The theory of gas-filled detectors is shortly introduced in this chapter. Starting with their general properties and their common behaviour an overview of these devices and their variety will be presented. The particular case of proportional counters and deeper, the gas flow proportional counters type on which the thesis is focused, will be discussed.

3.1. General properties

Particle radiation cannot be detected directly, but rather only through their interactions with matter. One can say that every interaction process can be used as a basis for a detector concept [Gru99]. The variety of interactions is quite rich and, as consequence, a large number of detection devices for particle radiation exist.

As it has been already mentioned in a previous chapter, the most common type of instrument is a gas-filled radiation detector. These detectors can be designed to detect α, β, γ, and neutron radiation. These instruments work on the principle that as radiation passes through a gas, both ionization and excitation processes of the molecules in the gas along its path occur. Radiation ionizes the gas as it enters into the chamber, creating free electrons and positively charged ions both called *ion pairs*. The number of electrons and positively charged ions created is related to the properties of the incident radiation type. α particles produce many ion pairs in a short distance, β particles produce fewer ion pairs due to their weaker interaction, and photons produce relatively few ion pairs as they are uncharged and interact with the gas significantly less than α and β radiation. These ion pairs serve as the basic constituent of the electrical signal. Ions can be formed either by direct interaction with the incident particle, or through a secondary process in which some of the particle energy is first transferred to an energetic electron.

Regardless of the detailed mechanisms involved, the practical quantity of interest is the total number of ion pairs created along the track of the radiation. The most important fact is that if the particle is fully stopped within the gas, the deposited energy is proportional to the number of ion pairs formed, which can be measured.

However, without the presence of an external electrical field charges would simply recombine. Only when a high voltage is placed between two areas of the gas filled space, the positive ions will be attracted to the negative side of the detector (the *cathode*) and the free electrons will travel to the positive side (the *anode*). Normally, a wire serves as anode, and the chamber as cathode. The collection of these charges by the anode and cathode forms a very small current in the wire going to the detector. Obviously, the more

radiation which enters the chamber, the more charges and hence, current are produced. By placing the right devices, this small current can be measured and displayed as a signal.

The voltage applied to the chamber can be separated into different ranges that distinguish the types of gas-filled detectors described below. In ascending order of applied voltage we can find the three gas-filled detectors models: the ion chamber, the proportional counter, used both for measuring large amounts of radiation, and the Geiger-Müller (or GM detector), used to measure very small amounts of radiation.

There are some general features common for the three of them. The most relevant of them are described here.

3.1.1. Number of ion pairs formed

The particles must transfer at least a minimum amount of energy equal to the ionization energy of the gas molecules in order to permit the ionization process to occur. In most gases of interest for radiations detectors, the ionization energy for the least tightly bound electron shells is between 10 and 25 eV [Kno96].

Nevertheless, there are other possible ways for the particle to lose its energy. In average, the energy required to produce an electron-ion pair in a gas (denoted as W) depends on the gas, the type of radiation and its energy (consult Table 3.1). W values for fast electrons in common filling gases range from 26.4 eV per ion pair in argon to 41.3 eV per ion pair in helium. The presence of non-ionizing energy loss processes accounts for the W values greatly in excess of the ionization energy [Fra00].

Gas	W (eV per ion par)
Ne+ 0.5% Ar	25.3
Ar+ 0.5% C2H2	20.3
Ar+ 10% CH4	26

Table 3.1. Characteristics values of the energy required to create an ion pair (W) for common proportional counter gases [Fra00].

If that W is assumed constant for a given type of radiation, then the deposited energy in the detector will be proportional to the number of ion pairs formed and can be determine if a measurement of the corresponding ions pairs created is carried out.

3.1.2. Behaviour of charged particles in gases

The neutral atoms or molecules of the gas are in constant thermal motion. Free electrons and positive ions created within the gas also take part in the thermal motion leading to diffusion away from regions of high density.

Different types of collisions take place between ions, free electrons and neutral gas molecules in the gas and can influence the behaviour of gas-filled detectors. The most frequent interactions are three: *charge transfer*, *electron attachment* and *recombination* (Fig. 3.1). The first one occur when a positive ion encounters a neutral gas molecule. This

is particularly significant in gas mixtures containing several molecular species because of the transfer of electrons from the neutral molecule to the ion. The gas with the highest ionization energy tends to transfer its positive charge to the lowest one. In the electron attachment, are the neutral molecules which form negative ions by catching the free electron in the collisions that this undergoes in its normal diffusion. Oxygen is an example of gas that easily attaches electrons diffusing in air converting them to negative ions. Lastly, collisions between free electrons and positive ions may result in recombination through which the state of neutrality is again reached. Could also be that the positive ion undergoes a collision with a negative ion and both are neutralized. The most common recombination occurs on this last way. Thus, ions collection and charge separation should be as rapid as possible in order to minimize recombination. High electric fields are used for that.

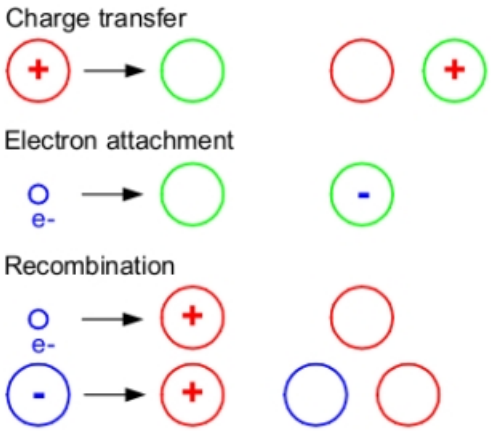

Figure 3.1. The most frequent types of interaction of charged species in a gas that can influence the behaviour of gas-filled detectors. Neutral atoms or molecules are shown as simple circles. The interacting species are depicted on the left-hand side of the plot and the products of the interaction are on the right-hand one [Phy12].

All these possible processes must be taken into account in the fill gas selection in order to avoid them as maximum as possible.

3.1.3. Operational modes of gas detectors

Operating with a radiation detector, each individual pulse carries important information regarding the charge generated by the particular incident radiation that interacts within the detector. In order to characterize its performance and establish an operating point at which the maximum stability in the device response is obtained, the pulse amplitude distribution must be studied. Variations in the amplitude of the pulses may be due to either differences in the radiation energy or to fluctuations in the inherent response of the detector to monoenergetic radiation. For this reason, an analysis of the amplitude pulses for the voltage values applied is necessary.

For a general gas-filled detector, as it has been mentioned before, depending on this high voltage applied, there are several operation regions that are related to the three possible types of detectors. In each one a different pulse amplitude is associated. These regions are shows in Figure 3.2. On that way can be distinguished:

I. Recombination region: At very low values of the high voltage the charge collection is incomplete seeing that the voltage is not enough to prevent recombination effects of the ions pairs. They will recombine before they reach either the cathode or anode and the collected charged is less than the real formed.

II. Ionization region: As soon as the voltage is increased a complete *primary charge* collection is reached. Nevertheless, no multiplication effect of the charges is still possible. The main feature of this region is the fact that the collected charge is proportional to energy, so the detector gives a *spectrometric response.*

    Ionization chambers work in this region. However, because signals produced are small, they are typically used only for heavy charged particles or large fluxes of radiation.

III. Proportional region: In the next range of higher voltage applied, the value is sufficient to create ions with enough kinetic energy to generate new ion pairs, called *secondary ions,* on their paths to the anode. If the produced electrons have a higher energy than the ionization energy of the gas, a multiplication effect comes and large amplification ($\sim 10^6$, [Kno96]) are produced.

    This is the region of operation for proportional counters. The quantity of secondary ions increases proportionally with the applied voltage, in what is known as the *gas amplification factor.* The signal pulse heights produced can be discerned by the external circuit to distinguish among different types of radiation.

IV. Limited proportional region: At a certain value, depending on the features of the detector (like size or fill gas), the applied high voltage is too big and the proportionality between the charge collection and the deposited energy in the detector is ended. Due to space charge effects: the positive ions reducing the electrical field, non-linear effects appear.

V. Geiger Müller region (GM-region): If the high voltage continues being increased, secondary avalanches along anode wire are produced. The space charge becomes sufficient to reduce the electric field below the multiplication threshold and no further multiplication takes place. Thus, a situation in which the same number of positive ions are produced for all initial ion-pair populations can be reached, and the pulse amplitude is independent of the initial conditions.

    This characterizes Geiger-Müller counter operation. Under this conditions there is an independence of primary charge and no energy measurement is possible. The detector works as an only simple counter.

VI. Discharge region: If after GM-region the voltage continues increasing, a constant breakdown with or without radiation takes place. This situation must be avoided to prevent damage to the counter.

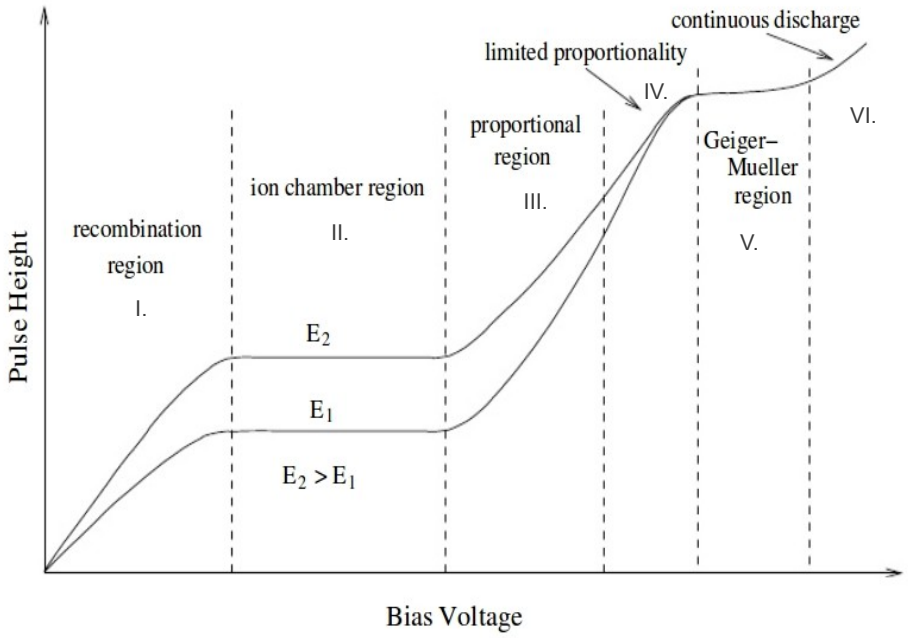

Figure 3.2. Variation of pulse height as a function of the voltage applied. Such variation leads to the different operation regions of gas-filled detectors. The two curves correspond to two different energies of incident radiation [Scr12].

3.2. Proportional counters: gas multiplication effect

As it has been already explained in the previous section, the small pulse amplitude encountered in ion chambers can be remedied by just increasing the high voltage applied. A proportional counter utilizes the phenomenon of *gas multiplication* to increase the pulse size by factors of hundreds or thousands. As a result, pulses are considerably large than those from ion chambers. Fortunately, secondary ionization is proportional to primary ions formed, so the pulse size reflects the energy deposited by the incident radiation in the detector gas.

The main advantage that this kind of detectors give is the possibility of differentiate between the ionization produced by heavily and lightly ionizing radiations, distinguishing the larger pulses produced by α particles from the smaller pulses produced by β particles or γ rays.

The gas multiplication factor of a proportional counter can be defined as the ratio of the charge on the electrons collected at the wire to the charge on the electrons produced by an ionizing particle passing through the gas [Cur49].

As it has been previously explained, gas multiplication is a consequence of the motion of free electrons in a strong electric field. When the strength of the field is the adequate, the electrons gain enough energy between collisions to cause secondary ionizations. After such an ionizing collision, two free electrons exist in place of the original one. The size of the output pulse increases with the voltage applied to the proportional tube, since each avalanche is more vigorous as the electric-field strength increases. The proportionality between the size of this output pulse and the amount of energy lost by the incident radiation in the gas is the basis of the term proportional counter.

In an uniform electric field, the number of electrons will grow exponentially along their paths to the anode. The growth of the population of electrons finish only when they reach the anode. The production of such a *shower* of electrons is called a *Townsend avalanche* and is triggered by a single free electron.

In a proportional counter, the objective is to have each original free electron that is formed along the track of the particle create its own individual Townsend avalanche.

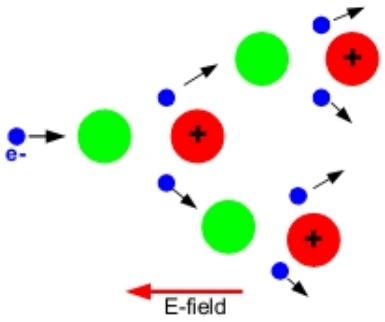

Figure 3.3. Gas multiplication effect: as the voltage increases, free electrons reach higher energies than the ionization energy of the gas and by that, they are able to ionize the neutral particle along their paths through the gas producing secondary electrons [Phy12].

This charge amplification within the detector itself reduces the request of external amplifiers what improves significantly the signal-to-noise ratio.

For proportional counters of normal size, only heavy charged particles or other weakly penetrating radiations can be fully stopped in the gas. Therefore, they can be used for energy measurements of α particles but not for longer-range β particles or other fast electrons. Even though fast electrons do not deposit all of their energy, the gas-multiplication process results in a pulse that is generally large enough to record. Therefore proportional counters can be used in simple counting systems for β particles or γ rays.

3.3. Gas flow detectors

Gas-flow detectors are nuclear detectors in which the fill gas is continuously flowing through the chamber. They are available either as hand-held devices or as bigger units

designed with a much larger detection areas, which are useful in accelerating surveys of open floor areas.

In gas-filled detectors, the gas can be either permanently sealed within the counter or circulated slowly through the chamber volume like in designs of the continuous flow type. This latter one, require gas supply systems and its design permits the flexibility of choosing a different fill gas for the counter when is desired.

Gas-flow detectors are designed to detect α and/or β radiations depending on the radiations of interest and the way the instrument is set up. A variety of different counting gases are used (all heavier than air, as will be explained in the next chapter, in section 4.1) to provide a slow flow of gas into the probe.

4. Experimental set-up

A description of the experimental set-up including the detector and its nuclear electronic associated will be given in this chapter. The details of the detector components and the different electronic devices with the chosen parameters as optimal for α detection are described on the following pages.

4.1. Detector

The function of the detector is to produce a signal for every single particle entering into it. Every detector works by using some interaction of radiation with matter. As it has been already mentioned, the present thesis in focused in a *windowless gas flow proportional counters*. The particular features chosen for its optimal operation on α particles detection such as the geometry of the device, the size and shape of the electrodes and the fill gas are described in the next sections.

As it has been already explained, gas flow proportional counters are a specific type of proportional counter with the characteristic that the gas inside the chamber is not static, flows through the detector with a flux than can be adjusted by adding a flowmeter. In the used set-up, the gas feed to the detector is through a separate gas supply line that consists in two cables, one for the gas input and another one for the output. The gas enters and exits the detector through two holes located at the top of the detector body through these both cables (see Fig. 4.1).

These detectors are generally used to detect α and β radiation, but also detect γ radiation. Nevertheless, the detection efficiency for γ emissions is considerably lower than the relative efficiencies for α and β activities.

There are several types of gas flow proportional counters. The concrete type of windowless gas flow has some particular characteristics. The most important is the fact that the source is introduced directly into the counting volume of the detector. This has the great advantage that there is no entrance window between the radiation source and active volume of the counter which can attenuate soft radiation severely. Because of this, like the sample is inserted into the chamber by sliding a tray, both the amount of air introduced and the loss of radiation on its track to the wire through the gas are minimized. On the other hand, the presence of no window leads to a counting geometry with an effective solid angle very close to 2π, and the detectors have an efficiency close to the maximum.

The particular counter that was used for this work is a reconstruction from a commercial Methane-Gas flow detector from the company *Berthold* [Ber12]. A deeper description of its technical features can be found in Chapter 2 of the *manual of use*.

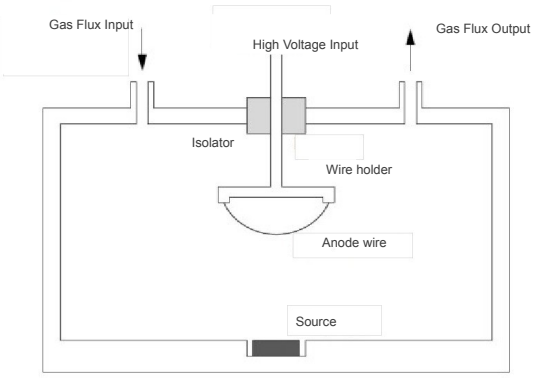

Figure 4.1. Schematic structure of a 2π gas flow proportional counter [Rwth12]. The source is introduced into the chamber by sliding a tray. The wire is placed by fixing a wire holder in the top of the chamber with an adjustable position. In the external upper part of the detector are placed the high voltage input and both the input and output for the gas. A flowmeter of the gas supply controls the gas flux inside the chamber with a adjustable flow rate from 0 to 0.5 in liters per minute (LPM).

4.1.1. Choice of geometry

Typically, all proportional counters are constructed using a wire anode of small diameter placed inside a large cathode that also serves to enclose the gas. Proportional counters are normally build with cylindrical geometry.

In the detector used, the anode is a fine wire positioned in the top of the hemispherical chamber, which works as cathode, into a metal holder (see Fig. 4.2).

Because of several reasons the cylindrical geometry was chosen. Under these geometrical conditions, the electric-field strength is non-uniform and reaches large values in the immediate vicinity of the wire surface. The main purpose of this particular shape is to procure a region of the extremely high field gradient surrounding this fine wire electrode, required for the gas multiplication. By having such a region of high electric field gradient it is possible to achieve a long chain of series of secondary ionizations (*avalanche*) from the primary ionizing event, increasing greatly the gas amplification factor.

In cylindrical geometry, the electric filed value is given by:

$$E(r) = \frac{V}{r \ln(b/a)} \tag{4.1}$$

where r is the distance from the wire, V is the voltage applied between anode and cathode, a is the anode wire radius and b is the cathode inner radius.

For a wire of 15 μm, as was selected as the optimal one for the detector (explanation will be found in Chapter 6), for the detector chamber size and the wire position, electric field values between around $6{\times}10^3$ V/m at the source position, and $150{\times}10^6$ V/m approximately in the vicinities of the wire are produced for a voltage value of 1.2 kV.

In order to achieve an uniform multiplication is achieved for all ions pairs formed by the

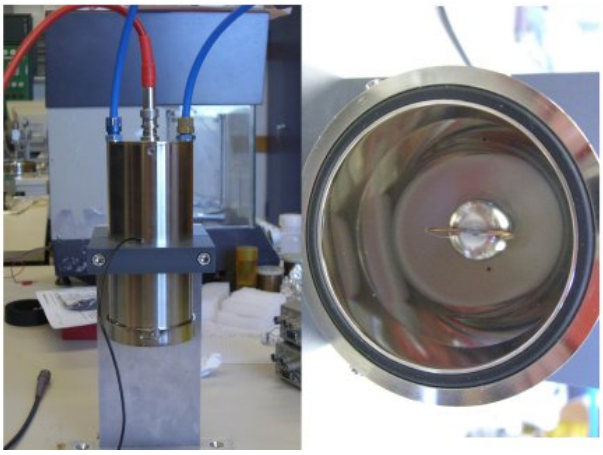

Figure 4.2. Detector available: 2π-windowless gas flow proportional counter in the right-hand side of the picture and the wire holder with a wire that makes the function of anode in the left-hand side. The current wire has flat shape.

original radiation interaction, almost all of the volume of the gas must be located outside of this high-field region. In this manner, the electrons formed at a random position in the gas by the incident radiation, drift toward the wire without creating secondary ionization. Hence, the region of gas multiplication is confined to a very small volume compared to the total volume of the gas. As electrons are drifted closer to the wire, they are subjected to higher values of the electric field, as is shown in Fig. 4.3. At some point, the field become high enough to cause the initiation of the Townsend avalanche that will grow until all the electrons reach the wire surface.

On this way, almost primary ion pairs are formed outside the multiplying region and drifts to it before multiplication takes place, ensuring the same multiplication factor for all original ion pairs.

4.1.2. Wires

As it has been just mentioned in the below section, the anode is a fine wire settled in a holder, as shows Fig. 4.4.

In the initial measurements, the available wires had a hemispherical shape and were made of several materials with different diameters that are summarized in Table 4.1.

Looking for the maximum sensibility, for being the thinnest one and hence, according to Eq. (4.1) produce the largest electric field value, the experiments were started with wire number four, with size 10 micrometers and composition of tungsten (gold-plated).

It must be noted that anode wires are extremely delicate and damage on them can result in total failure of the counter or a failure of a segment of the counter.

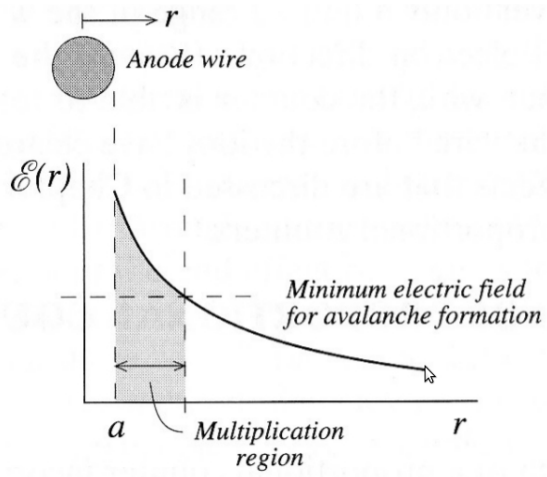

Figure 4.3. The rapid decrease in the electric field strength with the distance from the anode wire surface limits the multiplication region to a small volume [Kno96]. The multiplication begins only when this field becomes larger than its minimum value required to support avalanche formation and extends to the anode surface.

name	material	diameter(μm)
1	copper-nickel	80
2a	copper-nickel	50
2b	tungsten(gold-plated)	50
3	tungsten	15
4	tungsten(gold-plated)	10

Table 4.1. Size and composition of initial available wires. Measurements were started with wire number 4.

4.1.3. Fill gas

Seeing that gas multiplication is critically dependent on the migration of free electrons, the fill gas must not have an appreciable electron attachment coefficient. Because air is not one of these, proportional counters must be designed with provision to maintain the purity of the gas.

In addition, apart from ionization, the collisions of the free electrons with the fill gas may also produce simple excitation of the gas molecule without creation of secondary charge. There is no contribution of these molecules to the avalanche, they decay to their ground state through the emission of visible or ultraviolet photons. However, these photons can create additional ionization elsewhere in the fill gas by interacting with less tightly bound electrons or interacting by the photoelectric effect in the counter wall, producing the loss of proportionality.

The ideal detector must produce a single pulse on entry of a single particle which is counted as a single pulse. Consequently, the extinction of this process is important because

Figure 4.4. Wire initially used with semicircular shape and features: size 10 μm and composition of tungsten (gold-plated).

the tube is unable to detect another particle until the discharge has been stopped. In addition, the tube is damaged by prolonged discharges. Thus, to reduce this effect the named *quench gas* are added. The basic properties of a fill gas can be changed significantly by small concentrations of a second gas whose ionization potential is less than that of the principal component. These quench gases are polyatomic gases that will preferentially absorb the photons. Often, the most used is methane (CH_4).

For this reason, an inert gas (which has the property of being non-reactive and is used to prevent undesirable chemical reactions from taking place because of their properties) is used to fill the tube as counting gas, with a quench gas added to ensure the end of each discharge. The gas mixture employed for the detector in the set-up is known as *P-10*, and consists in a mix of 90% argon like counting gas and 10% methane as quench gas, and it works at atmospheric pressure.

Some examples of the electro affinities of the most common contaminants molecules and ions can be found in Table 4.2.

Molecule	Electron Affinity (eV)	Negative Ion	Electron Affinity (eV)
O_2	0.44	O^-	1.47
C_2	3.54	C^-	1.27
OH	1.83	H^-	0.75

Table 4.2. Some examples of electro affinities of different molecules and ions. The gases used in radiation detectors are generally not free from contaminants. The most problematic of these contaminants are the electronegative molecules, which absorb electrons and form negative ions. The most commonly found contaminants in gaseous detectors are oxygen and water vapours. It is almost impossible to purify a fill gas completely of oxygen [Ahm07].

4.2. Nuclear electronics

In general, the output from the detector is not well shaped to work with it, so is necessary to surround it with a series of electronic modules which allow the interpretation of the data received from the detector. There are two main problems in the detection:

- The amount of charges produced in the detector depends on the number of ionizations that the initial radiation is able to produce within it. In general, this amount is very low, making its measurement really complicated and very sensitive to possible alterations produced by the noise.

- The electronic devices are commonly designed to work with voltage pulses, not charge pulses.

Hence, all radiation detector signals chains start out with linear pulses (which carry information in them shapes and amplitude) and, at some point, a conversion is made to logic pulses (which carry information only with them presences or absences).

Nuclear electronics is a subfield of electronics concerned with the design and use of high-speed electronic systems for nuclear physics and elementary particle physics research for pulse-processing [Wik12a]. Essential elements of such systems include a high voltage power supply, a preamplifier, an amplifier, a discriminator, a counter, a timer, a multichannel analyzer and an oscilloscope (Figures 4.5 and 4.6). The units are manufactured in standard modules called Nuclear Instrumentation Modules (NIM) and must be plugged into a NIM crate to obtain power.

The purpose of this section is to present a general description of the physical appearance and operation of the components of the radiation counting system used in the present thesis. Details about the construction and operation, as well as the particular features of the individual components are given in the following sections.

4.2.1. High voltage power supply: Model 3132 Canberra

All detectors have like common features that the radiation produces a certain amount of charge which is collected by applying a high voltage. They convert a radioactive event in a pulse charge. The electric field applied is obtained by applying a high potential. That is why the electronic chain starts with a high voltage power supply.

The sophistication required of the power supply depends on the detector type. But in general terms, the voltage may be as high as several thousands volts and the current requirements are very small. Furthermore, because of the plateau region characteristic of the tube ensure the relatively independence of the counting rate with the voltage, the stability of the supply can be very poor.

The particular model used in the electronic chain (*Canberra model 3132*, [Can12]) consists on a multi power supply of four cells, each one capable to provide voltage on a range from 0 to 1500 V that can be read on a screen located in the front panel with a precision of 0,1%.

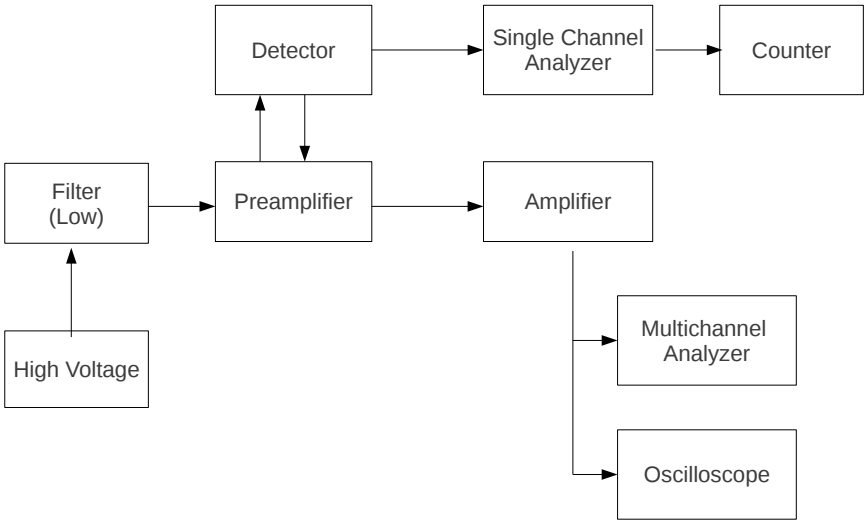

Figure 4.5. Schematic illustration of the full detection system used.

The unit is highly sensitive to fluctuations in the value of the voltage. The stability of the four supplies was checked and the lowest noise-to-signal ratio was founded for cell *C*. Thus, this has been the cell used for the present measurements shown in this work[1].

The high voltage is supplied by an SHV cable which passes the high voltage to the wire. The close of the detector is ensured by the black rubber ring.

4.2.2. Filter: Model A483 Caen

Because of the use of electronic devices, the presence of electronic *noise* is unavoidable. Noise is defined as any undesirable fluctuation of the system that superimpose on the signal. It is principal generated on the first stages of the chain, where the signal is yet small, and undergoes the same amplifications as the signal. It can appear in a broad range of frequencies (See Fig. 4.7). To avoid noise, the use of filters is recommended. In the present set-up, the biggest problems with noise were found for the hight frequency one, so a low-pass filter was introduced in the chain just after the power supply.

The filter *model A483* from *Caen* selected ([Cae12]) is a bidirectional passive high voltage filter with a maximum input voltage of ± 10 kV. The high voltage input and output are provided by SHV connectors. It possesses a ripple rejection of 20 dB, measured with 50 mVpp. The ripple is a small unwanted residual periodic variation of the direct current

[1]The characteristics sheets of this device and all the next that are going to be described in the following sections can be found with more detail in chapter 3 of the *manual of use*.

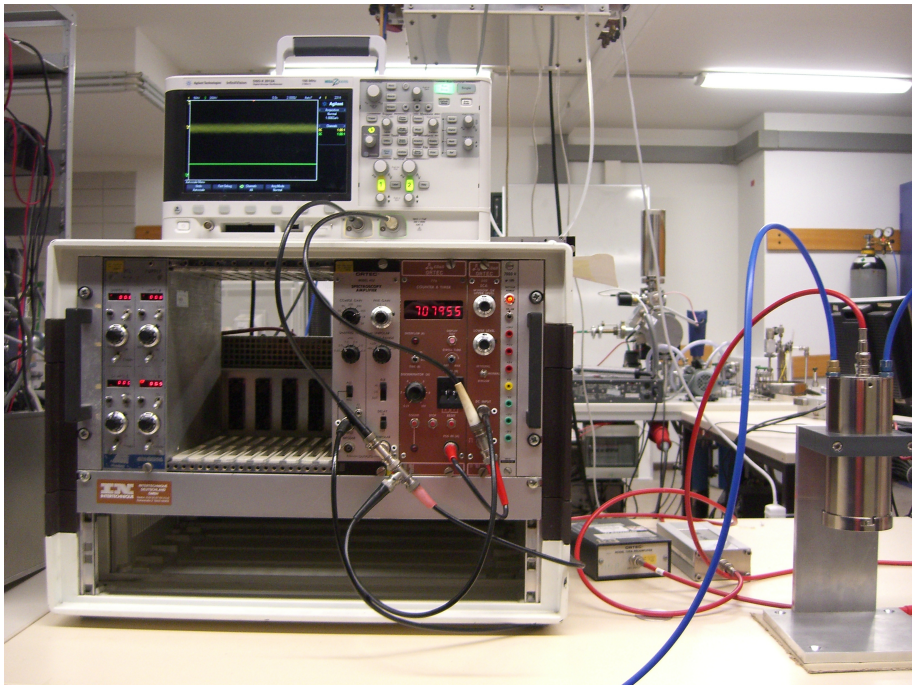

Figure 4.6. Photo of the full detection system used placed in the NIM crate.

(dc) output of a power supply which has been derived from an alternating current (ac) source and is due to incomplete suppression of the alternating waveform within the power supply, as define [Wikb12d]. It does not require any power supply since it is made up of passive components and is designed to be used together with a high voltage power supply when a low ripple is required.

4.2.3. Preamplifier: Model 109A Ortec

As the output of the detector is a charge pulse proportional to the source energy, an instrument to convert it must be included in the chain. This is the preamplifier. It transforms the charge pulse to a voltage one using a variable capacitor ($V = Q/C$).

The output from both the detector and the preamplifier has the shape shown in Figure 4.8.

The height of the output pulse is related to the intensity of the pulse obtained directly from the detector through a fix gain factor. By this, the spectrometric information is conserved in the conversion of the charge pulses to voltage. Nevertheless, the generated pulses are very weak, so the preamplifier must be situated as close as possible to the detector, in order to minimize the appearance of electrical noise. The use of short cables is recommended.

The noise can also be reduce by increasing the resistance value of the preamplifier circuit, but longer time constants leads to very long tails in the output pulses. This fact can produce problems of pile-up.

In summary, the preamplifier is the *entrance door* to the electronic chain, so its good

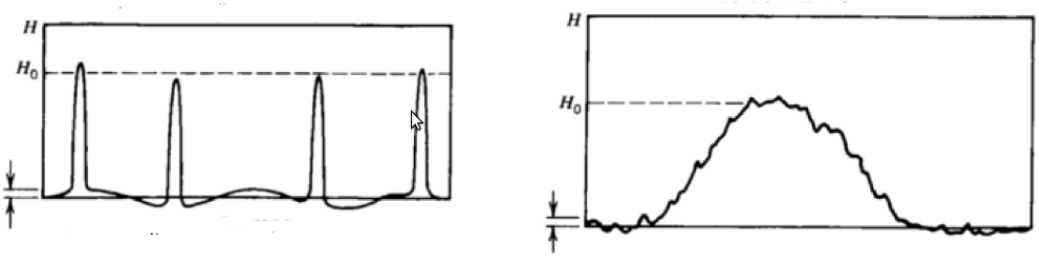

Figure 4.7. Different types of noise: low frequency and hight frequency. Each one affects the signal in single way. The first one can be detected as the appearance of signals each certain time and the second one as perturbations in the signal shape [Kno96].

operation is extremely important.

The preamplifier used in the set-up (*model 109A* from *Ortec*, [Ort12]) was carefully chosen taking into account that it should introduce an electronic noise as low as possible. A model from the company *Ortec* specifically designed for proportional counters was the final selected after testing multiple devices. The main features of this device are its high sensitivity, an accepted voltage until 3000 volts and a protection circuit for the input FET to prevent damage from inadvertently applied overvoltages.

The only parameter adjustable in this device is the horizontal amplification of the signals by a switch that allows to choose between $\times 1$ or $\times 10$. The first one was selected for the measurements.

4.2.4. Amplifier: Model 452 Ortec

The output pulses from the amplifier already are voltage pulses, however, two problems with them are again found:

- The gain factor of the preamp uses to be not really high, hence the voltage pulses have a low height. So, problems in their measure because of electric noise are again important.

- The pulse shape is not the most adequate. Analog-digital standard converters normally work much better with Gaussian shaped pulses. Therefore the pulse must be again processed.

For this reason, besides amplifying the pulse, it have to be correctly shaped. This is the function of the amplifier, which is the most important device in the chain. The amplification is carried out with an adjustable gain factor that must remain fixed for each single experiment. Only by this way, the spectrometric answer is not lost and the height of the output pulse keeps proportional to the energy of the incident radiation.

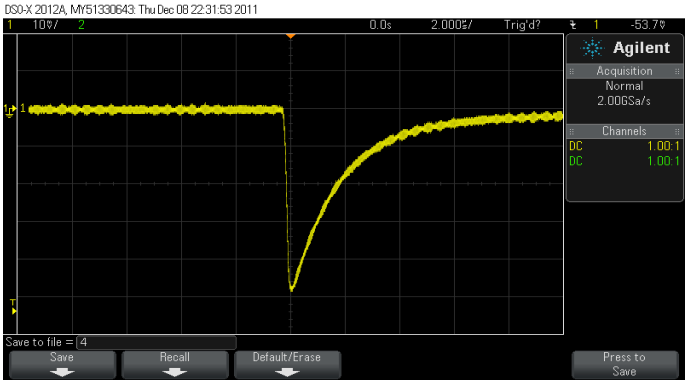

Figure 4.8. Preamplifier output signals. The signals can be visualized using an oscilloscope that allow to measure both amplitude (y-axis) and time (x-axis). The rise time of the output pulse is kept as short as possible ($\sim 10 - 100$ ns), consistent with the charge collection time in the detector itself. The decay time of the pulse is made quite large (typically 50 or 100 μs) in order to get full collection of the charge from the detector, which produce pulses of $\sim$0,01-1 μs.

The decay time of the pulse is much stronger than after the preamp (see Fig. 4.9 for a comparison of them). This is done to prevent pile-up of pulses in high count rate experiments.

In general, the multichannel responsible for analyzing the output pulse is able to discriminate pulses inside a fixed range of heights. Consequently, the main point is to adjust the amplifier gain factor so that the multichannel range corresponds to that under interest of study. Higher values of the gain accords better resolution on energy for the same channel. But in the other hand, a less range of energy can be measured [Kno96]. A brief explanation of how the amplifier input pulses are converted in Gaussian pulses introduce the concept of *shaping time*. A series of differential RC circuits are employed to get the Gaussian shape from a pulse like the preamplifier output one. The *time constant RC*, which is named *shaping time*, can be adjust using a potentiometer which makes the resulting Gaussian more or less broad (see Fig. 4.10).

At higher values of shaping time, broader Gaussian are get and more separated should be the pulses in order to be discriminated and the work for the converter is easier.

However, RC circuits are designed to obtain a Gaussian signal from an step function. If the input signals the amplifier receives have the typical shape of the preamp output signals, the final result is a pulse with a shape similar to a Gaussian but with a *tail* of negative voltage. This fault is known as *pole-zero problem*. A summary of its effect is shown in Figure 4.11. Can be solved by adding a potentiometer adjustable in parallel with the RC circuit that allows to recover the correct Gaussian shape when the value is well chosen. This potentiometer can be controller with a adjustable screw located in the front panel of the device.

Finally, another fact to take into account in the use of amplifiers is the *baseline restoration*. To ensure good energy resolution and peak position stability at high counting rates, the higher-performance spectroscopy amplifiers are entirely dc-coupled. As a consequence,

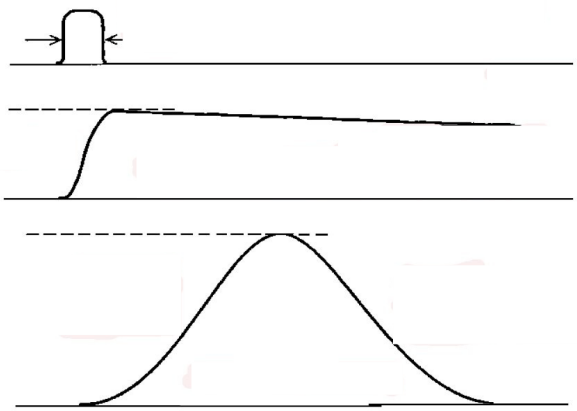

Figure 4.9. Comparison of typical pulses at sequential points along the signal processing chain. The first plot corresponds to the current pulse from the detector. Typically has a duration between 0.1 and 1 microsecond. The second one is the preamplifier output, with a tail of approximately 50 microsecond and a initial amplitude of a few microvolts. And the last one is the liner amplifier shaped output which presents a few microseconds width and a maximum height of a few millivolts [Kno96].

the dc offsets of the earliest stages of the amplifier are magnified by the amplifier gain to cause a large and unstable dc offset at the amplifier output. This phenomena can lead a shift in the baseline. Therefore, baseline restoration must be active. That control consists on a circuit which has the purpose to return to true zero the baseline between pulses as short in time as possible.

Therefore, this device is the most sophisticated of the whole chain and has a lot of parameters that can influence the signals processing. A description of them and the optimal values of those parameters found for the experiments carried out for the spectroscopy amplifier *Model 452* from *Ortec* company is presented here:

Coarse gain (A): The gain is adjustable over a wide range through a combination of this parameter and the fine control. The election is dependent on the kind of radiation that has to be measured, being the optimal value 500 for α particles .

An agreement between the signal-to-noise ratio, the pulse pile-up rejection and the amplitude of the signal not over the amplifier saturation limit must be found. If the product of input amplitude and gain goes beyond the maximum designed output amplitude, the amplifier will saturate and output pulse will appear deformed with a flat top at the amplitude at which saturation takes place (see Fig. 4.12).

In addition, the value of the gain determines the position of the peaks in the multichannel analyzer. Seeing that the range of value covered for the one used is 10 V (which value is translated by the analyzer into a certain channel), amplifier output signals can not have amplitudes that exceed the maximum channel.

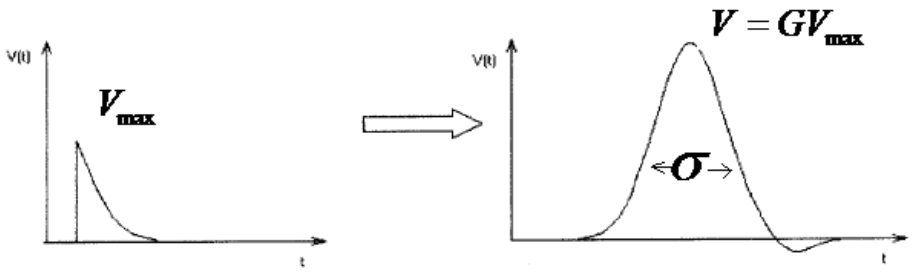

Figure 4.10. Conversion of the signals carried out by the amplifier. G and σ factors are adjustable (with G proportional to the gain and σ proportional to the shaping time). The amplification gain is higher than 1000, only on this way output signals between 1 and 10 V are generated and the analog-to-digital converter is able to recognize them [US11].

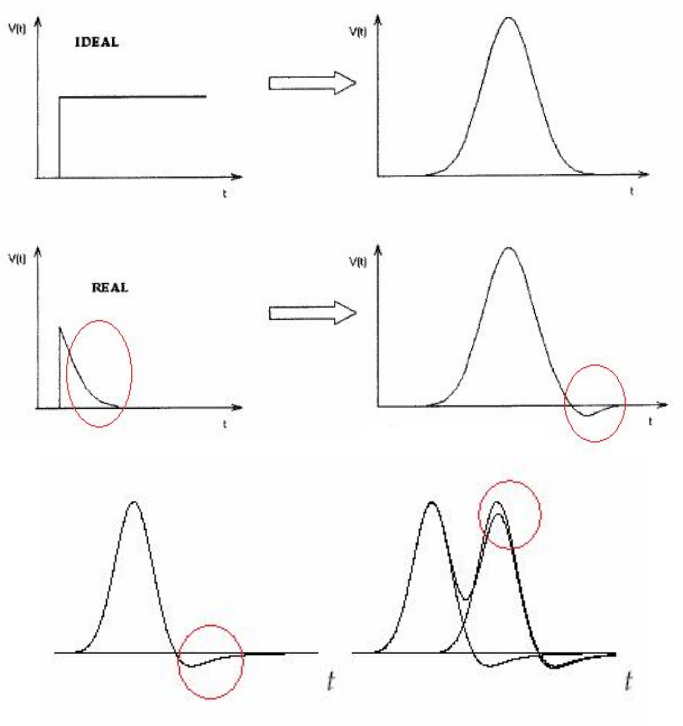

Figure 4.11. Summary of pole-zero problem effect: the amplifier output signal shows a negative tail when the input is not the expected step function. If the potentiometer is not well adjust, the pole-zero problem distort the height of the next Gaussian peak. If two very closed pulses pile-up, the height of the second pulse is lower than the expected, so the energy lecture of this pulse (shown in the left-hand side) is not the correct one [US11].

The procedure carried out for the choice of such concrete values and all next as optimal for our experiments will be explained with more detail in chapter 6 through all the systematic measurements carried out.

Figure 4.12. Examples of a bad gain amplification factor selection. The image on the left-hand side corresponds to a too low value and the signals are not recognize by the discriminator and no signals are produced in its output (channel 2, green signal). Opposite, the figure on the right-hand side, corresponds to a too high value and saturation effect in observed. The discriminator either is able to process the signal coming out form the amplifier.

Fine gain (A_f): Between the available values, 1.0 was the quantity decided for this gain.

Shaping time: There are a number of considerations in the choice of the optimal shaping time. It must be long enough to collect the charge from the detector, but short enough to achieve the high counting rates that are require. The main point is to choose a shaping time that filters as much of the electronic noise as possible.

In order to minimize problems with the pile-up and the noise, values somewhat larger than the lowest one are recommended [Kno96]. Thus, 0.5 μs was chosen as the optimal one (see Fig. 4.13).

Output Range: The amplitude range of the amplifier output signals can be picked. Whereas the multichannel analyzer employed has a range of 10 V corresponding with its 8191 channels, the output range must be the same.

Base Line Restorer (BLR): With the correct value chosen, besides to restore the zero position to its real value, the noise can be reduced as well. The *hight* mode was selected for being the one indicated for shift the zero line from a higher position than real zero level (see Fig. 4.14).

Delay: With the delay on, pulse pile-up can be prevented.

Input and Output: There is only one possible input for the amplifier and two outputs available: the unipolar one and the bipolar one. The first one must be the one chosen for signals with a single polarity (chosen as positive in the internal circuit on this case).

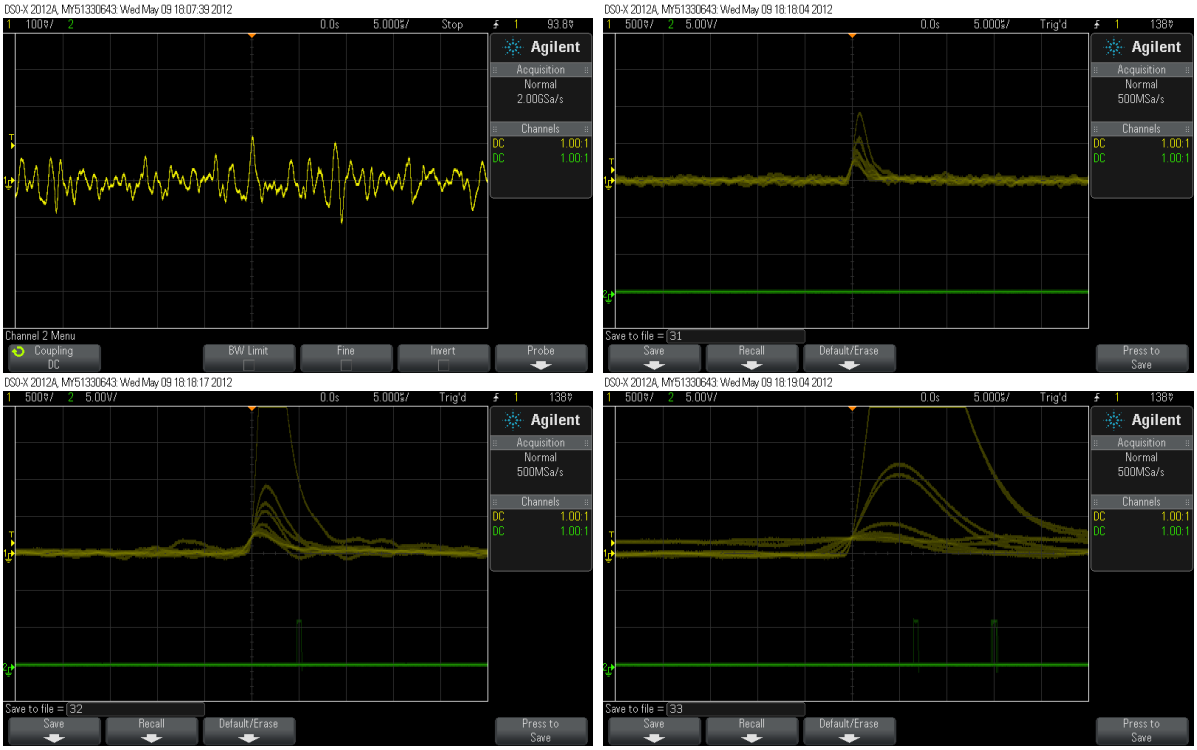

Figure 4.13. Signals measured for different values of shaping time of 0.25, 0.5, 1.0 and 3.0 μs are shown this in order (starting from the upper left-hand part to the right one and then to the lower part of the plot). The broadening of the signals can be perfectly observed with the shaping time increasing. At the smallest value available signals cannot be distinguished and at the highest one are too broad and pile-up. The better results are get in the second image, corresponding to a shaping time of 0.5 μs.

4.2.5. Single channel analyzer: Model 550 Ortec

It is essential to distinguish signal from noise, otherwise no reasonable counting is possible. In addition, the shape linear pulses must be converted into logic pulses in order to be counted. This roll is carried out by the Single Channel Analyzer (SCA).

This device produces a logic rectangle output pulse only if the Gaussian input pulse amplitude exceeds a discrimination level set. If the input pulse amplitude is below the chosen discrimination level, no output pulse is generated (see Fig. 4.15).

The signals that are coming out of the main amplifier are selected by the SCA. For this purpose, the SCA possesses two independent and adjustable controls: lower-level (LLD) and upper-level (ULD). The lower level serves to separate the decay signals from noise. A threshold voltage is set so that only signals that exceed it can pass. The upper level is used to exclude signals of great intensity. If the signals exceed the threshold given by the upper level, then the signal is not routed. On this way, a logic output signal is only produced if the input linear pulse amplitude lies between the two levels.

To use the best settings this device can be used in the SCA three operating modes: normal, window and integral. By designed, in the integral mode of operation, the device

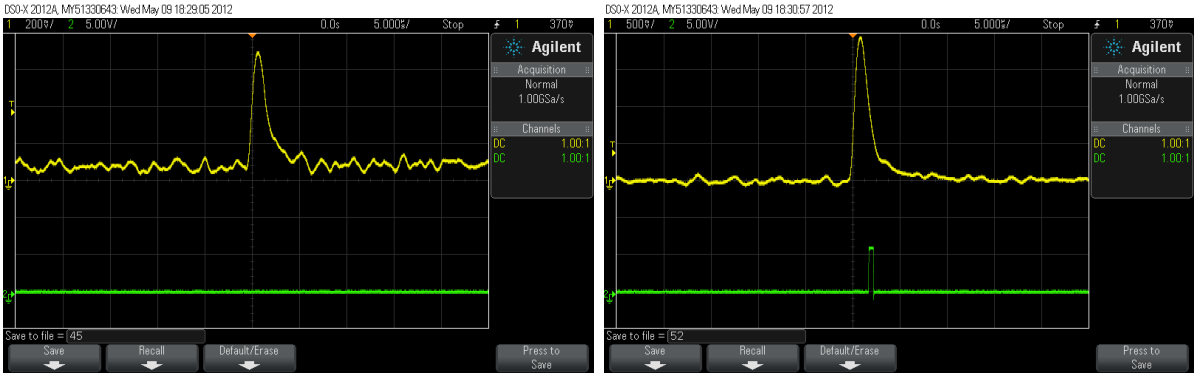

Figure 4.14. Example of the improvement of the noise as well as the change of the baseline position with the correct choice of the Base Line Restorer value. The image on the left-hand side shows the signals for the *low* mode and the other one for the *high* mode. On this last signals are much cleaner.

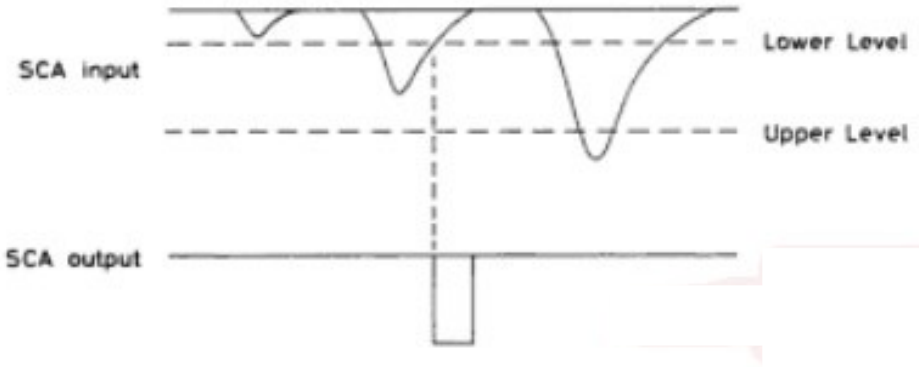

Figure 4.15. Basic operation of a single channel analyzer: only signals whose amplitudes fall within the window defined by the upper and lower level threshold trigger a signal [Leo99].

can function as an integral discriminator. In the normal mode of operation, the upper-level and lower-level thresholds are independently adjustable. In the window mode, the upper-level threshold control is used to establish a voltage level that is added to the lower-level threshold voltage to yield the upper-level discriminator threshold level (more details in chapter 3 of the *manual of use*).

Of the three of them, the normal mode must be the one used in order to just select a band of amplitude in which the input amplitude must fall in in order to produce an output pulse.

On the other hand, looking for the the maximum signal range, the lower level was set just above the system noise so that the maximum sensitivity for counting detector pulses of all sizes is obtained. This leads to a value of 0.20 V. On the other hand, the upper level was just fixed as the maximum value of the output signals, that is, 10 V.

4.2.6. Counter & Timer and oscilloscope

As the final step in a counting system, the logic pulses must be accumulated and their number recorded over a fixed period of time. The device use for this is called *counter* and is a simple digital register that increments by one the number of counts each time a logic pulse reaches its input. In a lot of cases, the counter unit includes as well the *timer*. This device has the function to start and stop the accumulation period . It must be very precise in the determination of interval of time.

The available device, an instrument *model 776* from *Ortec*, work as both: counter an timer. The counts can be visualized on a screen located in the front panel. This device includes its own discriminator, however, its use in not necessary due to the presence of the single channel analyzer. It just must be on its lowest position.

On the other hand, in order to be able to visualize the output signals another device is required. This is the oscilloscope. It is an instrument that permits the study of rapidly changing phenomena, such as a sinusoidal voltage or the pulse of a counter. The phenomenon is observed on a fluorescent screen. The horizontal axis of he screen measures time, while the vertical one gives the voltage. *Model DSO-X 2012A* from the company *Agilent Technologies* ([Agi12]) was the instrument used in the lab.

The model available in the lab has as main features a bandwidth of 100 MHz and waveform capture rate of 50,000 signals per second.

4.2.7. Multichannel analyzer: Model 926 Ortec

The amplifier output goes to the multichannel analyzer. On this way, the complete output signal (i.e. without any low or up limit imposed by the discriminator) reaches the device.

This versatile instrument is an analogical-digital converter (ADC) and gives a plot of the pulse height spectrum of all of the pulses which input on it. It takes each pulse, converts its height into a digital number and increments the bin count that number falls within. The width of the peaks is a measure of the energy resolution of the system.

In the case of the MCA used for the present work (*Model 926* from *Ortec*), the voltage span of 0 to 10 V is divided into 8191 bins of equal width. What is displayed is a plot of the number of pulses versus pulse height.

Seeing that the answer of the chain is linear, the channel where the count appear is proportional to the energy of the incident pulse. This device use to be integrated into a PC acquisition system which allows the control and the analysis of the data.

The presence of this device introduce the concept of *dead time* due to the problem of the pile-up of the signals. The dead time is defined as the minimum amount of time that must separate two events in order that they be recorded as two separates pulses [Kno96]. In some cases the limiting time is may be set by processes in the detector itself, and in other cases the limit may arise in the associated electronics. When a count is received, the detector is disabled for another count processing during a certain time. For proportional counters, it will take some time for the avalanche process to finish and be counted before counting the next event. This amount of time is described as dead time and usually is

about 0.5 microsecond [Wat12]. The counts that reach the detector during this time are ignored leading to a lost of information. On the other hand, in counting systems, the single channel analyzer introduce a dead time as well related to the width of the linear pulse presented into its input. It use to be around a microsecond [Kno96]. But the main dead time is introduced by the MCA because of the time required for the processing time by the ADC and the memory storage time. Consequently, the known as *dead time* is the total time lost due to all these contributions. In the ideal case, must be zero, otherwise means the ADC is not able to convert all the signals.

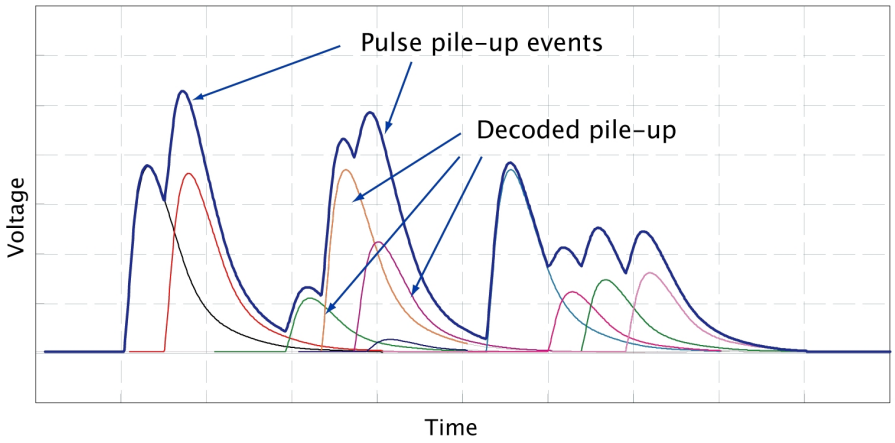

Figure 4.16. Description of the problem of the pile-up. The height of the second peak is higher than it should be due to it is a sum of both contributions, composed of its own hight and the first peak tail. It can be due to a amplifier gain value too high. A lower shaping time value can reduce it [Web12c].

The amplifier output goes to this device input which distribute the different received amplitudes on its 10 V representing by 8191 channels.

The result can be visualized as an energy spectrum on a PC thanks to the program *Maestro* which allows taking data of the total number of counts under the peaks as well as the measurement time (real and live times).

The device possesses its own lower level discriminator as adjustable parameter as well as another control what allows to select the zero position by choosing the voltage value at which the x-axis starts.

If some undesirable signals are detected at certain low voltage values, using the *zero control* is possible to make them disappear of the screen just moving the zero position to a voltage slightly above that value. For our set-up, the zero level was established at 0.24 V, close to the noise value measured with the oscilloscope. The difference may be due to some internal noise included by the own multichannel analyzer.

A summary of all the parameters chosen as optimal for the devices of the electrical chain in the present work for α detection can be found in Appendix A .

5. Previous results

A previous work with the detector was carried out in 2010 by Christian Buchholz on a Bachelor Thesis. A previous description of it and the most relevant results from which the present thesis started are briefly summarized in this chapter.

5.1. Initial set-up

There are some differences between the general set-up used by Christian in his experiments and the one developed for this thesis.

- First of all, as counter wire, the one made of a copper and nickel alloy fitted with a diameter of 80 μm was the one used. This is wire number one of the table 4.1. As was mentioned in section 4.1, we used wire number four, with 10 μm and made of tungsten (gold-plated).

- The high voltage power supply, the preamplifier and the amplifier inserted in the old chain were changed for the new models detailed described in the previous chapter in order to improve the signal quality and, specially, the signal-to-noise ratio. Therefore only the single channel analyzer and the counter remained as the same.

  Moreover, the low-pass frequency filter already mentioned and the multichannel analyzer were included as new units. The first one looking for a noise reduction and the second for investigating the energy spectra of the samples.

5.2. Main considerations

The key findings from the previous Bachelor Thesis ([Buc10]) considered in order to continue this study were:

1. A dependence of the starting voltage value of the plateau region with the gas flow rate could not be determined because of no relevant differences between the use of the different flux values were observed as is shown in Fig. 5.1. So was considered that the counting rate is independent of the gas flux value. It may only be said that a gas flow rate for the measurements is needed.

2. The plateau region for α sources shifts to higher or lower voltages as effect of the main amplifier gain changes.

3. A geometric effect due to the position where the sample is placed in the cover of the detector was discovered.

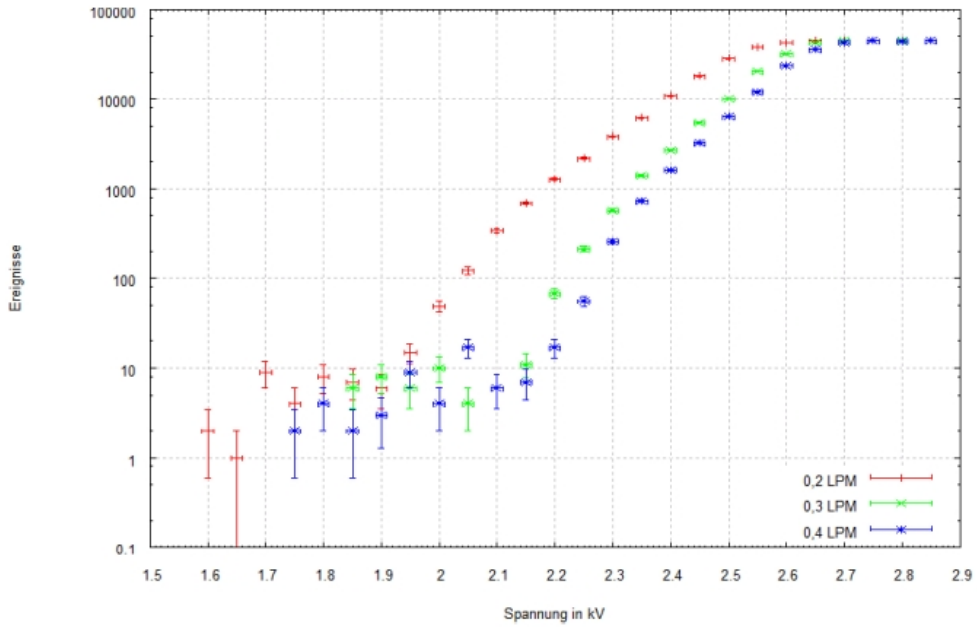

Figure 5.1. Measurement carried out to check the dependence of the counting rate with the gas flow. Such a dependence was non observed as shows Figure 4.13 of the thesis of Ch.Buchholz work, [Buc10].

4. The wall of the chamber must be conductive and grounded, so ionized gas atoms with missing electrons can be absorbed. Otherwise, a positive space charge cloud would form, that could prevent the ionization of other atoms.

5. A double plateau region was observed for the α sample at a voltage value of 1.5 kV in measurements carried out for a comparison between the counting rates for the different wires. In addition can be seen clearly how the plateaus regions shift their beginning value to smaller voltages for thinner values of the wire diameter (see Fig. 5.2).

6. The detection of β plateau regions is not possible (Fig. 5.3). Thus, the detector is unsuitable for the determination of the activity of β radiation samples.

7. The activity measured for the ^{241}Am α source ($A = 3.665$ kBq) used was $A_\alpha = (1.75 \pm 0.01)$ kBq. Consequently, the efficiency of the detector obtained for α-radiation was
$$\varepsilon = \frac{A_\alpha}{A_{source}} = (47.75 \pm 0.26)\% \tag{5.1}$$

8. The activity measured for a beta source ($A = 1.065$ kBq) used was $A_\beta = (752 \pm 4)$ Bq. Thus, the efficiency of the detector obtained for β-radiation was
$$\varepsilon = \frac{A_\beta}{A_{source}} = (70.61 \pm 0.33)\% \tag{5.2}$$

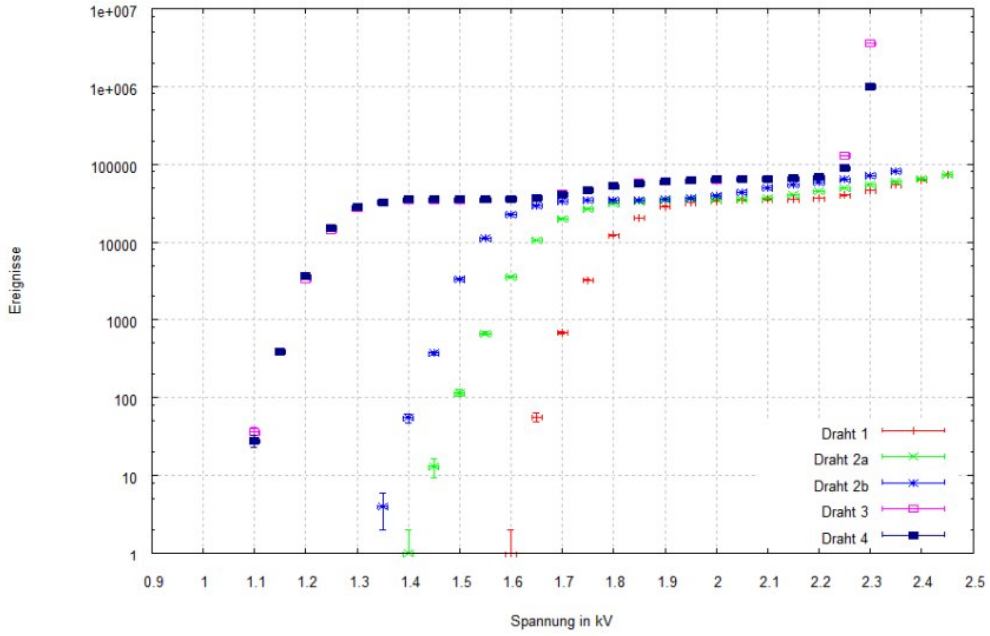

Figure 5.2. Study of the counting rates for the different wires. A double plateau was detected for wire number three and four according to Figure 4.13 from Cristian's work [Buc10].

9. The problem with the measurement of both α and β sources is considered of electronic nature.

5.3. Required improvements

In sight that the device was not working as well as was expected and some were a lot of opening questions due to some measurements were not possible (like β detection) or still confusing (like α detection), a Master Thesis was proposed. Its main aim was fixing the set-up completely in order to can be use for the practical exercises by the students in the University in a regular way for both counting and spectrometric analysis.

The presence of a double plateau for the α source, as well as the low value of the efficiency for its detection, and the impossibility of the detect the β plateau were the main problems considered to require improvements. So the aim of the present work was to work out them.

The following chapters present all the ideas that were tried and all the measurements that were realized as well as all the innovations introduced with the purpose of achieve the improvement of the detector focusing in α decay measurements, and the results attained thanks to all of them.

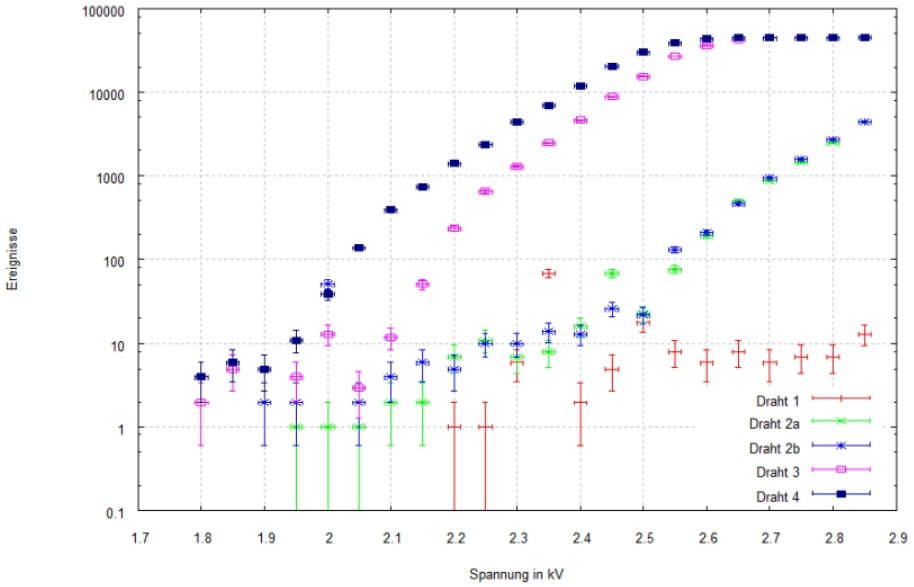

Figure 5.3. β source measurements with the detector and the available different wires. No well defined β plateaus are detected [Buc10], Fig.4.12.

6. Systematic studies and optimization of the experimental set-up

This is the main chapter of the thesis. All the optimization measurements performed with the detector set-up for α decay will be presented. The main points of interest during these tests were firstly to study the problem of the double plateau for the ^{241}Am α source. Because the α decay is the simplest one to detect due to its strong interaction with matter in which the α particles lose their whole energy and for the fact that this radiation is monoenergetic, it was considered this the most reasonable starting point. Once α detection was solved, it was expected to be possible to measure β particles easily. It was considered since the beginning that both problems, the double α plateau and the impossibility of detect β radiation correctly were related.

Nevertheless, a lot of unexpected problems were found in the measurements performed. But it was precisely the study of all them which allowed the optimization of the detector. The outcome of all the measurements and the ideas carried out to get these improvements are described in the followings sections.

6.1. Study of the output signals

To have a first contact with the detector and the whole assembly, a study of the output signals from each device of the electronic chain was carried out. It must be noted in that point that all the studies developed were carried out with another high voltage power supply. This one has the same features as the one described in section 4.2 with the single difference of having a broader voltage range, from 0 V to 3000 V. Both studies were made with the purpose to achieve the good working of the setup and all the systematic measurements done looking for the optimal values of the parameters of the electronic devices that influence in the measurements It was decided to make this study with such a device because, due to the unknown operation of the detector, a wider range of working voltage provides more possibilities for a deeper study. Once the optimal configuration was found the power supply was replaced.

The double plateau was of course easily observed. Nonetheless, a much more serious problem was found out. The expected output signals from a monoenergetic source as is the ^{241}Am sample used, output signals of fixed amplitude, were not observed. Signals of several sizes were visualized in the oscilloscope for both cases, preamplifier and amplifier output pulses, as can be seen in Figures 6.1 and 6.2. As was discussed in section 4.2, the amplifier gives an unipolar output, nearly with Gaussian shape, while the discriminator gives a rectangular output signal. Nevertheless, for the signals observed in both cases,

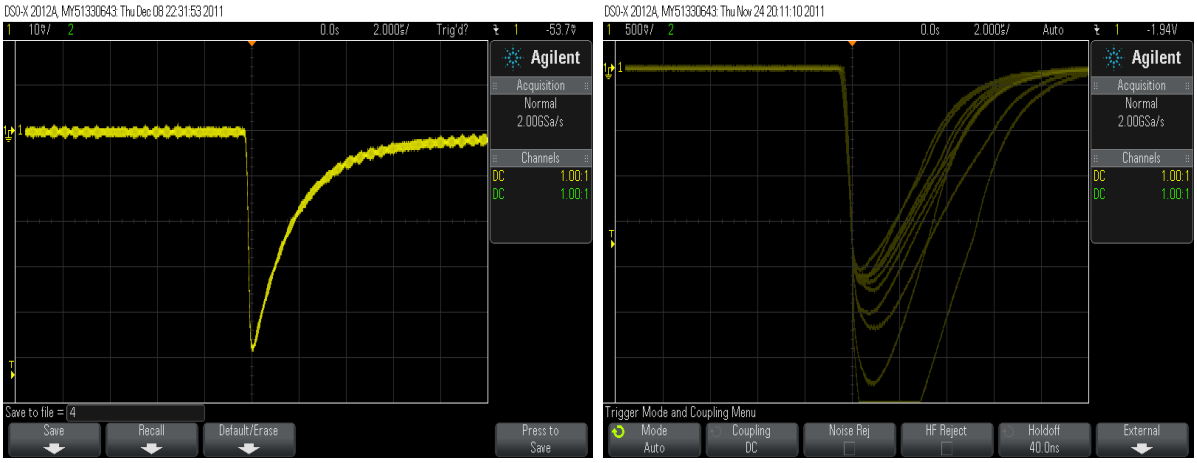

Figure 6.1. Output signals from the preamplifier expected for a monoenergetic source in the left-hand side of the figure and signals visualized for the ^{241}Am source on the oscilloscope with the available preamplifier on the right-hand side. Pulses of several amplitudes are observed for the monoenergetic α source.

the amplitude was not fixed. A broad range was observed what indicated that radiation of different energy values was detected.

However, it must be pointed out that in these initial measurements the electric chain used was the old one (already explained in Chapter 5) and the electronic noise introduce by this assembly was really high. Consequently, very high voltage values were required to be able to visualize any signal, even with the high energy ^{241}Am source, which increased the noise more, affecting the output answer giving by the chain.

The most logic explanation for the strange pulses measured was that the combination of such high voltage and the fill gas produced discharges through some mechanism still unknown. Actually, for the hemispherical shape of the wire used, different amplitudes can be explained because this shape makes the detector non-isotropic. Depending on the part of the electrode the particles hit, they will produce a different pulse because the value of the electric field is not the same. So several amplitude values could be expected for such wire. But in addition, perhaps due to the small thickness of the diameter of the wire it was very sensitive, actually too sensitive, and the high voltage value required for visualize any signal provokes discharges of random energies between the wire and the chamber walls.

However, in spite of this idea, several initial checkings were firstly try in order to explain these output pulses of diverse amplitudes:

- As starting point, was considered that maybe the detector was not well cleaned. In that case, some contaminants could be inside the chamber and produce signals through their interactions with the α particles. Hence, the detector was perfectly cleaned with isopropanol observing no new results after that.

- Maybe the cables used to connect the high voltage power supply and the detector were non adequate (could be the currently used was not high voltage cable). So a

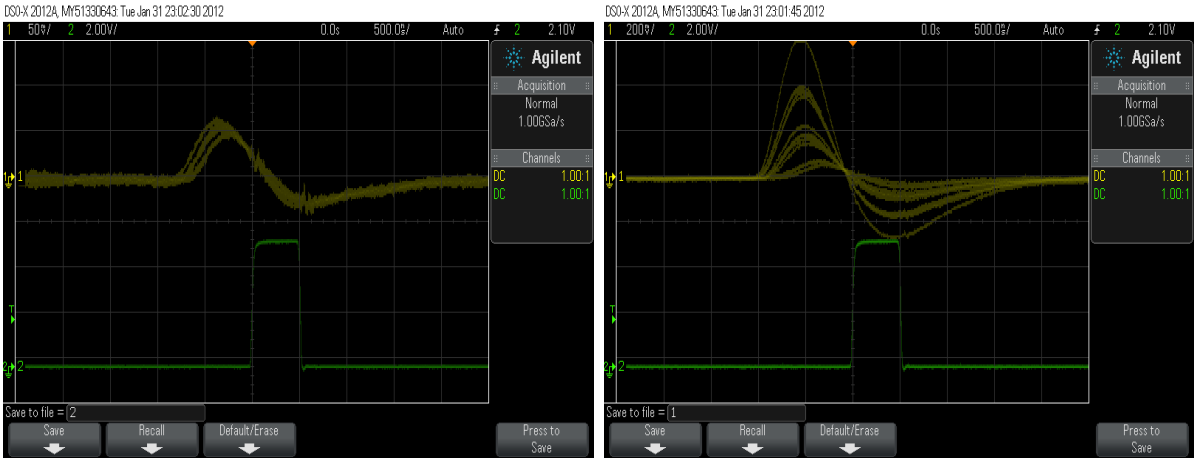

Figure 6.2. Signals expected at the output of both amplifier and discriminator respectively in the left-hand side of the picture. The amplifier gives output signals with nearly Gaussian shape, while the discriminator produces rectangular signals. In the right-hand side, amplifier output signals in CH 1 and discriminator's in CH 2 for the ^{241}Am source measured. Several amplitude values are observed.

new one was built replacing the old one. But again no differences were observed.

- The good condition of the insulating material was checked as well. Sometimes a damage in it can occur caused by with some substances used for cleaning. But no imperfections were found.

- Finally, problems with the electronic devices, like bad operation or bad configuration of their parameters were studied. Only big problems with electronic noise were discovered. Thus, its deep analysis is described in the following section.

6.1.1. Disturbance of the output signals by background noise

By definition, noise is an undesired fluctuation that appears superimposed on a signal source. The most important sources of noise occur near the beginning of the signal chain where the signal level is at a minimum, as was explained in more details in section 4.2 in the part corresponding to filters.

The signals detected looked quite distorted by the presence of this noise. As output signals with a broad range of amplitudes were produced, the signals which the lowest amplitude values could not being distinguished from the big noise leading to the discriminator was unable to process them and consequently, were not counted, as shows Figure 6.3. The working hypothesis was that the presence of such a big noise required the use of very high voltage values and amplification gain in order to be able to visualize the real signals over the noise, which in turn, increased the noise. Under this supposition, the double plateau may be a consequence of these discharges observed which are consequence of this huge noise, being the *real* or the correct plateau only one of them. This is, α particles must produce a plateau region, the *real* plateau, and discharges with similar

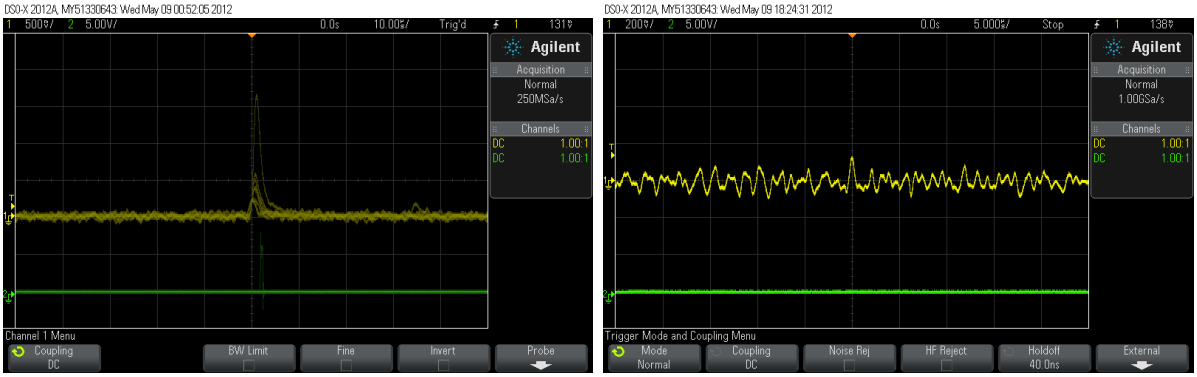

Figure 6.3. Noise visualized by the oscilloscope for measurements without source within the chamber. The plot in the left-hand side shows the output signals together with the noise. Sometimes, the signals with the lowest amplitudes were confused with noise and consequently, were not count by the discriminator as shows the plot on the right-hand side. The maximum amplitude observed for this noise was around 140 mV.

strength generated signals of similar amplitudes that were counted as pulses of the same energy and then produced a flat region interpreted as a plateau. On the other hand, β signals must be always there, but it was not possible to detect them also because of the big noise. Thus, a reduction of the electronic noise as much as possible was fundamental. It was expected that once got this, a lower high voltage operation value would be required for the detection and discharges would not be observed. Then, with the selection of a correct amplification factor, the output signals must be the expected ones.

Consequently, as next step, some modifications in the electronic chain were introduced in order to reduce that disturbing noise. They were already mentioned in Chapter 5: the preamplifier was replaced for another one specific for proportional counters and a low-pass filter was included just behind the detector. The low-pass filtering eliminates the contribution of high frequency noise of the output, which distort the signals the most, but will not affect the information carrying components of the signal.

Some advances were reached with these changes. An improvement in the noise was got and the discharges were reduced, they appeared with lower frequency. Nevertheless, they did not disappear. So a deeper study of them was necessary.

6.1.2. Presence of discharges

It must be noted that exist another sources of noise or background in spite of consideration the noise detected as electrical noise. The most significant is that the materials usually employed to build the detectors sometimes contain impurities. As most common, potassium, uranium and thorium can be found. These all are radioactive elements and therefore, can produce some extra radiation and a rather high background level.

The presence of discharges even with decrease of the noise-to-signal ratio gave the idea that signals were produced by *extra* radiation.

The behaviour of the discharges over time was considered relevant in order to be able

to find out their nature. Consequently, a study of them were carried out. The counting rate of the signals was measured during several hours. The data obtained are depicted in Fig. 6.4.

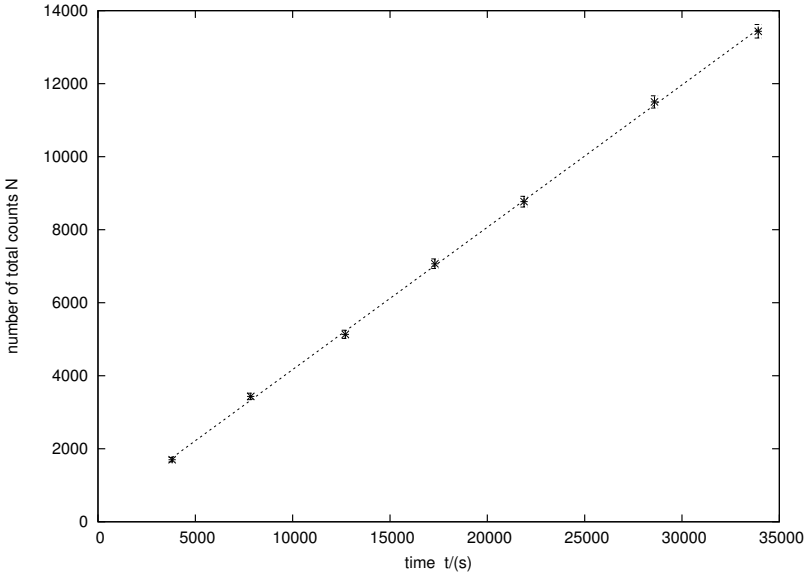

Figure 6.4. Number of counts produced by the discharges as a function of time. The line represents the least squares fit. A linear behaviour is observed: a counting rate of around 3 counts per second was detected. That means it could not be cosmic radiation.

Thus, according to the results lead from Fig. 6.4, can be concluded that the discharges are constant in time. That fact made consider the possibility of this radiation being *cosmic radiation*. As is well known, cosmic radiation bombards continuously the earth's atmosphere that makes all radiation detectors record some background signal. Cosmic rays are extremely energetic particles, primarily protons, which originate in the sun and other stars. They interact with the upper atmosphere of the earth and produce showers of lower energy particles. Many of these lower energy particles are absorbed by the earth's atmosphere. At sea level, cosmic radiation is composed mainly of muons, with some γrays, neutrons and electrons [Pri12].

So as to confirm this supposition it is necessary to know that every second the earth is exposed to 200 muons per square meter. The gas flow chamber of the detector has a diameter of 6 cm so an area of $A = \pi r^2 \backsimeq 28 \times 10^{-4}\,\mathrm{m}^2$. Hence, a counting rate of around 0.6 muons per second is expected to reach the detector. Nevertheless, around three discharges per second are detected with the set-up, so it could not be cosmical radiation. As conclusion, it only can be affirmed that the discharges must be *real* discharges.

The influence of other parameters was also checked in order to try to explain the presence of such discharges:

- Measurements without gas flow were done. No signals were observed, as was expected.

- A study of the signals produced with another α source of less energy than the ^{241}Am one and with both α and β emitters was done. However, the effect appeared independent of the source used: there was the presence of discharges again. Therefore, discharges are not due to the americium source for being too much energetic.
- A series of measurements only with holder (i.e. with no wire inside the chamber, so no anode) placed at different distances from the wall were carried out. The possibility of being the wire too close to the walls of the chamber and produce discharges with them wanted to be excluded with this analysis. Sorrowfully, no differences neither in the discharges, nor in signals were observed.

Another idea about the nature of these discharges was required. Looking for that, a study of the discharges on different measuring conditions were carried out on detail. The most significant results are summarized in Table 6.1. The analysis consisted on the observation of the differences between the discharges amplitude, frequency and voltage at which start for the α-americium source and the β-strontium source. The measurements made with no wire inside the detector (i.e. with only the metal holder placed on the top of the chamber) and two wires of different thickness, one of 50 μm and the other one of 10 μm (wire number 2b and 4 from Table. 4.1). The other three available were visibly broken and unusable.

	holder	wire (50 μm)
no source	- no signals	- no discharges - no signal
alpha source	- discharges start at HV= 2,7 kV - discharges and signals	- at HV= 2.0 kV discharges and signal - huge discharges at HV= 2.4 kV
beta source	- no signals	- discharges at HV= 2.7 kV - difficult to discern discharges or signals

	Wire (10 μm)
no source	- discharges at HV= 1.4 kV - big and very frequent
alpha source	- discharges at HV= 1.3 kV, but small - really big discharges start at HV= 1.5 kV - discharges at HV= 1.8 kV start signal
beta source	- signal at HV= 1.9 kV - discharges at HV= 2.2 kV

Table 6.1. Study of the presence of discharges under different measuring conditions. The voltage value at which they appear in every case is specified.

The main conclusions reached were:

1. For the α-source discharges were produced even without wire inside the chamber.

2. With the thickest wire discharges were always observed for the α-source.

3. With the thinnest wire the discharges appeared even without source. So maybe this size of wire was too small cause made the electrode too sensitive.

4. Discharges were directly related to presence of the source because they did not start at the same potential only with the wire without source and with it. The presence of the source changed the high voltage value required to start them.

On the sight of these results, the possibility of a damaged on the electrodes was strongly considered. The age of the wires and the treatment given in the past to them was completely unknown. In addition, as must be remembered, wires electrodes are extremely delicate and for the present experiments were removed and replaced several time, so a damage to them cannot be discarded.

However, to expedite the set up of the detector, the further experiments were still carried out with the normally used wire (this is wire number 4) and the next big problem, the double plateau, was studied hoping to find a correlation between it and the discharges.

6.2. Study of the ionization plateau region

In order to determine the proper operating voltage of the instrument, it needs to be characterized for its plateau curve. This is the study of the *counting rate*, i.e. the number of ions pairs collected, depending on the applied voltage.

For voltages applied too small, the voltage did not exceed *discrimination threshold* H_d and no counts are observed. When the voltage exceeds it, in the ideal case, all the pulses are collected and it is expected that all of them are generated equal.

The *plateau region* is a domain in which a slight variation in the counting rate is found with the variation of the high voltage value. It is generated by a series of source counts while increasing (stepping) the high voltage applied to the detector after each count. In the ideal case, it must be flat but in reality, it shows some finite slope as illustrates Figure 6.5. When the voltage applied exceeds such discriminator threshold, the pulses start to be registered. When all of them are detected, they lead to a flat region in the counting rate that is the one known as plateau region. In the ideal case, all the counts have the same amplitude as well a Gaussian shape, however, in the real case a low-amplitude tail appears producing a finite slope in the counting rate.

The length of the plateau is dependent on the instrument and the counting geometry.

6.2.1. Alpha counting

As the voltage across the cell electrodes is increased from zero volts, the first particles that create enough ion pairs to be detected will be α particles. When the gas proportional counter is set up, one of the first functions is to find the voltage region where the counting of a sample will yield a constant count rate for a pure α particle source. Must be noted that in this region, β particles do not create enough ion pairs to produce a measurable signal. The β particles ionize much fewer atoms per linear path length than α particles

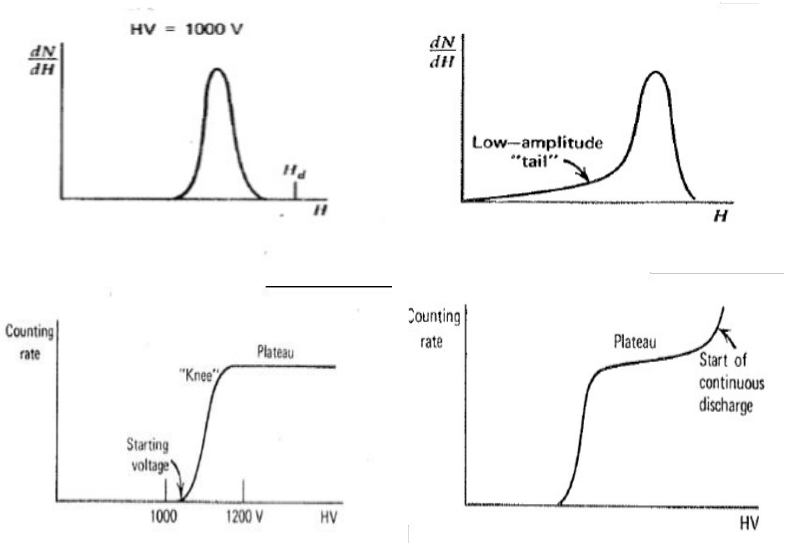

Figure 6.5. Differential distributions of the number of pulses exceeding the threshold in the upper part of the figure. The ideal case corresponds to the left-hand side of the plot whereas the right-hand side shows the real one. Their respectively plateau counting curves are in in the bottom of the figure. The low amplitude-tail on the pulse height spectrum in the real case causes a finite slope of the plateau [Kno96].

do. Thus, in order to accumulate enough collected charge for a measurable pulse, the amplification of the original β particle ionizations needs to be more significant than for α particles. Hence, there is very limited beta contribution to the pulse size in the α region. However if the voltage is increased, a similar plateau for beta particles as for α particles can be located. The major differences are the more gradual increasing in the number of counts until the plateau region, and the rate of change on the plateau is slightly greater than for α particles.

For charged radiations, a signal pulse will be produced for every particle that deposits a significant amount of energy in the fill gas. However, this behaviour is observed in proportional counters *only* for a special situation: in the case of working with monoenergetic charged particles whose range in the counter is less than the dimensions of the chamber. As is the case of α particles (is completely sure that the dimensions of the chamber are enough to satisfy the required condition). Under this circumstance, if almost all pulses from the detector are of the same size, the differential pulse height spectrum has a single isolated peak and the corresponding counting curve has a *simple plateau*.

Consequently, for the available α-source of americium-241 a plateau is expected and, most concretely, a single one. Hence, no reason to explain the double plateau observed are initially found.

However, by measuring the counting rate produced by the ^{241}Am sample as a function of the high voltage applied in a range of 0 to 2.1 kV, a double plateau depicted in Figure 6.6 was obtained. A first flat region was observed between 0.3 - 0.6 kV around 1350

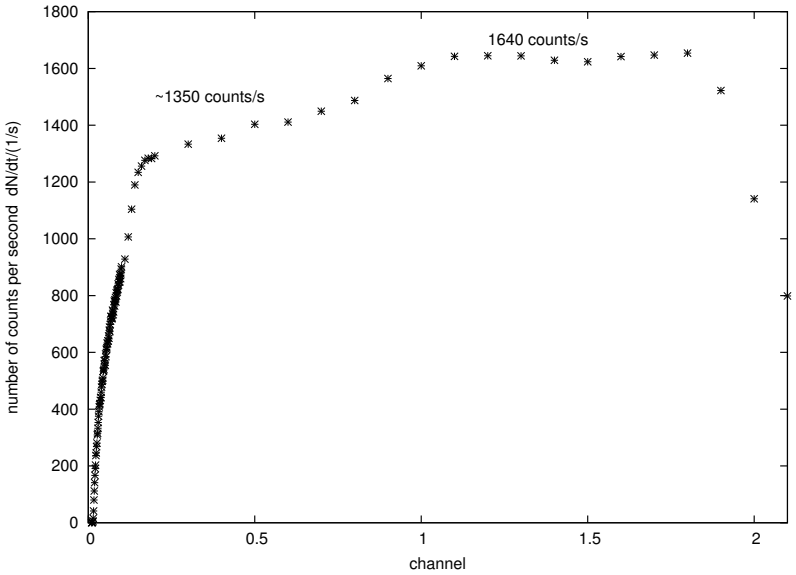

Figure 6.6. Initial double plateau detected. In the y-axis are represented the number of counts detected for a measurement with the americium source during 10 s versus the applied voltage in kilovolts. The first plateau is observed between 0.3 - 0.6 kV around 1350 counts and the second one in the interval of 1.1 - 1.6 kV with 1640 counts approximately.

counts and a second one region in the interval of 1.1 - 1.6 kV with 1640 counts approximately. Consequently, first of all, it was necessary to discern between both as the right one according to the activity of the source employed.

This can be easily using the relation between the activity A (given in Becquerels) of a certain source and the number of counts expected for a particular detection geometry:

$$A = 4\pi \frac{N}{t_{live} \cdot \Omega \cdot P_\alpha} \tag{6.1}$$

where t_{live} is the measurement period already corrected with the dead time, Ω is the solid angle (in steradians) subtended by the detector at the source position and P_α is the intensity of the α decay under interest.

In the specific case of the 2π counter use, the features of measuring are:

$$\left[\begin{array}{l} \Omega \sim 2\pi \\ P_\propto = 1 \\ A(^{241}Am) = 3.7\,\mathrm{kBq} \\ t_{live} = 10\,\mathrm{s} \end{array}\right.$$

Thus, the counting rate expected for the ^{241}Am source used was around 1850 counts per second. However this result did not match with any of the counting rates corresponding to the two plateaus regions obtained in Fig. 6.6 (with flat regions around 1350 and 1640 counts per second). Hence, any of the plateaus measured was the correct one.

Besides that, the energy spectrum was also taken for the source. As the sample was a monoenergetic α emitter, a single sharp peak was expected. Nevertheless, spectrum plotted in Figure 6.7 was obtained. A peak can be distinguished over the rest of radiation that was considered background or noise. However, when the spectrum without source was taken, no counts were detected.

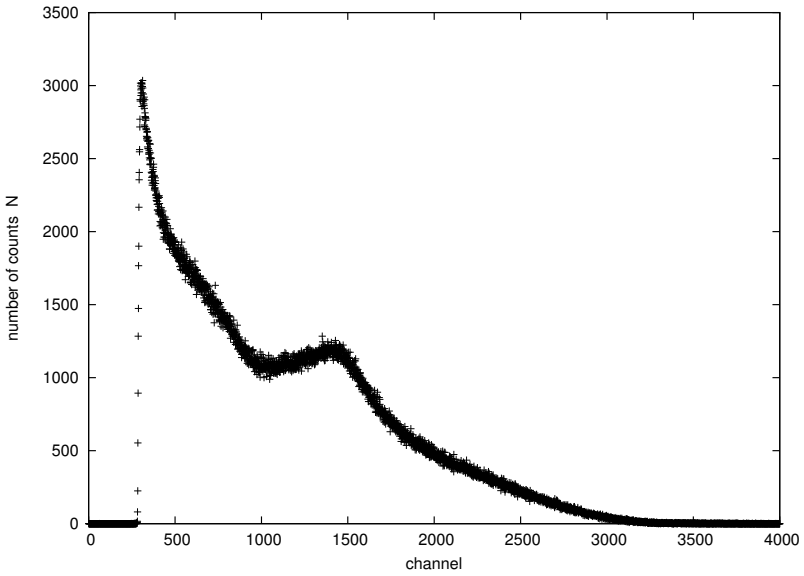

Figure 6.7. Alpha spectrum measured at HV= 1 kV. A peak at channel around 1500 was observed. The rest of the counts were expected to be explained as background, but when a measurement without source was taken, the spectrum obtained was empty. So there was no background, neither noise presence.

So clearly, that showed serious problems in the detection and was essential to to find out from where they came from.

6.2.2. Analysis of the possible causes for the double plateau

Several reasons could explain the presence of this double plateau. These ideas and the experiments designed to check them are described in the following section.

6.2.2.1. Gamma radiation detection

The first idea that came up to try to explain the presence of the double plateau was take under consideration the fact that besides being an α emitter with its main peak at 5.6 MeV, ^{241}Am is also a γ emitter with a peak around 60 keV (if it is recalled the decay scheme of americium-241 of Fig. 2.5). Therefore, was logical to wonder about the possibility of the detector was so sensitive that it was viable to measure γ radiation at low energy.

Assuming this hypothesis as possible, γ particles which would interact with the medium bias fotoelectric effect or Compton effect, will produce electrons (of 60 keV) able to reach

the detector and be counted. That would lead to the second plateau region, a gamma one. Cause, as it has been previously explained, the first one would be the α one seeing that α particles are the first particles able to ionize.

Therefore, an experiment to check this possible reason was designed. The basic point was that if an aluminium plate of known thickness enough to attenuate all the α radiation was put covering the source, under the previous hypothesis, only the γ particles which were no attenuated by the plate would be detected. Consequently, only the plateau region corresponding to the γ emission energy (the second to appear) must be observed.

As a quick reminder, is well known the attenuation of α and γ radiation behaves in a different way for each kind of particle:

Alpha attenuation: the range of α particles in an absorber material, according to [US11], is given by:

$$R(solid) = 3.2 \times 10^{-4} \cdot \sqrt{\frac{A}{\rho}} \cdot R(air) \quad \text{with} \quad R(air) = 0.318E^{3/2} \tag{6.2}$$

with A the mass number, ρ the density (in g/cm^3) and R the α particle range (in cm).

Gamma attenuation: a beam of photons is not degraded in energy as it passes through a thickness of matter, is only attenuated in the intensity, according to [Vil12], on a way given by:

$$I(x) = I_0 e^{-\mu \cdot x} \tag{6.3}$$

with μ the lineal attenuation coefficient (in cm^{-1})and x the thickness (in centimeters).

With the available data:

$$\begin{cases} \rho_{Al} = 2698,4\,\text{kg/m}^3 \\ A_{Al} = 26,98\,\text{u} \\ \mu_{Al}(59keV) = 0,213\,\text{cm}^{-1} \end{cases}$$

According to Eq.(6.2) the α particle range in aluminium is 41,3 μm. Thus, if a thickness for the plate of 60 μm is chosen, according to Eq.(6.3), the attenuation of γ particles is less than 0.5%. So the lost of γ radiation is negligible for this thickness of the plate.

Measuring first the spectrum without the plate covering the α-source using the multichannel analyzer, the already mentioned spectrum of Fig. 6.7 was obtained. Nonetheless, surprisingly, when the spectrum with the aluminium plate over the α-source was taken, an empty plot was acquired. Any counts were detected, not even background or noise. However, under the working hypothesis it was supposed to be the same spectrum as the one obtained without the aluminium plate except from the peak (which to α particles).

Thereupon, the conclusion reached was that the *extra* radiation manifested as the second plateau was not due to neither γ radiation, nor background or noise.

6.2.2.2. Damage of the source

The next logical step seemed to be wonder about the source quality. It could be possible maybe a damage on it. The ^{241}Am source used is an *open source*. That means that, in order to minimize the lost of radiation because of internal absorption, the sample has radioactive substances non-encapsulated. The radioactive material is deposited in the surface. So possible damages on its active area are not difficult to happened.

The most normal harm expected was that α particles were extended over the whole plate instead of be localized in the active area as a result of touch the source directly. In oder to check it, a plate of known thickness (150 μm) with a hole of diameter 2 mm in its center, was placed over the sample.

The same spectrum as in the last check (Fig. 6.7) was measured again but no changes were observed. Hence, could be affirmed that the source was not damaged.

6.2.2.3. Damage of the wire

Once discarded the γ radiation detection and an injury in the source, the next question was the state in which was the wire. As it has been already mentioned, electrode wires are very sensitive and all the discharges it was suffering could had damaged it.

In addition, the possibility of being something wrong with the wire was took under consideration since the beginning as a possible solution of the discharges problem. Furthermore, the hemispherical shape of the electrode did not seem the best one due to signals of different amplitudes must be getting depending on the part of the wire the electrons hit. Maybe the continuous distribution instead of a isolated peak obtained in the energy spectrum of the ^{241}Am source showed in Figure 6.7 could be also explained by this effect. Particles hitting the wire in positions with lower electric field values (this is, the extreme positions of the wire which are a higher distance from the radioactive sample) would produce signals of lower amplitudes that, consequently, would appear in lower channel values in the energy spectrum.

Consequently, the wire was finally changed. A new one with a diameter of 15 μm and flat shape using tungsten was built.

The new measurements carried out with this new electrode were really good in the first checks. A counting rate with a single flat plateau, as well as nice spectra with a well defined α peak were obtained as is shown in Figure 6.8. A plateau region extended from 200 V to 1700 V and a counting rate around 1640 counts per second was measured. In addition, a well defined peak, although a little bite broad, was observed. Consequently, the change of the wire apparently solved the two biggest problems: the presence of discharges and the measurement of a double plateau for a monoenergetic alpha source.

However, a lot of different measurements were made in order to to guarantee completely the veracity of the good results. And in some cases, still strange counting rates or the double plateau were observed. In some measurements, apparently taken under the same conditions, strange plateau curves were obtained. Again double plateaus or inexplicable increasing or decreasing of the number of counts were observed for the same source measured with the new wire as illustrated by Figure 6.9.

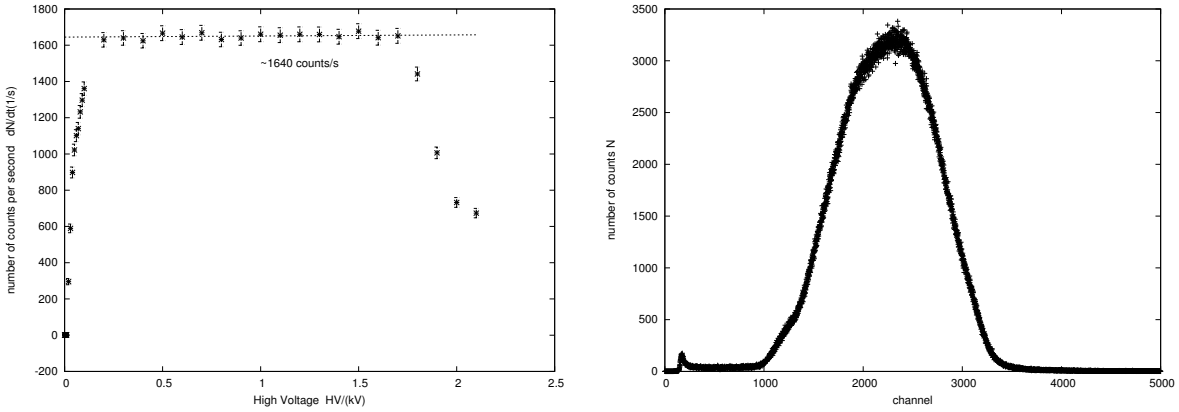

Figure 6.8. Good results were obtained in the first checkings for both energy spectrum and plateau curves after replacing the wire. A single flat plateau can be observed from around 0.2 kV to 1.7 kV with a counting rate of 1640 counts per second. The decreasing of the counts around 1.7 kV is due to the amplifier saturates as evidence the signals cut visualized in the oscilloscope from the output of this device. A defined peak is obtained as well in the energy spectrum of the radioactive sample, although with the incorrect counting rate in both cases, curve and spectrum.

Thereupon, the possibility of a change in the measurement conditions between the various controls had to be covered.

6.2.2.4. Influence of the source and its position

Always a measure was done, the data acquisition was not started until a couple of minutes after the introduction of the source inside the chamber of the detector in order to assure the purity of the fill gas afterwards the elimination of all the air. Specifically, for the chamber dimensions, for a flux of 0.2 LPM, around five minutes is enough. Hence, the only parameter that seemed to be possible to change between the measurements was the position of the source. Must be reminded that the sample is directly manually introduce and placed on the plate that closes the detector. Thus, some movements of it are probable. Perhaps the counting rate was very sensitive to this parameter and the position of the source was extremely important.

Several measurements were effectuated to confirm if this supposition was correct. The results of the analysis are the corresponding to Figure 6.10 and effectively they affirmed it. If the source was placed on purpose in one of the extremes of the cap which closes the detector chamber, completely different plateau curves to the correct one showed in Fig. 6.8 were obtained, with no flat regions or even with the appearance of the double plateau again.

In the light of these results was clear that the position of the source was extremely important due to its big influence in the plateau curves obtained. Consequently, it must be fixed to ensure measuring always under the same conditions.

Thus, a modification in the detector was implanted: a hole some millimeters bigger

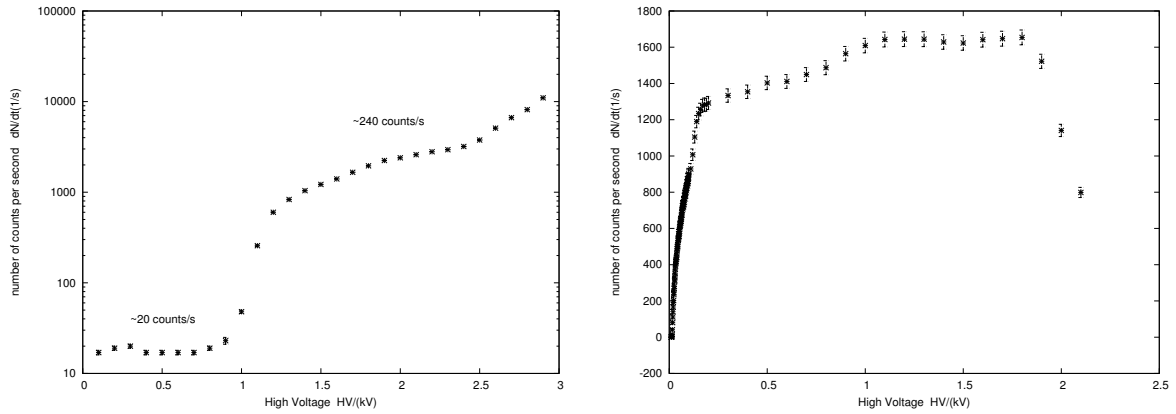

Figure 6.9. Strange spectra as the one shown on this figure were obtained sometimes in the checking measurements with the new flat wire placed on the chamber. Double plateaus in the counting rates or strange curves were get, but only in some measurements apparently carried out under the same conditions: the same high voltage value applied, gas flux, wire and source.

than the diameter of the sample was made in the plate (see Fig. 6.11). In this way, the source is always in the same position with no doubts.

The new analysis carried out were completely satisfactory, good results for the plateau region and the energy spectrum as the one shown in Figure 6.8 were obtained with complete reproducibility. Consequently, after all the improvements carried out, it was concluded that a nice flat plateau with a counting rate around 1640 counts per second and extended on a range from 0.2 to 1.7 kV was measured for the ^{241}Am source. In addition, a energy spectrum with a well defined α peak was also obtained and corroborated this counting rate value. However, is must be reminded that a counting rate of 1850 counts per second was expected for the source employed according to the fabricator certification. Therefore, this problem should be solved yet. It was though that such difference was related to the parameters of the electronic chain used for the measurements, so a study of their influence was developed, as is discuss in the next section.

6.3. Choice of the measurement parameters : search of the the optimal configuration

Once that all the parameters which have some influence in the measurements with the detector are under control, it was necessary to chose the most adequate values of the different electronic devices in order to optimize the use of the set-up for α decay detection.

The main parameters which had to be studied are the high voltage value of operation and the amplifier gain (adjustable trough coarse and fine gain). The rest of the parameters were previously selected taking into account general recommendations as was explained in section 4.2.

The first parameter under study must be of course the high voltage applied between

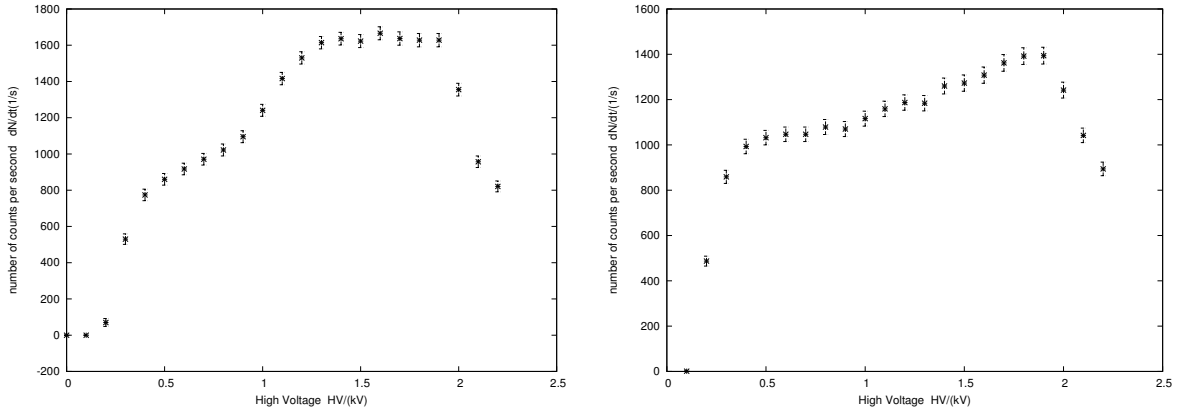

Figure 6.10. Measure of the α-source with the sample placed in the bottom side of the plate in the left-hand side of the image and placed in one of the extreme sides of the plate in the right-hand one. Plateau curves completely different to the expected one were observed indicating the big influence of this parameter in the measurements. Double plateaus or any plateau regions were obtained.

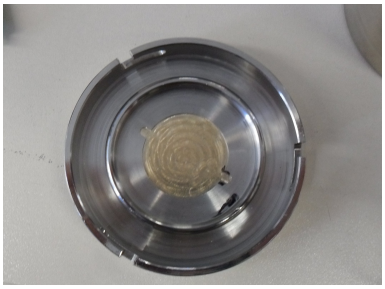

Figure 6.11. Mechanism used to fixed the position of the source. A hole some millimeters bigger than the sample was made in the center of the cap where it is placed.

the electrodes since the collected charge formed in the detector chamber and hence, the visualized signals, depend on it. The determination this proper value needs to be characterized for the plateau curve of the instrument for a specific radiation. It should be chosen around the middle of the region where is supposed that the stability of the number of counts is the highest one.

Considering the final plateau obtained with the set-up showed in the last section (Fig. 6.8), the plateau region extends approximately from 200 V until 1700 V. Consequently, the optimal voltage value adopted must be inside this region, normally around its middle (950 V). Thus, diverse studies were carried out in order to select the optimal operation voltage value.

First of all, to assure the right selection of the best voltage to work, a deeper study of the counting rates get for each voltage value was developed with the analysis of the energetic spectra. Spectra taken at several volts (from plot a) to f) in Fig. 6.12) were measured. The evolution of the spectrum shape with the high voltage is perfectly illustrated. At low values, more acutely in those values out of the plateau region, several peaks appear.

On a qualitative way, a possible explanation is that the lowest energy peak may be due to the α particles lost. Those which hit the walls and do not ionize much on their paths produce electrons that hardly reach the holder due to the weak electric field they are exposed. The second peak can be formed through those α particles which do not travel straight along the chamber and hence, the electrons produced cover a longer path in the chamber, loosing energy in the collisions with another electrons or with the molecules of the gas. Finally, the last peak may be due to the α particles which reach the wire directly: they are emitted, travel straight into the chamber, ionize on their paths and the electrons produced reach the wire. These electrons carry the real α decay energy. The plateau region starts around 200 V as was showed in Fig. 6.8, however, the spectrum shape is not still the correct one, as can be seen in the spectrum e) of Fig. 6.12. As the voltage increases, the shape of the spectrum improves and the three peaks get closer and form a single one. That occurs around 1000 V (spectrum g) of the figure), being at the value of 1200 V (spectrum h) of the figure) when the observed peak has the nicest shape. At higher values of voltage the shape is still the correct one but the electric noise starts to be important, being visible at low channels and it increases with the high voltage value, so preferable not exceed that voltage. Indeed, at maximum voltage value, 1500 V, the noise is much bigger than the alpha peak (spectrum j) of the figure). Hence, according to the figure, the best shape with the lowest noise is get for spectrum h), this is, for the spectrum taken at 1200 V. Therefore, from the several possible values, this was the chosen as the optimal one to measure α-sources. In addition, the spectra in the left-hand side of the figure 6.12 are plotted with the same scale between them, while the spectra from the right-hand side are plotted with another scale but the same between them. That was made in purpose in order to show in a clear way how the mean value of the distribution, which gives information related to the amount of energy collected of the energy deposited by the alpha particles in the detector volume, increases with higher voltage values applied as must be.

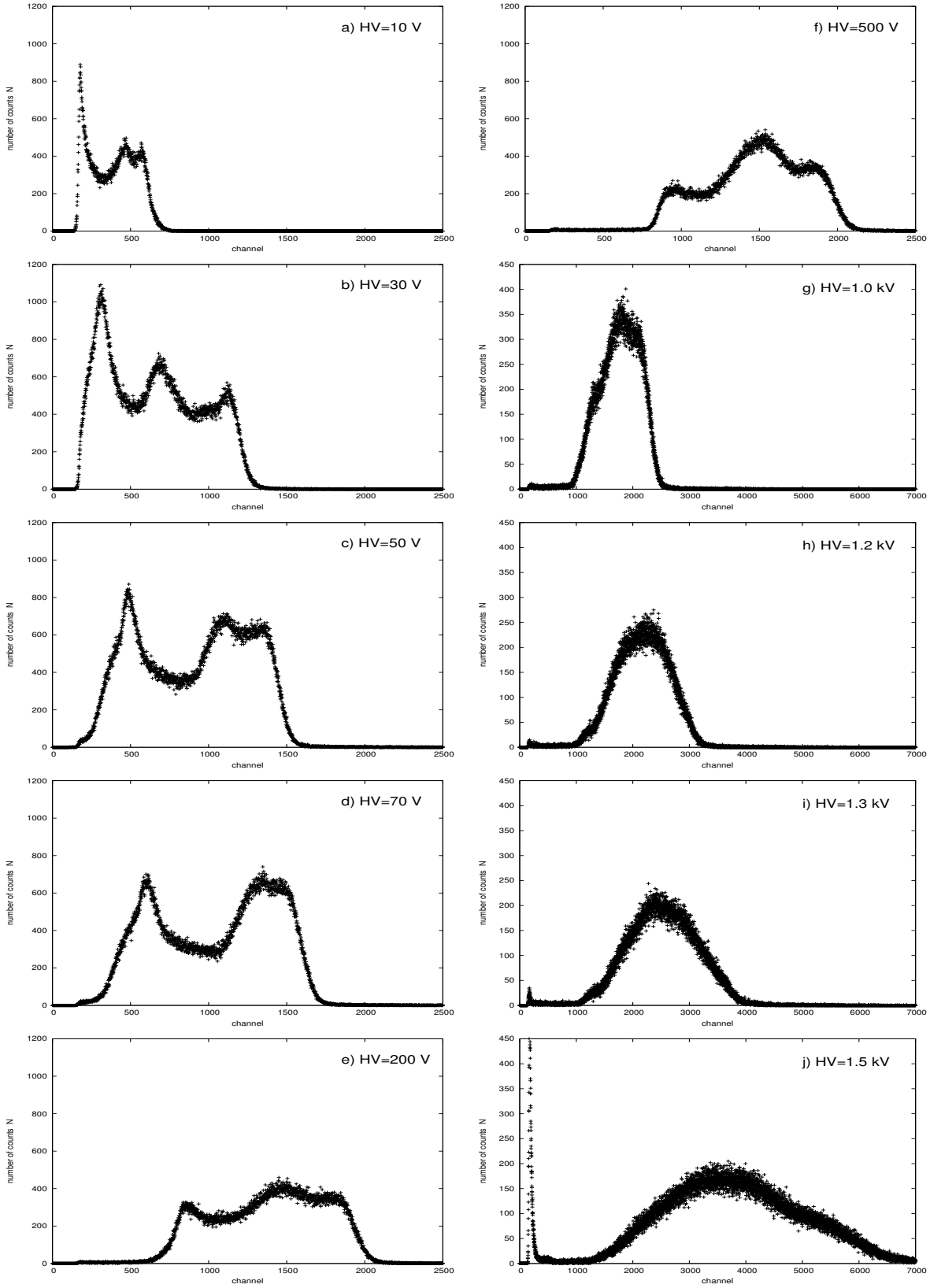

Figure 6.12. Energy spectra taken at several voltage values. At low high voltage values, as in the case of spectrum a), the shape shows the presence of three peaks. On the contrary, at very high voltage values, as 1300 V like in spectrum i), the shape is good but the electronic noise is too big. The best shape is get for the spectrum at 1200 V, h). That is why this value is chosen as the optimal one to measure α-sources.

Apart form that, a study of the amplitude of the output signals as a function of the applied voltage can be carried in order to define the voltage ranges of the different operation regions of the detector. Such study is shown in Fig. 6.13. It must be reminded that the attempt of the present thesis is to optimize the performance of a gas flow proportional counter, so the measurements must been carried out with a voltage value corresponding to this region. As shows the mentioned figure, for voltage values below 200 V recombination effect is too strong due to the low electric filed. As the voltage raises, the recombination is avoid and the ion saturation region is found between 200 and 900 V approximately. Around 1000 V the collected charge begins to multiply and the observed amplitude pulse increases. That corresponds to the proportional region and it extends until around 2500 V. In this region must be selected the working voltage in order to operate as gas flow proportional counter. After it, the Geiger-Müller region starts and non linear effects are introduced. Thereupon, the selected 1.2 kV voltage values is certainly inside the proportional region, so is a good election.

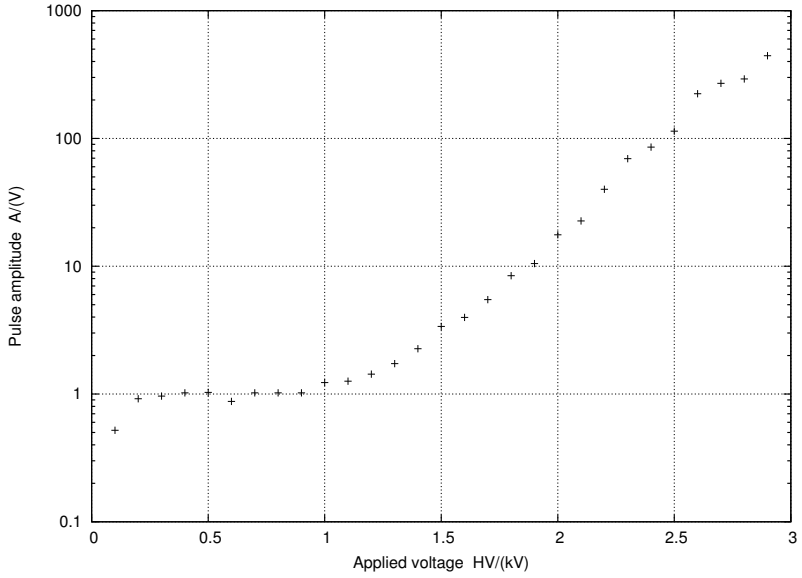

Figure 6.13. Study carried out in order to determine the different operation regions of the detector used to check that the high voltage value selected as optimal, i.e. 1.2 kV is inside the proportional region. For voltage values below 200 V electric filed is too low and recombination effect predominate and very few number of ion pairs are collected. As the voltages raise, the recombination is avoid and the ion saturation region starts. It extends from 200 V until 900 V approximately. At a higher values, around 1000 V, the multiply effect starts and the collected charge multiplies, so the observed amplitude pulse increases. That corresponds to the proportional region and it extends until around 2500 V. The working voltage value In this region must be selected in order to operate as gas flow proportional counter. After it, the Geiger-Müller region starts and non linear effects are introduced.

Besides that, another test were performed in order to consolidate the high voltage value chosen. Both the mean value and the standard deviation of the energy spectra were

analyzed. The coefficient between this values leads to an idea about the energy resolution of the the detector for each high voltage applied. That study is depicted in Figure 6.14 and shows that the best resolution are achieved for values around 1.0 kV with resolution around 20%. The best comprise between the energy spectrum shape (discussed in Fig. 6.12) and the resolution value are get for a high voltage value of 1.2 kV, so the right choice of this value as operation voltage was again confirmed.

It must be noted that the proportional counter was not designed to make spectroscopy analysis. The energy spectra were taken in order to provide additional information used to confirm the counting rates or just to take a look to the shapes, so the resolution value obtained is not very important.

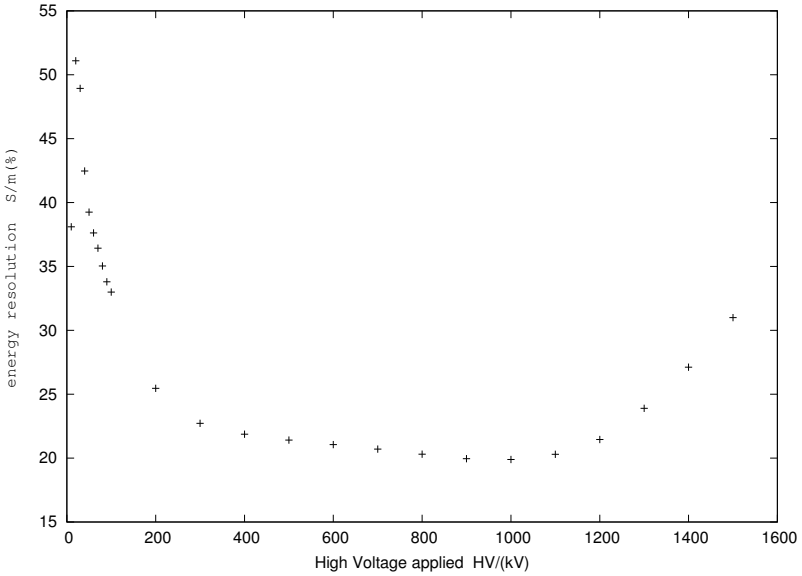

Figure 6.14. Study of the detector resolution through the mean value and the standard deviation of the energy spectra, as a function of the high voltage applied. S represents the standard deviation and m the mean value of the energy spectra distributions. Once again, such analysis reaffirmed the high voltage value chosen as optimal for α decay detection seeing that the best values of the resolution are found around 1.0 kV.

Finally, a study of the signals pulses visualized in the oscilloscope showed that the amplitude of the output signals did not change with voltage variation in the plateau region as was expected. This is perfectly illustrated in Fig.6.15. Hence, the high voltage value was reinforced once again.

Accordingly, the optimal high voltage value for α decay detection chosen using both the plateau curve and the energy spectra was selected as 1.2 kV. All the future measurements with all α sources will be taken at this voltage value.

Once chosen this variable, only the amplifier gain had to be adjusted so that the optimal configuration of the electronic chain was completely fixed for α detection. In order to do so, the plateau curves were again observed but this time, at fixed voltage value for different gain values.

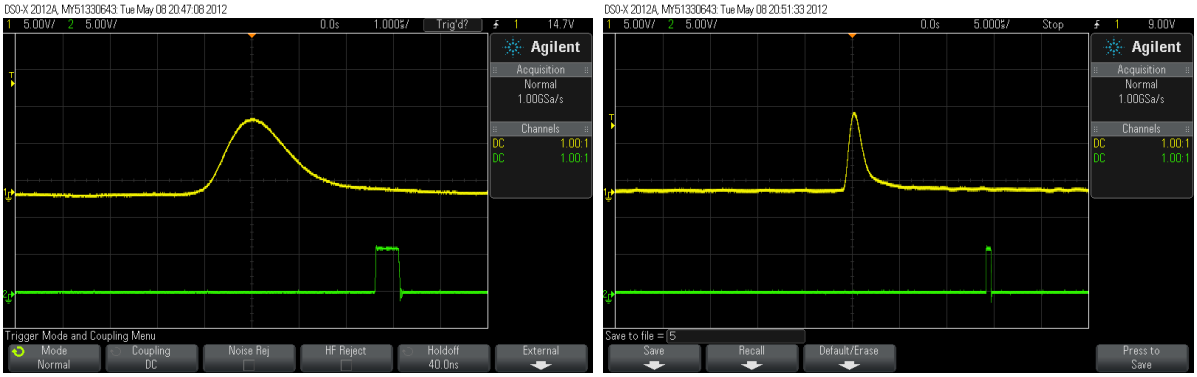

Figure 6.15. Output signals from the amplifier (channel 1) and the discriminator (channel 2) visualized in the oscilloscope for different values of the high voltage both inside the plateau regions, concretely 0.9 kV and 1.3 kV. It can be observed that the amplitude of both signals of the same as should be (note that the y-axis scale in the same in both cases although the x-axis is not).

The study was realized with a fixed value for the lower threshold of the discriminator, concretely the value chosen for the optimal configuration, this is 0.2 V. Two measurements were carried out for values of the gain of 500 and 1 k respectively. The results obtained for the plateau curves are the corresponding to Fig. 6.16.

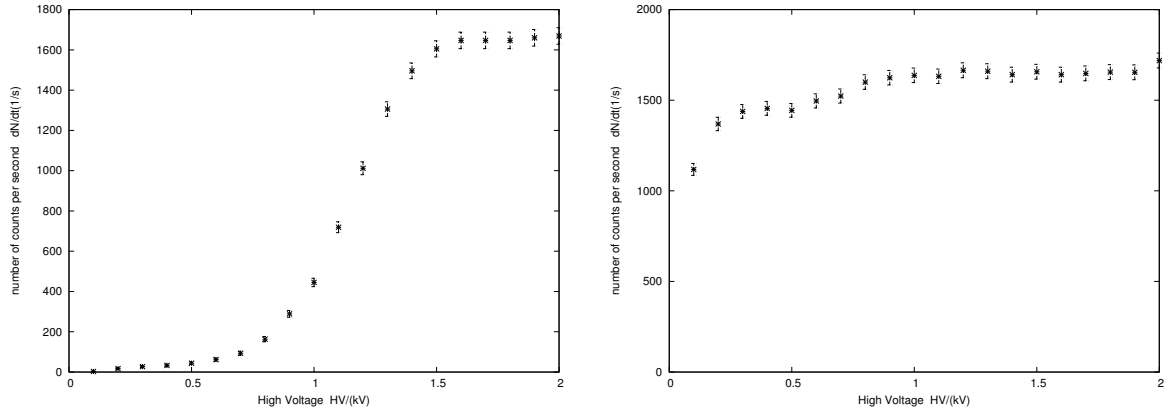

Figure 6.16. Plateau curves measured for two different values of the coarse gain, 500 and 1 k respectively at fixed high voltage (HV= 1.2 kV) and lower discriminator level (0.20 V). For the lowest value the plateau region starts at too high voltage. For the second one, the plateau curve is nice but the output signals form the amplifier are cut in the oscilloscope as shows Fig.6.17.

For the choice of this parameter it must be pointed out that a compromise between the voltage value at which the plateau region started and the quality of the output signals must be found. From Figure 6.16, it can be observed clearly that at the lowest gain value (A=500) the plateau starts at too high voltage ($\sim$ 1.3 kV). That means that in order to

visualize the complete plateau region, very high voltage values must be reached which is very inconvenient for several reason. First of all, the anode wire can be resulted hurt with such a strong electric field. Secondly, discharges could appear again because of the high sensitivity of the wire. And finally, if such high voltages are necessary to detect α, higher ones would be need to detect β and maybe the range of the power supply is not enough. On the other hand, for a higher gain value (A=1 k) the plateau curve obtained is quite nice but signals are cut in the oscilloscope (see Fig. 6.17). That means that the amplifier saturates.

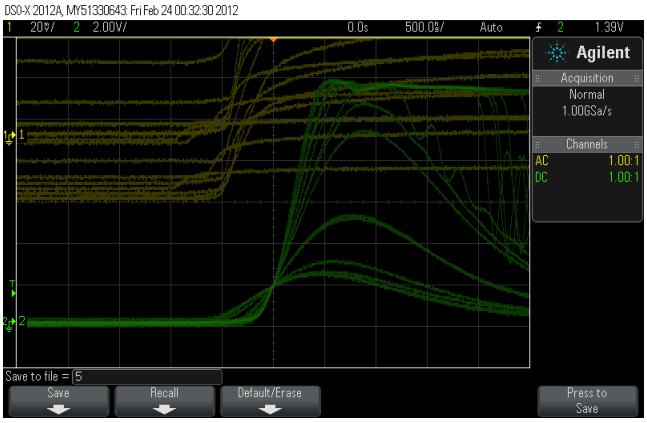

Figure 6.17. Signals in the oscilloscope at 1200 V for a gain value of G=1 k. They are cut, what indicates that the amplifier saturates for such combination of high voltage and gain values.

In view of these results, a value of the gain at which the signals in the amplifier were not cut must be chosen. That leaded a value of 500. But also was needed that the plateau started at not high voltage so that working at high values which produce strange effects in the output signal was avoided. In oder to get the appearance of the plateau region at lower voltage values the fine gain value was adjusted as well. Playing with the fine gain and analyzing the plateau curves for each case, a value for the fine gain was finally selected: 1.0. For such value, well signals were visualized in the oscilloscope (see Fig. 6.18).

Then, after all the measurements carried out, we could conclude that the *optimal configuration* for α detection is:

$$\boxed{\text{HV= 1.2 kV, A=500, A}_f\text{=1.0, LL= 0.2 V}}$$

Where must be remembered from section 4.2 that A indicates the coarse gain value, A_f the fine gain value and LL the lower level threshold of the discriminator.

Measurements done for this selection are shown in Fig. 6.19. According to them a counting rate of $N = (1584 \pm 3)$ counts per second was detected with the current set-up working at the optimal configuration, which correspond to an activity of the source of $A = (3.2 \pm 0.1)$ kBq. This results were checked for different orientations of the source and for all the possible values of the gas flow and the same spectra and counting rates

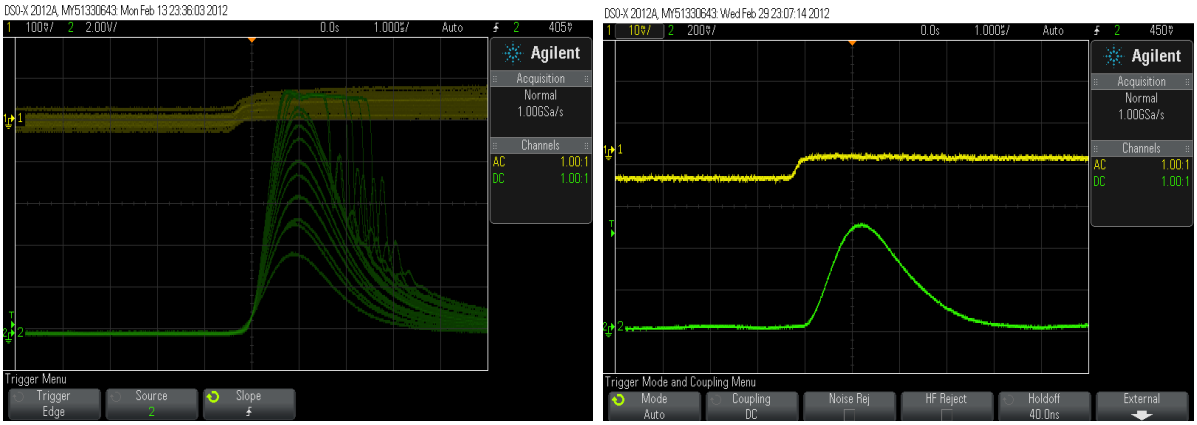

Figure 6.18. Comparison of output signals from the preamplifier and the amplifier respectively visualized in the oscilloscope for values of the voltage out of the plateau region (at 1.9 kV) and inside it (0.7 kV) at the optimal gain value. The results are really good.

were obtained. Consequently, neither of those two parameters has any influence in the detection.

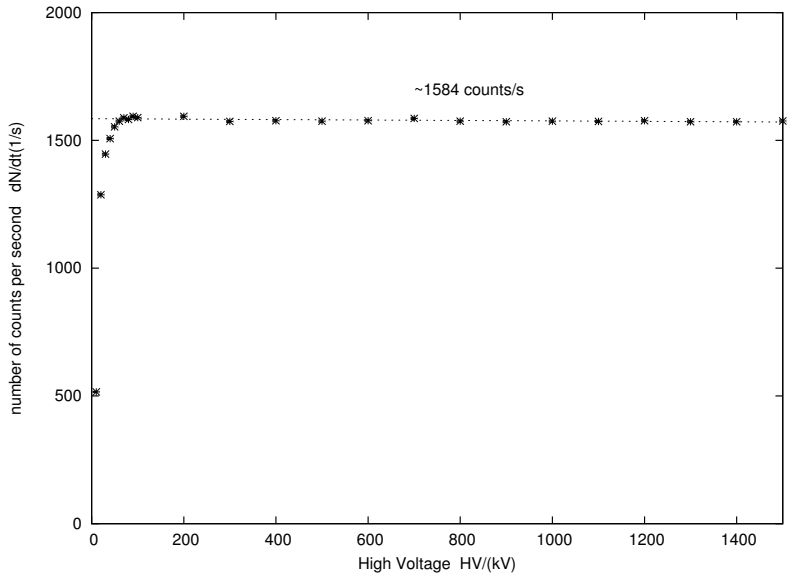

Figure 6.19. Plateau region measured with the source fixed in its position at the optimal configuration. In addition, with complete reproducibility the same results were always obtained. The plateau region is observed between approximately 100 V and 1500 V with (1584±3) counts per second or average in the voktage region from 100 to 1500 V. However, it must be reminded that the measurements were carried out with certificated source of 3.7 kBq of activity, which corresponds to a counting rate around 1850 counts per second for our geometry detection.

6.4. Determination of real activities: Silicon detector

Nevertheless, despite all the improvements obtained, still was not clear the counting rate measured with the detector. It must be reminded that counting rate of 1850 counts per second was expected for the source measured according to its certified activity. But 1584 counts per second was the amount obtained with the proportional counter, so around a 14% of the radiation was lost in the detection. Consequently, was necessary to carry out an analysis in order to identify a possible problem with the efficiency of the detector or just with the activity considered of the source.

The first experiment carried out was to measure the amount of radiation emitted by the ^{241}Am source with a different active area. Such analysis could provide information useful to check if the same amount of radiation was missed in the case that only a certain part of the source was emitting radiation and in the case that the whole sample dimensions were considered as active area. In that case, a problem with the efficiency of the detector could be identified.

With this aim, an aluminium plate with a hole in its center of known diameter (7 mm) was used to cover the source. The counting rate produce by the source was measured giving a plateau curve corresponding to Fig. 6.20. The main features of the curve obtained were the presence of a single plateau which started around 2 V with an average of (896±30) counts per second and the fact that the counting rate increased around 1.4 kV suddenly and then decreases around 1.8 kV with no apparently reason (no saturation was observed in the oscilloscope for the output amplifier signals).

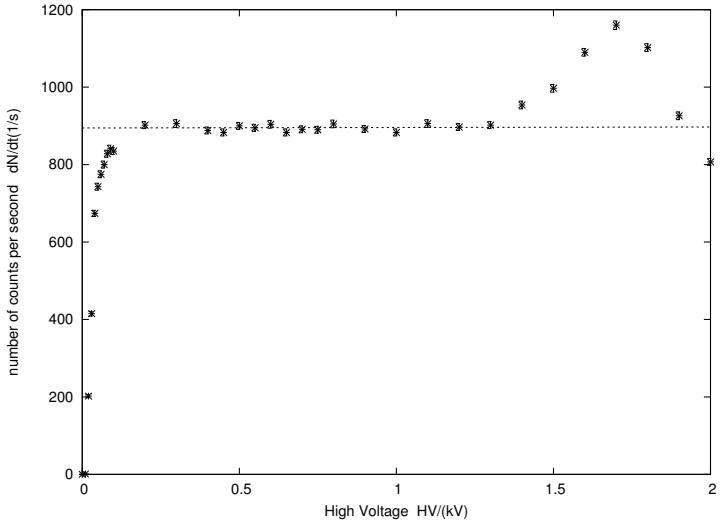

Figure 6.20. Plateau curve measured with the ϕ= 7 mm aluminium plate in order to check the activity of the source. The line correspond to the leads square fit. A counting rate of (896±30) counts per second was obtained. The appearance of the peak at high voltages could not be explained yet.

However, for an active area of 7 mm, according to a Monte Carlo simulation for the solid angle value carried out for our detection geometry, a solid angle of Ω= 4,0323 steradians

was subtended by the detector at the source position. Applying Eq.(6.1) a counting rate of around 1200 counts per second corresponds to the certified activity of the α source. That involved a amount of approximately 25% of radiation lost. Maybe, was possible to attribute this bigger difference between counting rates to a lose of counts because of interactions of the particles with the plate. In any case, seeing that the age of the sample was unknown, the determination of the exact activity of the source was necessary in order to discern a problem between the set-up or just with the data used for the calculations.

To find the answer, a new experiment was designed: a new set-up with a silicon detector was built.

6.4.1. Experimental set-up.

Silicon detectors are a type of semiconductor detectors. These devices use the fact that when the ionization radiation pass through them creates a big number of electrons-holes pairs along its path. The number of ion-pairs formed is proportional to the energy transmitted by the radiation to the semiconductor. As a result, a number of electrons are transferred from the valence band to the conduction band, and an equal number of holes are created in the valence band. Both particles can be collected applying an intense electric field and generates the basic electrical signal from the detector. Besides that, the energy required for creation of an electron-hole pair in these detectors is well defined (3 eV for silicon), so the detector has a spectrometric answer. In addition, the lower energy value required to form an ion pair results in a much larger number of carries for a given incident radiation event than is possible with any other common detector type. Consequently, they provide the best energy resolution.

Apart form that, solid-state detectors have the advantage of have relatively fast timing characteristics. However, they must be cooled to very low temperatures to avoid excessive generation of carriers due to thermal agitation, which can generate a problematic electronic noise and must be set up in vacuum.

For more details about these devices, [Kno96] can be consulted.

In the present set-up, the detector used is a *model BA-23-50-300* from company *Ortec* which is a silicon surface barrier detectors for charged particle spectroscopy able to cover a wide variety of applications. It has as main features a low background and high resolution charged particle spectroscopy. This device is equipped with a very thin gold window that is sensitive to light, so the experiment must be developed in darkness in order to avoid noise. It also requires an operation in vacuum [1].

On the other hand, the nuclear electronics associated is the basic one: a voltage power supply, a preamplifier, an amplifier, a multichannel analyzer and an oscilloscope.

6.4.1.1. The experiment

The idea was to design an experiment as simple as possible. Looking for this condition, the source must be faced to the detector at a distance sufficient for the sample to be punctual. That simplify all calculations. To get that, an aluminium plate with a hole of

[1] More details about this Si device can be found in chapter 4 of the *manual of use*.

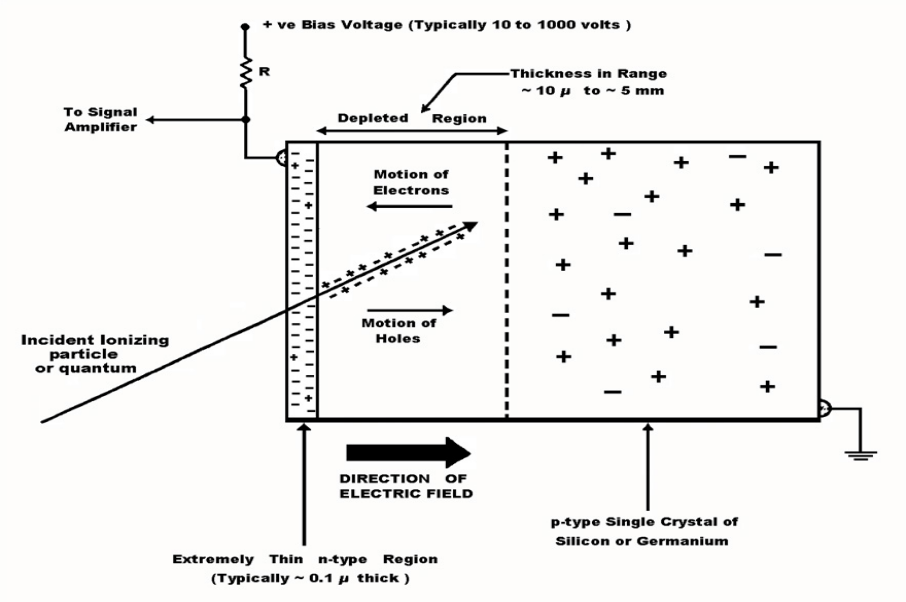

Figure 6.21. Operation of semiconductor detectors [Web12d]. When the ionization radiation pass trough them creates a big number of electrons-holes pairs along its path due to the excitation of the less binding electrons of the valence band which jump to the conduction band creating free electrons and holes.

known diameter (ϕ) in its center and 100 millimeters of thickness (enough to attenuate α particles) was interjected between both of them. The whole assembly was set-up in a tube connected to a turbo molecular vacuum pump (4.6×10^{-4} mbar) by means of plastic rings in order to isolate the tube and reduce noise as much as possible.

In order to not make excessively long measures, a compromise between measurement period and the counting rate, which assure to get good statistic, must be found. A reasonable counting number in an experiment is around 10000 counts, what leads to an error of 1%. Hence, with the constrains of this counting rate and a distance from the source to the detector (d) long enough to be possible to treat the sample (with an active area $A = \pi a^2$) as punctual and so the solid angle (Ω) is completely defined, the time of measure must be calculated.

For a punctual distribution the solid angle is given by:

$$\Omega \cong \frac{\pi a^2}{d^2} \tag{6.4}$$

Thus, the time of measure for a punctual source, according to Eq.(6.1), can be calculated as:

$$t_{live} = \frac{4\pi N}{AP_\alpha \Omega} = \frac{4Nx^2}{AP_\alpha a^2} \tag{6.5}$$

with the total number of counts N around 10000.

If the values for the parameters are chosen as:

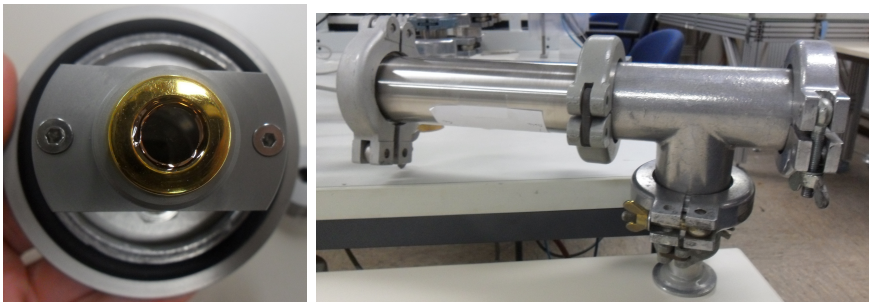

Figure 6.22. Silicon detector *Model BA-23-50-300, Ortec*, available for the experiment and the tube where is set the assembly. More details can be found in chapter 2 of the *manual of use*.

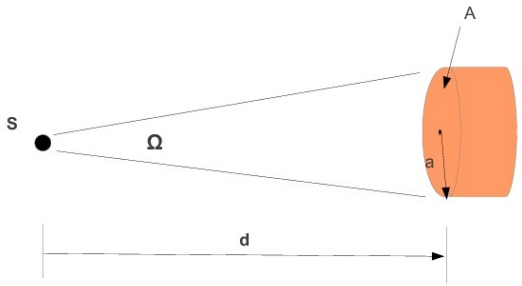

Figure 6.23. For $d >> a$, the source can be considered as punctual (where d is the distance between the source and the detector and a is the radius of the active area of the source) and the solid angle Ω reduces to the ratio of the detector plane frontal area A visible at the source to the square of the distance [Kno96].

- Active source area: $\phi = 2a = (6.0 \pm 0.1)$ mm
- Distance source-detector: $d = (298.2 \pm 0.1)$ mm

Then, according to Eq.(6.4), the solid angle is $\Omega = (3.43 \pm 0.20) \times 10^{-4}$rad. And for this parameters, using Eq.(6.5), is obtained that a time of measure of 37 hours is enough to have a good counting statistics.

6.4.2. Activity measured

Taking the α spectrum with this new set-up, Fig. 6.24 is obtained. That leads to an activity of the source of $A = (3.6 \pm 0.2)$ kBq. Thus, the expected counting rate for this activity according to Eq.(6.1) is (1800±100) counts per second.

So it can be concluded that the counting rate measured with the windowless proportional counter is not exactly the correct one. Some part of the radiation is lost in the detection.

However, no happy with the results obtained, a possible explanation of this lower number of radiations detected was looked for. The idea was that maybe, owing to a *ping-pong*

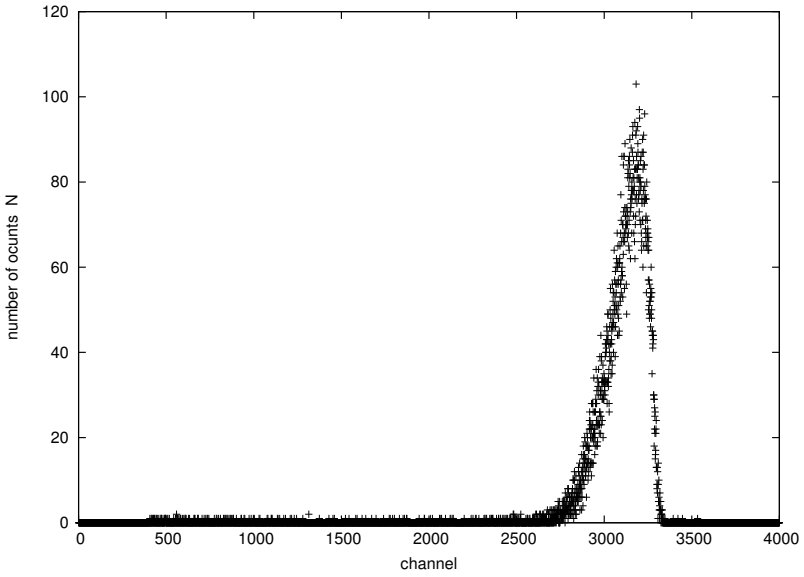

Figure 6.24. α spectrum taken with the Silicon detector measured during a $t_{live} = 247476.32$ s at 145 V (after several measurements the nicest shape was found for this voltage value). A total number of counts of $N = 22583 \pm 150$ was obtained. Hence, an activity of $A = (3.6 \pm 0.2)$ kBq was measured for the source and considered as *the real one*.

effect of α particles in the tube walls, the particles were arriving to the detector with another orientation (not like proceeding from a punctual source) and consequently, the solid angle subtended by the detector at the source position was a different one and the activity calculated was then incorrect. The consideration of the particles crash with the walls on elastic collisions and change their trajectory along the tube but not their energy, wanted to be checked. If this supposition was true, by placing an absorber material of enough thickness in the interior walls of the tube, whether the particles undergo ping-pong effect they must lose their energy in their collisions with the plastic. In this case, either they would not reach the detector or they would do it with a lower energy reflecting this with the appearance of another α peak at lower channels.

In order to check up on that the thickness of the material used for the attenuation, a very simple experiment was carried out. By knowing the channel on which the peak of the normal spectrum (non-attenuated) appears, measuring the channel in which the peak appear in a spectrum taken with a piece of the attenuator plastic material (of 30 μm) of thickness placed over the source, a lose of energy and can be checked. In the case of the non-attenuated spectrum, showed in Figure 6.24, the α peak appeared around channel 3200. By taking a quickly look to the spectrum measured with the attenuator material placed covering the source, could be determined the position of the α peak around channel 1400. It must be pointed out that this spectrum is not included because it was not taken during the whole time required to have a good statistic (i.e. 37 h), it was just measured during time enough to know the position of the α peak and check the that attenuation effect took place.

The realization of the experiment provided the spectrum of Fig. 6.25. Except form the peak at low energy, whose presence perhaps can be explained by the difficulty of placing the plastic around the tube walls, no differences are observed between this spectrum and the one from Fig. 6.24. In both cases the activity measured is $A = (3.6 \pm 0.2)$ kBq. It must be noted that this mentioned small peak can not be an α peak. However, this small peak appears around channel 500. So the positions do not match. Consequently, the existence of no *ping-pong effect* in the tube walls can be concluded and then, the activity determined for the source with the silicon detector is the real one with no doubts.

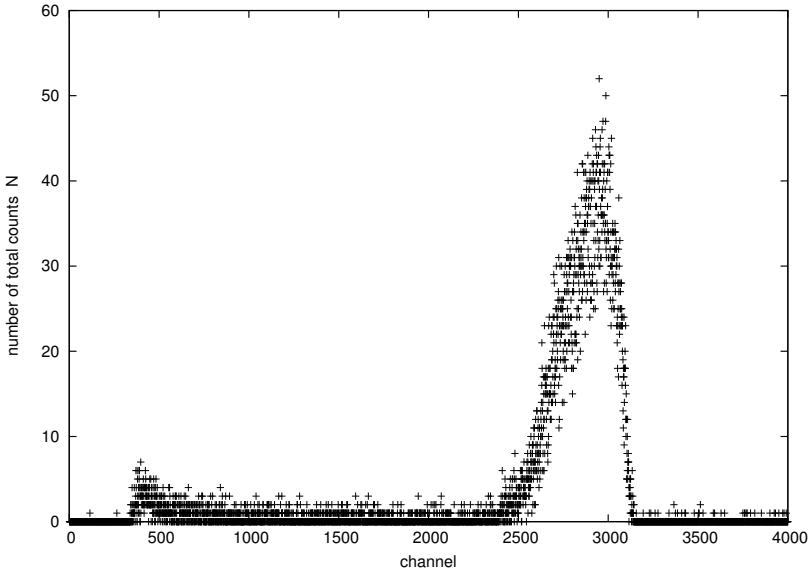

Figure 6.25. α spectrum measured with the Silicon set-up with the wall of the tube covered with a foil for a measurement time of $t_{live} = 154478$ s at 145 V. The small peak cannot be an α peak as a result of an attenuation of the α particles because of its position. A number of counts of $N = 14139 \pm 120$ was measured. So, an activity of $A = (3.6 \pm 0.2)$ kBq corresponds to the source .

6.4.3. Proportional counter detector efficiency

The results of the previous section show that the counting rate measured with the set-up is no the correct one. Some counts are lost by an unknown mechanism.

Looking for possible explanations, a check of possible anisotropy of the active area of the source was carried out. For that, a new series of measurements with the source placed with different orientations was taken. However, the same results were obtained, the counting rate measured was always the same. Besides this, the same measurements were again repeated with different values of the gas flux from the minimum value, i.e. 0.1 LMP, for which the counting rate obtained as (1598±29) 1/s, to the highest available one of 0.5 LPM, that leads to a counting rate of (1577±29) 1/s. So no significant changes were observed again.

Thus, this only could mean that the efficiency of the detector for α particles is not 100%. The detector has a lower efficiency and its value can be detected.

$$\varepsilon_\alpha = \frac{A_{measured}}{A_{real}} \times 100 = \frac{(3.2 \pm 0.1)}{(3.6 \pm 0.2)} \times 100 = (89 \pm 6)\% \tag{6.6}$$

Is must be pointed out that the efficiency of the detector was considered as 89% according to the fabricator of the commercial detector used to rebuilt the one used in this thesis [Kho12]. Hence, this value obtained for the efficiency is very satisfactory. In addition, from the previous results with the detector (chapter 5) the α efficiency was considered around 48%. Thus, a really good improvement was obtained.

Nonetheless, it was necessary to study the reproducibility of the efficiency for α detection. What happen inside the chamber so that some α particles are lost and no counted. As it has been already explained in chapter 2, these particles interact very strongly with matter and lost their total energy in some centimetres of air. Like the fill gas P-10 has higher density than air, α particles must lose their energy completely inside the detector for the present chamber dimensions.

The only possible explanation is was found for this value of the efficiency was the fact that the solid angle subtended by the detector is, by definition of the device itself, 2π. Perhaps, this value is not completely correct. It may be that in a certain region the electric field is too low and the recombination processes are important. Thus, is may exists a *blind angle* for the detector in which the α particles emitted collided with the walls and do not ionize the medium (see Fig. 6.27).

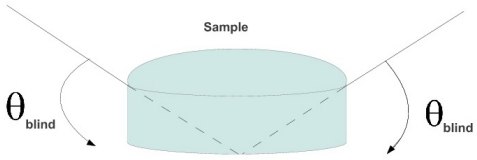

Figure 6.26. *Blind angle* for the sample. It makes the counting geometry lower than the theoretical 2π.

To verify this hypothesis, the solid angle correspondent to the value of the efficiency obtained for the detector needed to be estimated. Using again Eq.(6.1)

$$\Omega = 4\pi \frac{N}{P_\alpha \cdot A \cdot t} = (1.92 \pm 0.04)\pi \tag{6.7}$$

where N/t is the counting rate measured with the proportional counter (this is (1584±3) 1/s) and A is the real activity of the source (the one measured with the Si detector, i.e. 3.6 kBq).

The *blind angle* can be calculated as

$$\theta = \frac{1}{2}(\Omega_{theoric} - \Omega_{experimental}) = \frac{1}{2}(2 - 1.8)\pi = (0.10 \pm 0.05)\pi = (18 \pm 9)^\circ \tag{6.8}$$

Thus, according to this result, α particles may be detected with the set-up with an *effective angle* of $(1.8 \pm 0.01)\pi$, so it is considered that the non maximum value of the efficiency is due to this region *blind*. However, this value of the angle is too big to be realistic. The lower efficiency value may be a combination of the existence of such a blind region and the fact that the straight geometry of the wire makes the chamber anisotropic.

As a future possible experiment in order to check on a deeper way the problem with the isotropy of the chamber could be to cover the source with an aluminium plate again, but this time with a hole in its center with a certain inclination so that α particles are emitted only with this angle. Because the plate can move over the sample, the anisotropy of the chamber could be studied.

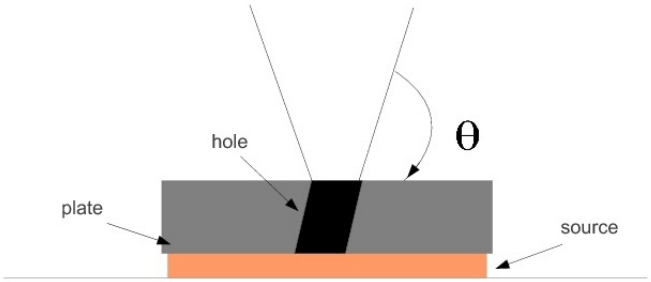

Figure 6.27. Aluminium plate with a hole in its center with a certain angle proposed as possible future experiment in order to study the isotropy of the chamber.

7. Alpha decay measurements of solid samples

In this chapter, the results of the measurements of two α solid samples are presented. Once the detector was fixed for α detection, its good running was strengthened trough both counting and spectrometric analysis of other α emitters. For this, a stone that contains natural uranium and a plate with natural thorium were used. All the measurements were carried out using the optimal parameters for α detection discussed in the previous chapter.

7.1. Natural uranium measurement

Natural uranium is composed of 99.2745% ^{238}U ($T_{1/2}$= 4.468×10^9years), 0.720% ^{235}U ($T_{1/2}$= 703.8×10^6 years) and 0.0055% ^{234}U ($T_{1/2}$= 2.455×10^5 years) [Kae12]. Thus, ^{238}U is the most common isotope of uranium found in nature and is the one expected to be detected in the stone. Uranium-238 decays into thorium-234 by α emission with an energy of 4.270 MeV. Neither the size of the source, nor the concentration of uranium are known. The source emits α particles from different deeps, so the expected spectrum must have a main peak corresponding to those particles emitted from the uppermost layer and a continuous part corresponding to α particles from the internal layers. The penetrating range of α particles in the stone was estimated as 50 μm. Consequently, the present analysis can only be a qualitative one.

Figure 7.1. Photo of the natural uranium stone available for the measurements. The concentration of uranium is unknown as well the dimensions of the stone. Its irregular shape difficulties estimations.

The plateau curve of the source was studied. The results obtained are shown in Fig. 7.2. A plateau region between around 300 and 1500 volts with a counting rate on average of (53±7) counts per second was detected. This results are quite satisfactory because the plateau obtained is consistent concerning to the length with that one observed for the americium-241 presented in the previous chapter 6.

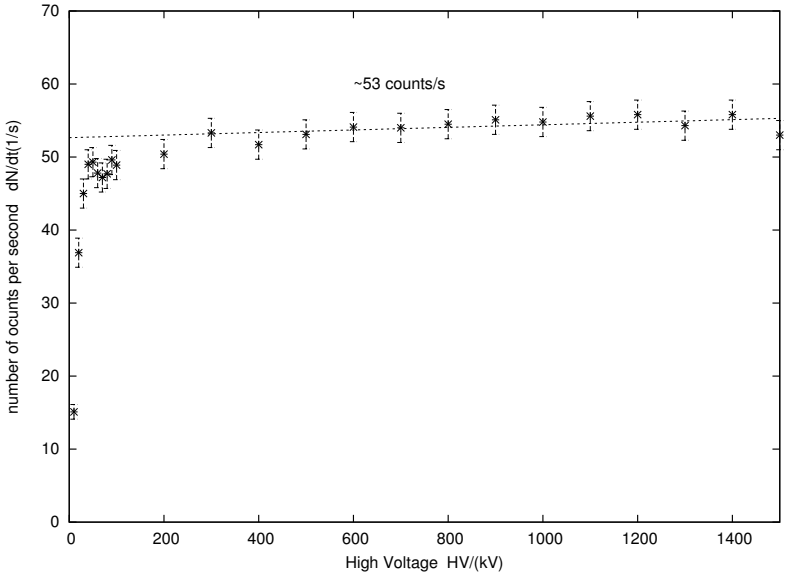

Figure 7.2. Plateau curve measured for the natural uranium source for a high voltage of 1200 V. The flat region extends approximately from 300 V until 1500 V with a slope of 2% and an average counting rate of (53±7) counts per second. However, the activity of the source cannot be determined because not enough data are available. A estimation of the size of the sample is too complicated because of its irregular shape and without it, no estimations of the activity are possible cause the counting rate measured is nearly almost due to the uppermost layer.

In addition, a spectroscopic study was carried out with the source, shown in Figure 7.3. The uranium spectrum was taken for a high voltage of 1200 V (plot a)). A mean and very broad peak was observed as it was expected but also a continuous part at low energy. It was necessary to check if that contribution corresponded to a big background which was distorting the spectrum or to the α particles emitters from greater depths. Hence, the background spectrum without source was measured as well. It showed that it was completely negligible (plot b)). According to this spectrum, the counts at low channels must be for another reason.

If the uranium chain is considered (see Appendix B, Fig. B.1), there are several β emitters on it, so could be that β radiation was being detected. To check this, the α spectrum was again measured but, this time, with the source covered with a piece of Aluminium (that was previously used in another experiments and was able to attenuate α particles from ^{241}Am) in order to attenuate α radiation. The third plot was obtained (c)), which shows a tail of counts at low channels. From this spectrum it was clear that

β emitters from the stone were detected. The corrected spectrum (i.e. the α spectrum without the β contribution) corresponds to the fourth plot (d)). Note that the counts at low energies do not disappear completely. This could be either due to background changes over time what makes a full removal of it impossible, or maybe to the deeper α particles contribution. Nevertheless, an improvement of the spectrum is observed what means that β radiation was affecting the α spectrum.

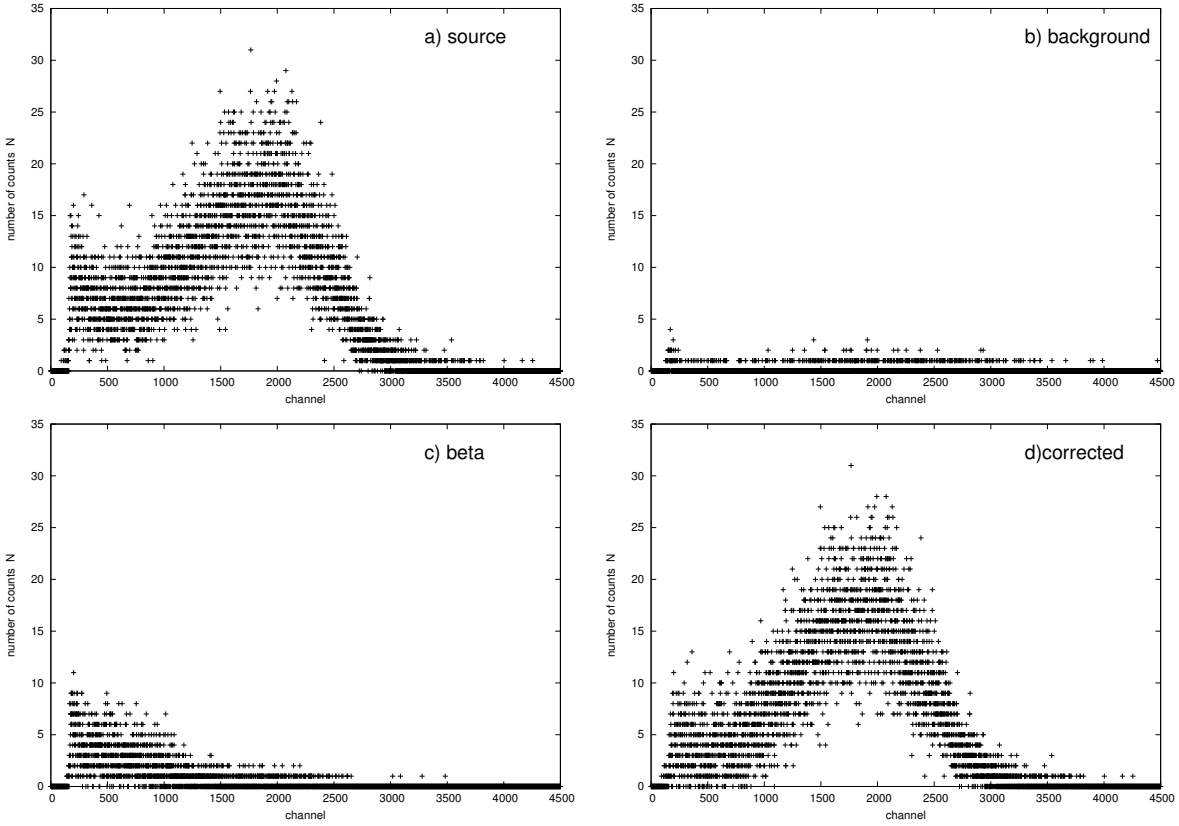

Figure 7.3. Spectroscopic analysis of the uranium stone. a) Spectrum of the stone containing uranium. b) Background spectrum at 1200 V taken without source just some minutes after the α spectrum. c) Spectrum with α particles attenuated with an aluminium plate. d) β corrected spectrum without the presence of β counts.

7.2. Natural thorium measurement

The same analysis as with the natural uranium source was carried out with a natural thorium source, this is ^{232}Th ($T_{1/2}$=1.405×10^{10} years). This element decays by α emission into ^{222}Ra ($T_{1/2}$= 5.75 years) with an energy of 4.083 MeV, which in turn decays to ^{228}Ac by β particles of 0.046 MeV energy [Kae12]. The whole decay chain for thorium-232 can be found in Fig. B.2). This source is a flat metal piece of thorium of of 24 mm of thickness with a mass of 0.2336 g. Considering the relation between the mass of a

radioactive element and its activity, according to [Buc10], given by equation

$$A = \frac{m}{M}\frac{\ln 2}{T_{1/2}} \cdot N_A \cdot h, \tag{7.1}$$

whit A the activity of the source, m its mass, M its atomic mass, $T_{1/2}$ the half-life of the radioactive element, N_A the Avogadro number and h the concentration of the radioactive element.

Considering the concentration of thorium as 100% and the thorium of the source *pure thorium*, an activity of (948.7±0.4) Bq corresponds to this source. The contribution of the daughters elements were neglected for being the composition of the sample not well known.

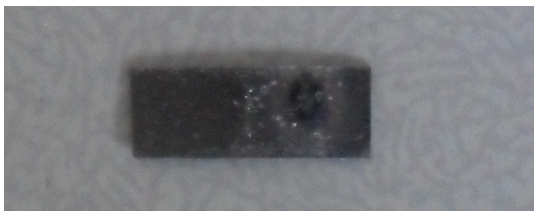

Figure 7.4. Photo of the thorium source. The concentration of thorium, as well as the rest of the components, are unknown.

The plateau curve was taken for this sample. The measurement of the counting rate as a function of the high voltage value applied at the counter tube obtained is plotted on Figure 7.5. An average value of (117±11) counts per second was detected. According to Eq.(6.1), assuming 100% efficiency, an activity of (235±7) Bq was measured. However, this value is much lower than the expected one. Even taking into account the efficiency of the detector for α decay calculated on Section 6.4.3 (i.e. (89±6)%), that leads to an activity of (264±6) Bq, still much smaller. Consequently, the concentration of natural thorium in the source is really small and the amount can be calculated using Eq.(7.1) as around 30% considering only the contribution of the uppermost layer.

With a spectroscopic study, the previous counting rate measured was confirmed by analysing the thorium spectra plotted in Fig. 7.6, as was done with the uranium one. In that case, a small peak at low energies was again observed (plot a)). Nevertheless, both background (plot b)) and the spectrum with only beta radiation (plot c)) contained a really low counting rate. The spectrum corrected without the beta radiation (plot d)) is nearly the same as the normal one (plot a)), so another reason must produce these counts.

Another possible contribution that remained to be studied was the detection of γ radiation. Several components of the thorium chain emits γ particles. Thus, an analysis of this radiation was carried out. For this, both α and β particles where attenuated with a thick piece of lead. The resulting spectrum was measured. However a really low number of counts were detected (so the spectrum plot was not included because of did not contain any useful information). Consequently, no γ radiation was detected.

On the light of these results, the contribution of other α emitters was taken into consideration as causative of the peak at lot channels. However, as was mentioned in chapter

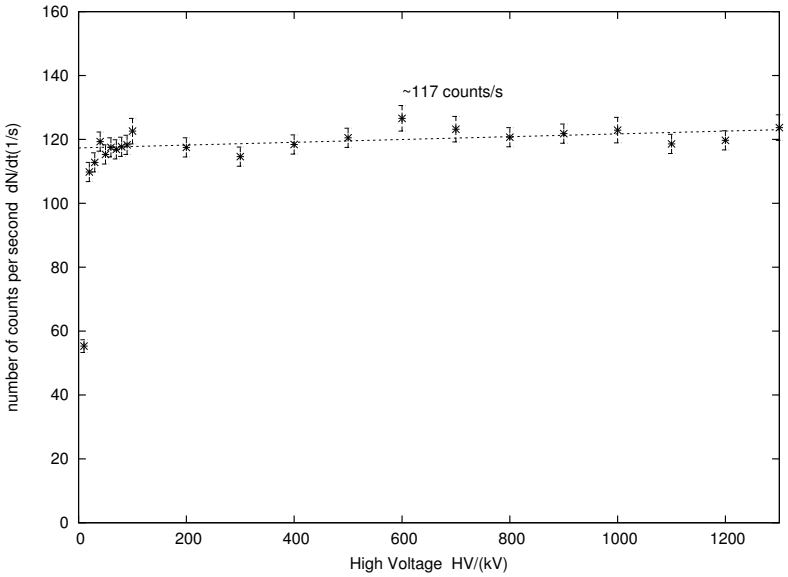

Figure 7.5. Plateau curve for the natural thorium source measured. The plateau region is found between around 100 V and 1300 V with a slope of 4% and (117±11) counts per second. That leads to an activity of A = (235±7) Bq.

2, α energies used to be between 4 and 6 MeV. Taking in to account the position of the ^{241}Am peak visualized in the energy spectrum taken for this source (shown in Fig. 6.8) around channel 2500, any α peak would be expected as such a low channels as the peak found in the thorium spectrum (channel 200, see Fig. 7.5-d)). In addition, the shape expected for an α energy spectrum is a Dirac delta peak. However, seeing that sources have a certain thickness, this peak become broader and a tail associated to low radiation energy appeared. Consequently, the small peak can not be due to the presence of other α emitter into the source. Most probably, can be explained as a low energy β radiation contribution that must been cut off by using the attenuator aluminium foil.

In any case, the shape of the peak is quite interesting due to no presence of the tail at low energies expected for thick sources. This may be an indicative of an effect that takes place in some materials that is the natural accumulation of the radioactive elements in the uppermost layers of the materials.

The measurements were repeated for different orientations of the source and the same results were obtained.

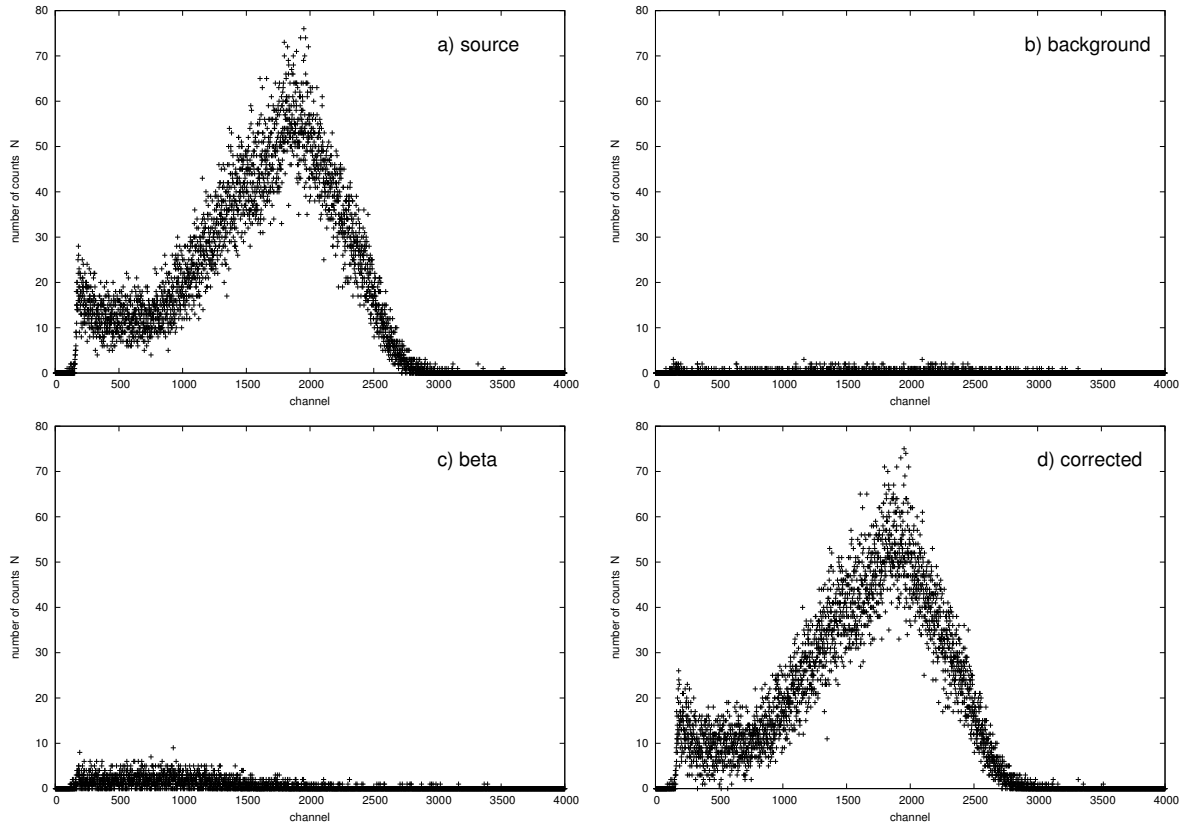

Figure 7.6. Spectroscopic analysis of the thorium sample. a) Spectrum of the source containing thorium. b) Background spectrum at 1200 V taken some minutes after the α spectrum. c) Spectrum with α particles attenuated with an aluminum plate. d) Corrected spectrum without the presence of β counts.

8. Beta decay measurements

In this chapter a qualitative analysis of two β sources with quite different energies was carried out. Thereby, difficulties of β detection were found. Particularly, those typical in the use of proportional counters.

8.1. Qualitative measurements

As it has been already mentioned, the instrument set-up establishes where the voltage regions are for counting α or β particles. These regions may be very detector specific.

The pulse size (that is the height) generated by an α particle event is much larger than that generated by a β particle event. It is the size of that pulse that discriminates between the two different particles. That is why the alphas are separated from the betas because of the fact that the signal rise time of the α pulses is shorter (due to higher ionization density) than for the β pulses.

It must be remembered that the pulse height is proportional to the the energy deposited by the particle. α particles in general deposit higher amounts of energies according to the Bethe-Bloch equation. The α particle energy has a distinct maximum with some amount of lower energy straggling. The β peak, on the other hand, is relatively broad. This difference in peak shapes is due to α particles being monoenergetic and β particles having a wide range of possible energies due to neutrino formation during the decay process. In the first particular case measured of the ^{90}Sr source, the β spectrum also has the complicating factor that there are two different β emitters present, ^{90}Sr and its progeny, ^{90}Y.

8.1.1. Activity measured of strontium-90

The first β measurement carried out was with the strontium-90 source described in chapter 2. For do this, a high voltage power supply with a higher voltage range (up 3 kV) was used.

According to the decay scheme of the ^{90}Sr (Fig. 2.5), a spectrum with both, a contribution of the strontium-90 ($E_\beta = 0.546$ MeV) and one of yttrium-90 ($E_\beta = 2.280$ MeV) is expected, as shows Fig. 8.1. In the case that β particles deposit their whole energy in the detector volume, two well defined peaks must be differentiated in the energy spectrum if the energy resolution of the detector is good enough.

Both, the energy spectrum of this source as well as the background spectrum without the source in the chamber were measured at a high voltage value of 3 kV and the same gain value used for α detection ($A = 500$, $A_f = 1.0$). The result obtained is depicted in

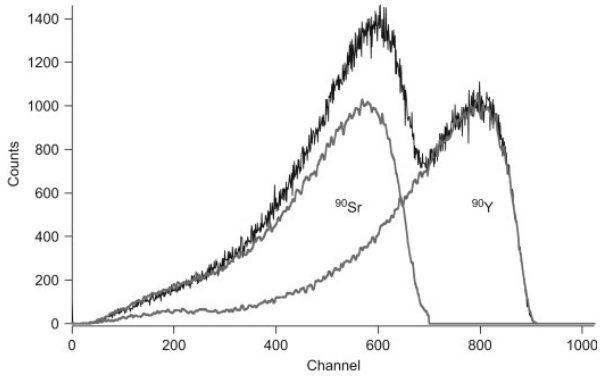

Figure 8.1. Theoretical ^{90}Sr energy spectrum expected. The contributions of both strontium-90 (E_β = 0.546 MeV) and yttrium-90 (E_β = 2.280 MeV) are present. This leads to two peaks that can be distinguished. That must be obtained in the ideal case that all β particles loose completely their energies in the detector volume [Web12e].

Fig. 8.2. The background showed a high counting rate registered at low channels. With its contribution already subtracted from the spectrum of the source, a counting rate of (551.4±0.3) 1/s was detected for the ^{90}Sr sample. Seeing that currently the certificated activity of the source is 2.01 kBq, a counting rate of 1005 counts per second is expected for the 2π detector. Consequently, the counting rate registered corresponded to an efficiency of (54.9±0.1)%.

Such a low value of the efficiency can be explained by the fact that β particles must not lose their whole energy in the dimensions of the detector chamber due to their weaker interaction with matter. The bad shape of the distribution completely different to the theoretical one (Fig. 8.1) is attributed to the rough energy resolution that incapacitate two distinguished the two peaks expected.

8.1.2. Activity measured of a potassium-chloride salt

A sample of potassium chloride present as salt was measured as well. This compound contains some Potassium-40. This element decays into Calcium-40 via β^- emission with a ratio of 89.28% and a decay energy of 1.311 MeV, and via electron capture to Argon-22 with an intensity of 10.72% and a decay energy of 1.505 MeV, according to [Kae12]. Nevertheless, the process of electron capture is not possible to be observed with the gas flow proportional counter, since no gas atoms are ionized. This means that only up to 89.28% of the 40-K decays could be observed.

With the use of a precision balance, a certain amount of salt was weighted. As has been already explained in the last chapter, the activity of a certain amount of a radioactive sample is related with its mass by the relation given by Eq.(7.1):

$$A = \frac{\ln 2}{T_{1/2}} \cdot \frac{m_{KCl}}{M_{KCl}} \cdot N_A \cdot h$$

where, for the KCl used, according to [Buc10]:

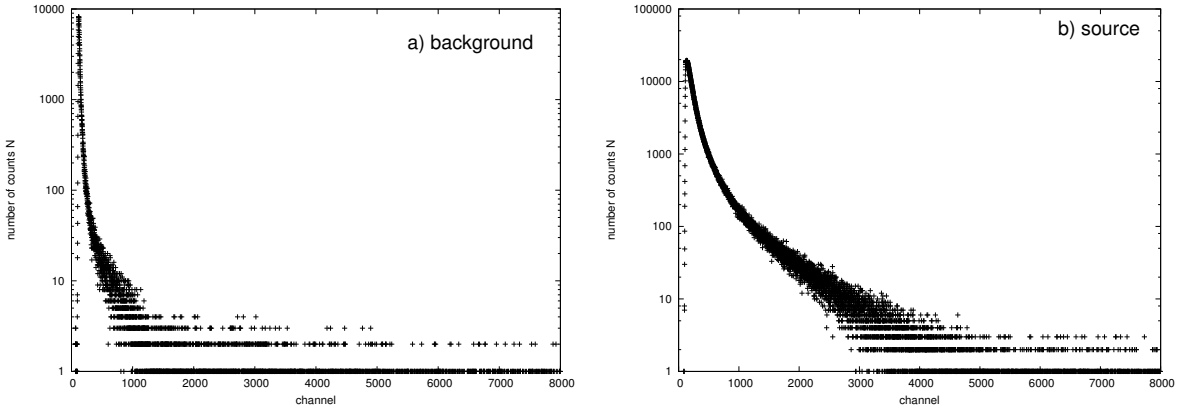

Figure 8.2. Background and ^{90}Sr source spectra measured for a high voltage value of 3 kV. a) The background spectrum shows a counting rate of (52.0±0.1) 1/s. b) ^{90}Sr -source spectrum with the background contribution already subtracted. A counting rate of (551.4±0.1) 1/s was detected. That leads to an efficiency of (54.9±0.1)% for this source. The bad shape of the distribution is attributed to the bad energy resolution that incapacitate two distinguished the two peaks expected.

$T_{1/2} = 1.248\times10^9$ years is the K-40 half-life

m_{KCl} = (6.875±0.001) g is the mass of KCl measured in the detector

M_{KCl} = 74.55 g/mol is the molar mass of KCl

$N_A = 6.023\times10^{23}$ is the Avogadro's Number

h is the concentration of K-40 in the salt

In the case of an amount of KCl of 6.875 g, the spectrum measured is plotted in Fig. 8.3. A counting rate of (38.9±0.5) 1/s was detected with the contribution of the background radiation already subtracted. According to Eq.(7.1), a β activity of (102.18±0.01) Bq was expected for this amount of salt. Nevertheless, due to the geometrical limitations of the detector (solid angle of 2π), just the half of the activity is measured with the proportional counter. This is (51.09±0.01) Bq. Consequently, this leads to an efficiency of (76.10±0.01)% for this source.

However, this value is maybe lower due to some auto-absorption effect in the salt itself. The big amount of salt measured may have provoked the lost of the contribution to the spectrum of the deeper molecules due to the thickness of the sample. To avoid this possible effect, measurements with a thin layer of salt could be carried out.

Consequently, taking into account the two efficiency values obtained for the two β sources measured (around 51% for the ^{90}Sr source and 76% for the KCl), it can be affirmed that this parameter depends on the energy of the β radiation detected, being lower for higher β energy values. Nonetheless, this fact is completely reasonable due to the different energy losses experimented by the β particles into their tracks trough the gas along the chamber according to their energies. According to Bethe-Bloch equation, faster particles,

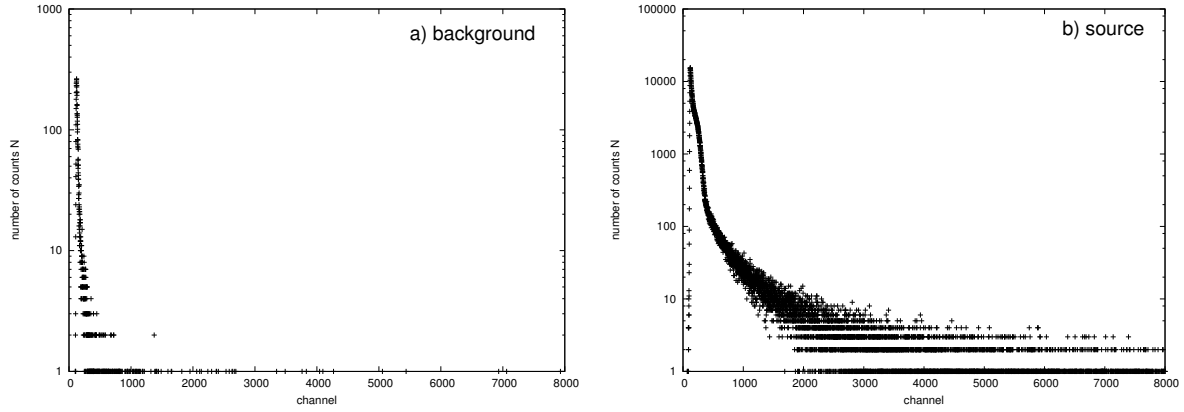

Figure 8.3. Background and KCl salt source spectra measured for a high voltage value of 2.5 kV and the same gain value used for α detection. a) The background spectrum shoes a counting rate of (23.9±0.3) 1/s. b) KCl salt source spectrum with the background contribution already subtracted. A counting rate of (38.9±0.5) 1/s was detected. That leads to an efficiency of (76.10±0.01)% for this source. The shape of the distribution is attributed again to the bad energy resolution that incapacitate two distinguished the two peaks expected.

this is, particles with higher energies, lose more energy in their interaction with matter. Nonetheless, as particles do not lose their whole energy in the detector volume, bigger fractions of energies are expected to be deposited in the chamber detector for lower energy sources. That agrees completely with the shape of the spectrum obtained. Big numbers of counts are registered at low channels corresponding to lower energy values whereas the counting rate decreases as the energy does.

For α particles it is expected that they lose their whole energy in the detector chamber dimensions. However, that was not the case for β particles. Due to their weaker interaction with matter, β particles lose their complete energies in some meters of air. Hence, for the size of the chamber, only a small portion of their energies was expected to be left in the particles tracks trough the gas. Consequently, lower amounts of ion pairs than the corresponding to such beta particles energies are formed. Accordingly, higher values of the high voltage applied than those theoretically predicted would be required to produce all the ion pairs that correspond to the β radiation energy.

A simulation of the gas multiplication factor as a function of the high voltage applied was carried out for the dimension of the detector chamber and the wire distance to the source [Ver12]. Such simulation is reproduced in Figure 8.4. It shows that for the detector dimensions, to reach an amplification corresponding to the proportional region of 4000 , voltage values around 1.3 kV are required. In the case that particles would lose their whole energy in the detector volume between the wire and the source, such voltage value would be enough to produce and collect all the ion pairs that should be created according to the radiation energy. However, in the reality, this value is not enough for β particles seeing that very few signals were observed in both the oscilloscope and the energy spectrum (not included). In addition, β particles ionize much fewer atoms per linear path length than

α particles do. Thus in order to accumulate enough collected charge for a measurable pulse, the amplification of the original β particle ionizations needs to be more significant than for α particles. Hence, higher voltage values are required to reach such amplification region with the gas flow detector. The mix of this fact and the reality that β particles do not lose their whole energies in the detector dimensions produces the lower efficiency values obtained for this radiation.

As a consequence, measurements with a more power high voltage supply must be carried out if higher number of ion pairs and then, higher efficiency values, wanted to be reached.

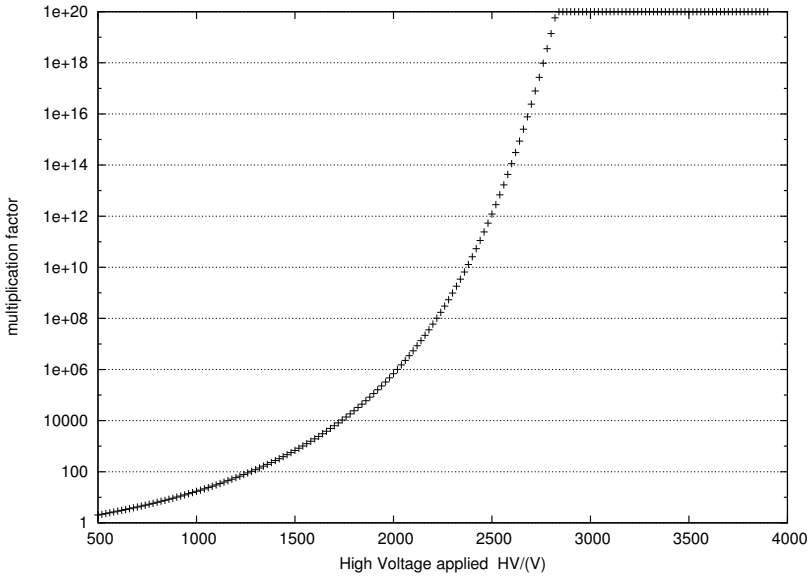

Figure 8.4. Simulation of the gas multiplication factor for the detector geometry for a distance of 10.5 cm between the wire and the source. The usual multiplication value for the proportional region is 4000 and is reached for a high voltage around 1.3 kV [Ver12].

As possible future improvements, in oder to increase the rate of energy loss by β particles in the chamber detector dimensions, two measurements can be carried out. Either the source can be attenuated by covering it with a piece of material absorber as Aluminium, or the distance between the holder and the source can be increased what increments the detector volume and so, the path in which β particles lose their energies. Studies about the influence of the wire position and its optimal value, as well as the high voltage value applied and the amplifier gain required are proposed as future work to optimize quantitative β detection.

9. Summary and outlook

To finish the thesis the most important results will be summarized in this chapter. A list of proposed measurements that still need to be completed in order to have the set-up ready for both α and beta detection is given at the end of this chapter as well.

9.1. Summary

The principal aim proposed in this thesis was the optimization of a windowless gas flow proportional counter rebuilt from an original commercial detector for α decay detection in order to be used in practical exercises by students at the university.

Initial measurements with the device have shown several problems for α detection related to the counting rate obtained and the device efficiency, as was described in chapter 5. The presence of a double plateau for an α monoenergetic emitter was the most important of them. Problems in β radiation detection were also found. Quantitative analysis of β samples were not possible. However, in deeper studies of the output signals at different steps of the electronic chain, a much more serious complication was discovered. Very frequent signals of several different amplitudes were visualized in the oscilloscope for the monoenergetic source. That provoked a development of a detailed analysis of the the whole set-up and and all the environment which could influence the measurements described in details in chapter 6. Thereby, there were considered discharges between the wire and the detector walls due to the combination of the wire shape and diameter and the high voltage values applied.

First of all, the nuclear electronic associated to the detector was revised. Looking for improvements in the noise, several devices where replaced for others specially designed for proportional counters or more specific for α detection. That was the case of the high voltage power supply, the preamplifier and the amplifier. Besides that, both a low pass filter and a multichannel analyzer were introduced in the chain. The first one with the aim of avoiding high frequency noise, which disturbed the signals the most, and the second one for the purpose of measuring the energy spectrum of the source, to have additional information useful for checking of the right counting rates and distribution shapes. As a result, improvements in the signal-to-noise ratio were obtained but the discharges remained present.

Checkings on the source condition were carried out as well and confirmed its isotropy.

Lastly, it was the replacement of the wire which solved both problems, the double plateau and the presence of the discharges. A damage of the wire was studied finding some irregularities in its silhouette. Moreover, the hemispherical shape of the anode wire was never considered the optimal one because depending on the position particles hit

it, several amplitudes were expected. As consequence, the old hemispherical wire was replaced by a new one with flat shape made of tungsten sightly thicker (15 μm) to reduce its sensitivity. With this replacement, discharges were no more observed.

In addition, it was figured out that the counting rate was extremely sensitive to the position of the source so a mechanism to fix the location of the radioactive sample was designed leading to a complete reproducibility of the results.

By these both changes, very significant improvements were obtained. The double plateau disappeared leading to a single flat plateau of 1.5 kV length with a counting rate corresponding to a 89% of α decay detection efficiency.

Afterwards, systematic measurements were carried out to determine the optimal parameters of the electronic chain devices for α detection, that were implemented for all the subsequent α samples measurements. In this manner, measurements of a source containing natural uranium and a natural thorium sample were analyzed in a qualitative way, reaffirming the good results.

So the problems with α detection were finally solved. The plateau curves obtained for the unknown sources measured were consistent with the plateau region observed in the calibration measurements. In addition, α particles were detected by applying high voltage values of just tens of volts. Since really low voltage values the energy spectra showed all the α were collected evincing the high sensitivity of the new wire and the detector.

Finally, the work presented in this thesis shows briefly the main aspects of beta decay detection with the proportional counter. Through measurements of two different samples, the dependence to the efficiency of the detector with the kind of particle and its energy for this radiation was figured out. However, deeper studies must be carried out in order to improve the quantitative detection of this radiation.

9.2. Outlook

Only lightly touched upon in this thesis is the fact that β radiation can be as well measured with the setup. Therefore, there are many proposing ideas in which future research with the detector can be taken focusing on these particles:

- Measurements with the wire holder located at different distances to the sample must been carried out. It was found that this parameter is really important in order that β particles lose their energies in the chamber dimensions. So a calibration of the position and the efficiency of the detector for beta detection would be very interesting.

  For α detection a significant change is not expected because of their strong interaction with matter makes them lose their complete energy in a few centimeters of material. In addition, the same efficiency value as the one provided by the fabricator was got for α detection. However, for β particles of typical energies, their ranges greatly exceed the chamber dimensions. The number of ion pairs formed in the gas is then proportional to only a small fraction of the particle energy lost in the gas before reaching the anode wire. A lot of variations in the possible path

lengths through the gas are possible for these particles, depending on these lengths the amount of energy deposited in the detector by the particles. This fact is not relevant for α particles because they lose their whole energy in the chamber dimensions in any case. But the same does not happen for β particles. Consequently, the wire holder position is expected to influence β detection through their energy loss.

- Checking measurements with more β-sources with a wide range of energies are recommended in order to determine a calibration for the detector efficiency as a function of the source and its energy. Also a range of β energies that is possible to study with the proportional counter can be developed. It may be both a minimum and maximum energy that the detector is able to read for β particles due to their weaker way to interact with matter and lose their energy.

- A study of the output signals and the energy spectrum distribution as a function of the high voltage applied with a power supply with a higher range is proposed to improve the efficiency of β detection.

  A higher number of ion pairs is expected to be produced with the increasing of the voltage applied by reaching the Geiger-Müller region of the detector.

- Measurements with the fill gas at other pressure values are proposed as a possible solution to the problem with the lower counting analysis of β emission samples. An increase in the pressure would lead to a higher energy loss and hence, high number of ion pairs produced. Whereas lower values of the pressure than the atmospheric one may reduce the recombination effect between the ion pairs formed. This effect could produce that although β particles ionize the gas molecules, the ion pairs generated are hardly collected.

- The possibility of having a bad isolation with the β source due to its plastic made nature can be checked by locating a metal grid above the sample in contact with the chamber walls that assures the correct grounding.

  The fact that the α source is metal made whereas the β one is plastic made is a big difference found as possible explanation of the problem with β detection. If the source is not well isolated, a cloud of positive ions can be formed above the sample altering the electric field, producing problems in the ion pairs collection. In that case, ions pair would be again created in the gas molecules, but not well collected.

- Finally, once the parameters required for measurements with β sources are under control, studies of mixed α and β emitters are proposed as very interesting in order to visualize the two plateau regions expected theoretically in the counting curve. The first one must correspond to α particles. In that point only these particles are counted because they are the only ones able to ionize the gas molecules. And the second plateau correspond to electric field values at which both α and β particles are counted. Just to be reminded, because of the β particles pulse height distribution is broader and less well separated from the low-amplitude noise, the β plateau is generally shorter and shows a greater slope than the α one.

According to [Kno96], absolute β activity measurements are often carried out in 4π flow counters which are able to detect radiations that emerge from both surfaces of the sample.

Appendices

A. Summary of the electronic basic settings

High Voltage	Filter	Detector	Preamplifier
-channel C -HV= 1.2 kV	-low-pass	-wire: 15 μm -material: tungsten -Gas flux: 0.1 LPM	-as close as possible to the detector
Amplifier	**SCA**	**Counter & Timer**	**MCA**
-Coarse Gain: 500 -Fine Gain 1.0 -Shaping Time: 0.5 μs -Output range: 10 V -BLR: High -Delay: On -Output: unipolar, positive	-LLD: 0.24 V just above noise -ULD: 10 V at maximum signals amplitude -Mode: Normal	-time selection: $m \times 10^{(n-1)}$	-8191 channels -range: 10 V

Table A.1. Summary of the parameter values of the devices of the chain selected as optimal for α detection in the present work.

B. Decay Chains

Figure B.1. The decay chain of ^{238}U is commonly called the *radium series*. All the elements are present, at least transiently, in any natural uranium-containing sample, whether metal, compound, or mineral [Div12].

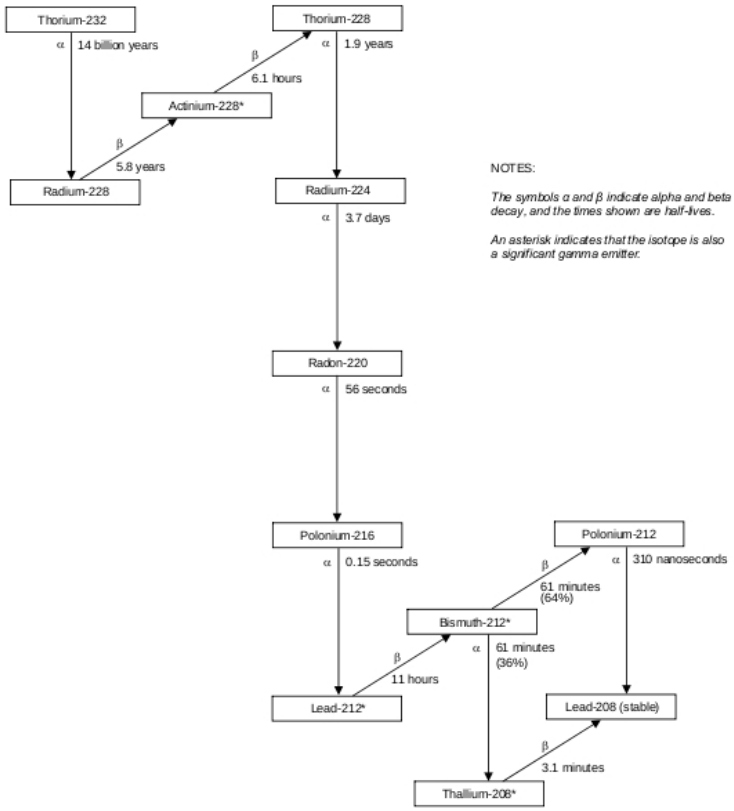

Figure B.2. The chain of Thorium-232 is commonly called the*thorium series*. Beginning with naturally occurring thorium-232. All the elements of the chain are present, at least transiently, in any natural thorium-containing sample, whether metal, compound, or mineral [Div12].

Bibliography

[Ahm07] Syed Naeem Ahmed *Physics & Engineering of Radiation Detection* First Edition, 2007, Academic Press

[Agi12] Agilent Technologies : http://www.datatec.de/

[Bau02] Baum 2002; DOE 1997b; ICRP 1983; LBL 2000; Lide 1998

[Ber12] Berthold Company: (https://www.berthold.com/)

[Bri12] Encyclopedia Britannica: http://www.britannica.com

[Buc10] *Dosismessung mit einem Proportionaldurchflusszähler*, Bachelorarbeit vorgelegt von Christian Buchholz, 2010

[Cae12] Caen: http://www.caen.it

[Can12] Caberra: http://www.canberra.com

[Cur49] S.C. Curran, J. Angus & A.L. Cockroft (1949): *II. Investigation of soft radiations by proportional counters*, Philosophical Magazine Series 7, 40:300, 36-52

[Div12] *Natural Decay Series: Uranium, Radium, and Thorium*, Environmental Science Division (EVS): http://www.ead.anl.gov/

[Fra00] Larry A. Franks, et. al.: *Radioactivity Measurement* Copyright 2000 CRC Press LLC

[Gal12] Galileo: http://galileo.phys.virginia.edu

[Gru99] Claus Grupen: *Particle Detectors.* Wiley (Third Edition), 1999

[Hua06] *Deng Huang, Rogene M. Eichler West, David V. Jordan, and Kim F. Ferris* IEEE Nuclear Science Symposium Conference Record, N35-5, 2006

[Isu12] Idaho Sate University: http://www.physics.isu.edu/radinf/cover.htm

[Kae12] Atom Kaeri: http://atom.kaeri.re.kr/

[Kho12] A.Khoukaz, private communication (2012)

[Kno96] Glenn F.Knoll: *Radiation Detection and Measurement.* Cambridge University Press, 1996.

[Leo99] William R.Leo: *Thecniques for Nuclear and Particle Physics Experiments* Springer-Verlag (Second Revised Edition), 1999.

[Nur12] *Instrumentation and measurement techniques*, NUREG-1575, Supp. 1

[Ort12] Ortec: http://www.ortec-online.com

[Phy12] *Radioisotopes and Radiation Methodology*, Chapter 3, Med Phys 4R06/6R03, http:http://www.sciencemag.org/.

[Pri12] Princeton University: http://web.princeton.edu

[Rwth12] RWTH Aachen Physics: http://www.physik.rwth-aachen.de

[Scr12] Scribd: http://www.scribd.com/doc/58227755/46/Regions-of-Operation-of-Gas-Filled-Detectors

[US11] *Manual for Experimental Nuclear Physics*, Técnicas Experimnetales en Física Nuclear 2011, Universidad de Sevilla

[Vil12] Vilniaus University: http://www.kkek.ff.vu.lt

[Wat12] University of Waterloo: http://www.safetyoffice.uwaterloo.ca/

[Ver12] Don Vernekohl , private communication (WWU Münster 2012)

[Web12a] http://www.cnstn.rnrt.tn/afra-ict/NAT/xrf/image/xrf11.png, 2012

[Web12b] http://web-docs.gsi.de/~wolle/Schuelerlabor/IMAGES/Sr-90%20Niveauschema.gif, 2012

[Web12c] http://www.southerninnovation.com/extras/557/Pulse%20Pile-up.png, 2012

[Web12d] http://nsspi.tamu.edu/media/155130/image26.jpg, 2012

[Web12e] http://ars.els-cdn.com/content/image/1-s2.0-S0969804308001085-gr1.jpg

[Wei12] *Kern- und Teilchenphysik; Vorlesung WS0910*, Prof. Dr. C.Weinheimer

[Wik12a] Wikipedia: http://en.wikipedia.org/wiki/Nuclear_electronics

[Wikb12b] Wikipedia: http://en.wikipedia.org/wiki/Uranium-238#Nuclear_weapons

[Wikb12c] Wikipedia: http://en.wikipedia.org/wiki/Beta_decay

[Wikb12d] Wikipedia: http://en.wikipedia.org/wiki/Ripple_%28electrical%29

List of Figures

List of Tables

Acknowledgements

On this final section I would like to thank all the people who have helped me during the whole master period.

First of all, I would like to express my gratitude to Prof. Dr. Alfons Khoukaz for giving me the opportunity of being a member in his group. Is remarkable how much I have lernt from him. Thanks for making me feel comfortable as foreign student, support me and always believe we would get it even in the hardest moments.

My next gratitude is to Paul Goslawski for all the help given during the whole period of the master. His advices in the laboratory work, the support and help on the writing of this thesis have been crucial for me to improve it. To Malte Mielke for his also important help with main details of this work but specially for all the talks and the particular German lessons. So many hours in the office were not so hard thanks to both Male and Paul. Furthermore, thanks to all the people who are or have been in the group during this time. All of them were kind enough to speak in English because of me and had a smile for me.

I would like to thank Daniel Bonaventura the design of Silicon detector set-up as well as the so delicate wires. Thanks for his great work and for his patient when I broke wires. In addition, I thank everyone on the electronic and mechanic workshop to help me with all the problems they were able to solve.

To Don Vernekohl thanks for his simulations which gave me useful ideas in the last moments. Thanks for dedicate some of your time to my problems. To Alexander Täschner thanks for his great help with gnuplot that made my thesis as it is.

I would like to give a special thank to Prof. Dr. Helmut Kohl, the coordinator of Müsters exchange students. For everything he has arranged to make our life in Müster easier. Thanks for always be so kind and have time for us and all our papers.

Finally, I would like to make a special mention to some Spanish people that were always there in the distance supporting me and giving me advices as are María Villa Alfageme and Santiago Hurtado. Your ideas really helped me and your support gave me force. To Manuel Perez Mayo all my gratitude for so many good moments in a foreign country and being always willing to help a friend in the lab and outside it. Some moments were more bearable thanks to you.

Thanks all you very much because otherwise this year wouldnt have been so much amazing.